Università degli Studi di Milano-Bicocca
Dipartimento di Biotecnologie e Bioscienze
Dottorato di ricerca in Scienze della Vita
XXIX Ciclo

FR051, a novel Hexosamine Biosynthetic Pathway inhibitor, induces cell death in breast and pancreatic cancer models

Francesca Ricciardiello
Matr. 787935

Anno Accademico 2015-2016

Dipartimento di Biotecnologie e Bioscenze

Dottorato di Ricerca in Scienze della Vita
Ciclo XXIX

Curriculum in Biotecnologie

FR051, a novel Hexosamine Biosynthetic Pathway inhibitor, induces cell death in breast and pancreatic cancer models

Ricciardiello Francesca

Matricola 787935

Tutor: Chiaradonna Ferdinando

Coordinatore: Vanoni Marco

ANNO ACCADEMICO

2015/2016

Abbreviations and acronyms

Atf4= Activating transcription factor 4
AZA= Aaserine
Grp78/HSPA5= 78 kDa glucose-regulated protein
Chop= CCAAT/-enhancer binding protein homologous protein
ER= Endoplasmic Reticulum
ERO1= ER oxidoreductin 1
GFAT= Glutamine:Fructose-6-phosphate amidotransferase
GlcNAc= N-Acetyl glucosamine
GlcNAc-6-P= N-Acetyl glucosamine-6-phospate
GlcNAc-1-P= N-Acetyl glucosamine-1-phosphate
HBP= Hexosamine Biosynthetic Pathway
IRE1= Inositol-requiring enzyme 1
Mgat= N-acetylglucosaminyl transferase
NAGK= N-acetylglucosame kinase
OGT= O-linked N-acetylglucosamine transferase
OGA= O-linked N-acetylglucosaminidase
O-/N-Gly= O-/N-Glycosylation
PARP= Poly ADP ribose polymerase
PERK= protein kinase RNA-like endoplasmic reticulum kinase
PGM3= Phosphoacetylglucosamine mutase 3
PDI= Protein disulphide isomerase
ROS= Reactive Oxygen Species
Tun= Tunicamycin
UPR= Unfolded Protein Response
UPRE= Unfolded Protein Response Element
UDP-GlcNAc= Uridine diphosphate N-acetylglucosamine
Xbp1= X-box binding protein 1

Abstract

Abstract

Cancer cells are able to reprogram their metabolism, increasing ATP synthesis, biosynthesis of macromolecules and maintaining the appropriate redox status, in order to sustain proliferation, survival and tumor development, also in different stress conditions.

Hexosamine Biosynthetic Pathway (HBP) integrates glucose, glutamine, fatty acids (Acetyl-CoA) and nucleotides (uridine-triphosphate) metabolism to synthetize a single metabolite, namely uridine-diphosphate N-acetylglucosamine (UDP-GlcNAc). This metabolite is recognized as a nutrient-sensing molecule because its level strictly depends on the availability of aforementioned nutrients. In addition it is a fundamental substrate for the enzymes involved in O-/N- protein glycosylation.

Since many proteins, engaged in a wide range of cellular functions (like shuttling of molecules, cell-cell contact, cell-extracellular matrix interaction, correct protein folding) are glycosylated, alteration of O-/N-linked protein modifications has been associated to various human diseases, including cardiovascular disease, neurodegenerative disorders, diabetes mellitus, and cancer.

In the last decades, in order to restore normal levels of glycosylation, especially in cancer, some modulators have been synthetized. These modulators act either binding enzymes directly involved in transferring of N-acetylglucosamine (GlcNAc) to proteins, namely *tunicamycin*, *alloxan*

and *benzyl-2-acetamido-2-deoxy-α-D-galactopyranoside*, or binding the glutamine:fructose-6-phosphate amidotransferase (GFAT) enzyme, the rate-limiting enzyme of HBP, namely *6-Diazo-5-oxo-L-norleucine* and *azaserine*, two structural analogues of glutamine. The need to synthetize new modulators rises from the low sensitivity and specificity of these compounds.

The purpose of my PhD project was the synthesis and then the characterization of several compounds acting as specific inhibitors of the phosphoacetylglucosamine mutase (PGM3), the enzyme involved in the isomerization of GlcNAc-6-P to GlcNAc-1-P in HBP. This enzyme has been selected for three main reasons.

First, as reported in literature, *PGM3* gene is evolutionary well conserved (i.e. *E. Coli, S. Cerevisiae*, *H. Sapiens*), suggesting an important role of this enzyme in cell and organismal physiology. Second, the reaction catalysed by PGM3 is downstream the enzyme N-acetylglucosamine kinase (NAGK), which directly participates to environmental recovery of GlcNAc (salvage pathway) necessary to fuel the HBP also in harsh conditions. Third, PGM3 inhibition affects both O- and N-glycosylation processes.

The library of possible PGM3 inhibitors has been designed by virtual screening and computational modelling, taking in consideration only chemical structures with high similarity to that of the natural substrate. Such molecules must act as competitive inhibitors for the catalytic pocket of PGM3.

FR051: a novel HBP inhibitor

According to a computational analysis, based on the affinity between the enzyme and new possible molecules, we screened a mini-library of compounds with the higher docking score, for their ability to induce cell growth arrest and/or cell death on MDA-MB-231 breast cancer cells.

Among the different compound tested, FR051 compound resulted to be the more effective, since it was able to induce cancer cell death upon 24-48 hours of treatment. For this reason a deeper investigation about the molecular mechanisms activated by FR051 was performed.

FR051 is able to block cell proliferation, cell attachment and also cell viability. As expected, these effects are associated to a decrease of N-glycosylation levels. Importantly, all these effects are not reverted by fuelling the salvage pathway by addition of GlcNAc, suggesting a downstream inhibition. As reported in literature accumulation of unfolded proteins in endoplasmic reticulum, due for instance to a decrease of protein N-glycosylation, leads to activation of the so called Unfolded Protein Response (UPR). Detailed analysis of UPR activation upon FR051 treatment indicate a reduction of the pro-survival branches as detected by measuring the level of mRNA and protein expression of chaperone 78 kDa glucose-regulated protein (Grp78) and X-box binding protein 1 (Xbp1), and an increase of pro-apoptotic pathways as detected by measuring the level of mRNA and protein expression of activating transcription factor 4 (Atf4) and of the CCAAT/-enhancer-binding protein homologous protein (Chop). Notably, FR051 treatment does not induce

Xbp1 splicing, suggesting a lack of activation of the other UPR branch, Ire1. This result is confirmed by the lack of activation of two Xbp1 transcriptional targets, GFAT1 and PGM3.

Further analysis of FR051 effect indicates a strong increase of Reactive Oxygen Species (ROS), partially due to the action of ER oxidoreductin 1 (Ero1), endoplasmic reticulum resident protein involved in protein disulphide bonds formation, process associated also to ROS generation.

A strong Erk1/2 activation is observed in association to such ROS production and to cell death upon FR051 treatment. Strikingly, specific inhibition of Erk1/2 activity, almost completely block the cell death induced by FR051 treatment.

To further evaluate the specificity of FR051, a de-acetylated counterpart of FR051, FR053, has been synthetized and in vivo tested. Strikingly, the FR053 does not influence cell proliferation, viability and cell surface N-glycans.

To confirm the specificity of FR051, experiments in normal cells and in other breast and pancreatic cancer cell models have been performed. Importantly, FR051 has a weak effect on normal cells and a higher specificity in all the other cancer cells tested as compared to MDA-MB-231 cells.

All these findings make FR051 an interesting molecule for cancer cell therapy and the starting point for the synthesis of more efficient molecules.

Riassunto

Le cellule tumorali sono in grado di riprogrammare il loro metabolismo, aumentando i livelli di ATP, sintetizzando macromolecole e mantenendo un corretto stato redox, al fine di sostenere la proliferazione, sopravvivenza e quindi sviluppo del tumore anche in condizioni avverse.
Nel pathway delle esosammine è prodotta l'UDP-N-acetilglucosammina mediante l'utilizzo di glucosio, glutammina, Acetil-CoA e uridina tri-fosfato. L'UDP-N acetilglucosammina è definita molecola sensore, poiché il suo livello è strettamente dipendente dalla disponibilità dei substrati sopra menzionati, ed è il substrato degli enzimi catalizzanti le reazioni di N- e O-glicosilazione proteica.
Un'elevata percentuale di proteine, coinvolte in svariate funzioni (trasporto di molecole, interazione cellula-cellula e cellula-matrice extracellulare, trasferimento di fattori di trascrizione, raggiungimento del corretto folding proteico), è modificata dalle glicosilazioni. Per tale ragione, sia l'aumento dei livelli di glicosilazione sia alterazioni nell'espressione degli enzimi (che controllano tale modificazione) rivestono un ruolo chiave in diverse patologie come ad esempio il diabete, le malattie neurodegenerative e infine il cancro. Studi recenti hanno evidenziato come un'alterazione del *pathway*, e di conseguenza un'alterata produzione di UDP-N-acetilglucosammina, sia in grado di favorire/sostenere la proliferazione, adesione, motilità, resistenza a

stress, angiogenesi e infine metastasi, caratteristiche tipiche delle cellule di cancro.

La progettazione razionale di strumenti chimici, che possano manipolare l'attività di enzimi coinvolti nell'HBP per ripristinare il normale livello di O-/N-glicosilazione, è un "problema" attuale ampiamente affrontato in ambito di ricerca. La maggior parte dei modulatori sino ad ora sintetizzati emula la struttura dei substrati naturali degli enzimi coinvolti sia nel trasferimento diretto delle catene glicosidiche sia nelle reazioni precoci del *pathway*. La tunicamicina, l'alloxano e il benzil-2-acetamido-2-deossi-α-D-galactopiranoside appartengono al primo tipo, mentre il 6-Diazo-5-oxo-L-norleucina e l'azaserina appartengono al secondo (questi ultimi sono in grado di inibire la fruttosio-6-fosfato ammido-transferasi 1, l'enzima limitante il pathway dell'esosamine. Nonostante i promettenti risultati ottenuti nei primi test effettuati, queste molecole sono poco sensibili e specifiche e in alcuni casi anche tossiche.

In funzione di ciò, ho incentrato il dottorato sulla sintesi e successiva caratterizzazione di modulatori dell'enzima phosphoacetil glucosammina mutasi 3, deputato alla conversione dell'N-acetilglucosammina-6-P in N-acetilglucosammina-1-P tramite una reazione di isomerizzazione.

La decisione di voler utilizzare la mutasi come target enzimatico deriva non solo dal fatto che si tratta di un enzima molto conservato e molto importante (la completa delezione del gene in topo non è compatibile con la vita) per diversi organismi (ad esempio *S.cerevisiae, H.Sapiens*), ma

anche perché inibendo la reazione da esso catalizzata si blocca la sintesi dell'UDP-N-acetilglucosammina, e quindi di entrambe le reazioni di glicosilazione. Inoltre in letteratura è stato dimostrato che la mutasi può utilizzare come substrato anche N-acetilglucosammina-6-P derivante dal meccanismo di salvataggio, una via di recupero di substrati che elude le prime reazioni del *pathway* delle esosammine, mediante l'azione dell'enzima N-acetilglucosammina chinasi. In questo modo si alimenta il *pathway* anche quando i livelli di glucosio e glutammina sono bassi. Quindi inibendo la mutasi si blocca anche il meccanismo di salvataggio rendendo la cellula più sensibile a trattamenti con specifici modulatori.

In collaborazione con il gruppo della Prof.ssa Barbara La Ferla, è stata progettata una libreria di possibili inibitori dell'enzima di nostro interesse, la cui struttura base è simile (glico-mimetici) a quella del substrato naturale dell'enzima e presentano delle modifiche in posizione C1 e C6. La progettazione delle molecole è stata basata non solo sulla struttura del substrato ma anche sul meccanismo di catalisi enzimatica, definito a ping-pong poiché si ha uno scambio di gruppi fosfati tra l'enzima e il substrato. Quindi la struttura base dovrebbe favorire il riconoscimento delle molecole nel sito catalitico, le modifiche in posizione 6 e 1 dovrebbero impedire la catalisi enzimatica diretta e inversa, rispettivamente (la reazione catalizzata è reversibile).

Mediante un'analisi computazionale sono state identificate le molecole con un maggiore valore di docking score e di cLogP, rispettivamente

l'affinità tra l'enzima e l'inibitore e il coefficiente di partizione ottanolo/acqua (indice dell'idrofilicità/lipofilicità di sostanze organiche). Gli inibitori con maggiore valore di docking score, sono stati poi testati in vitro utilizzando diverse concentrazioni su un modello di cancro alla mammella triplo negativo (MDA-MB-231) ed è stata valutata la capacità di indurre morte. Da uno screening iniziale, la molecola FR051 ha suscitato molto interesse. Infatti tale molecola FR051 è in grado di indurre distacco cellulare dalla piastra in associazione a una diminuzione delle N-glicosilazioni, a una forte riduzione della vitalità cellulare (attivando l'apoptosi) e influenza negativamente la capacità cellulare di formare nuove colonie. Inoltre, il co-trattamento con dosi crescenti di N-acetilglucosammina non è in grado di mitigare gli effetti dell'inibitore, suggerendo che FR051 stia bloccando effettivamente la mutasi.

E' noto che il mancato raggiungimento del corretto folding proteico, dovuto alla diminuzione dei livelli di N-glicosilazione, attivi il meccanismo di risposta all'accumulo di proteine non foldate che si compone di tre *sub-pathways* (Ire1, PERK e ATF6). E' stata valutata la variazione dell'espressione genica e proteica di alcuni fattori coinvolti in tale risposta. In particolare, FR051 riduce l'espressione genica e proteica di Grp78 (chaperone molecolare), aumenta l'espressione genica di ATF4 (fattore trascrizionale coinvolto nel *pathway* di PERK) e aumenta l'espressione genica e proteica della proteina pro-apoptotica coinvolta in tale meccanismo. FR051 induce un aumento del livello del messaggero Xbp1

(indice dell'attivazione del *pathway* di ATF6) ma non stimola il suo *splicing*, suggerendo un'inattivazione del *pathway* di Ire1.

Dopo 24h di trattamento, aumenta la fosforilazione di Erk, indice della sua attivazione, e rimane stabile anche a 48h. Tale aumento, probabilmente, è associato a morte cellulare, infatti l'inibizione di Erk (SCH772984) riduce la percentuale di morte cellulare.

Le analisi di espressione proteica suggeriscono una stabilizzazione post-traduzionale dell'enzima glutammina-fruttosio 6-fosfato amminotrasferasi 1, che rappresenta il più importante step di controllo della via dell'HBP, e della mutasi (enzima d'interesse). Invece le analisi di Real Time PCR rivelano una diminuzione dell'espressione genica di entrambi gli enzimi.

FR051 è un analogo strutturale del N-acetilglucosammina-6-P con gruppi acetili in posizione C3, 4 e 6. Tale molecola è stata sintetizzata anche in forma deacetilata (FR053), ma contrariamente a FR051 non ha alcun effetto né sulla vitalità cellulare né sui livelli di N-glicosilazione.

Inoltre linee di tumore alla mammella, con differente *background* genetico, e di tumore al pancreas sono molto più sensibili al trattamento con FR051, infatti si assiste ad un blocco della proliferazione e morte cellulare a dosi inferiori rispetto a quelle utilizzate per la linea MDA-MB-231.

Tutti i risultati ottenuti sino ad ora, rendono FR051 un'interessante molecola e punto di partenza per la sintesi di nuove molecole più stabili ed efficaci.

Introduction

Cancer metabolism

In 2010, De Berardinis et al. defined tumors as metabolic entities, due to their ability of drawing metabolites from blood into cells. Cancer abnormal metabolic phenotype is due to intrinsic genetic background (i.e. mutations of tumor suppressor and/or oncogenes) and by tumor environment (pH, O_2 level, nutrients availability). All these features make cells able to proliferate, to survive also in stress conditions (nutrient deprivation and cell dell detachment etc.), leading to tumor development and then to metastasis (Chiaradonna et al., 2012).

Among metabolites, glucose and glutamine are the mostly used substrates in several metabolic pathways.

Glucose is involved into glycolysis for ATP synthesis, in glycogen synthesis, in pentose phosphate pathway (PPP) for de novo synthesis of nucleotides, in Hexosamine Biosynthetic Pathway (HBP).

As reported in 1956, the Warburg effect is one of the hallmark of cancer, which consists of an high glycolytic rate also under normal oxygen concentration (WARBURG, 1956). This is an important adaptation, especially in tumors having defective mitochondria, since glycolysis, being less efficient in terms of ATP production, imposes a higher glycolytic flux to cancer cells.

Among altered signalling pathways in human cancers, there is that of Phosphatidylinositol-4,5-bisphosphate3kinase (PI3K), whose activation is

due to mutations in PTEN tumor suppressor or in the components of the PI3K complex (Wong et al., 2010). The activation of PI3K provides strong growth and survival signals and showing significant effects on cancer metabolism, contributing to several aspects of tumorigenesis (tumor development, invasiveness, metastasis, progression). It produces phosphoatidylinositol-3-4-bisphosphate or -3-4-5-trisphosphate, which is bound by Akt protein that increases expression of glucose transporters (Gluts) (Elstrom et al., 2004), of ectonucleoside triphosphate diphosphohydrolase 5 (supporting protein glycosylation) (Fang et al., 2010), and inhibits negative regulator tuberous sclerosis 2 (TSC2) of mTOR leading to protein and lipid biosynthesis and cell growth (Robey and Hay, 2009). In addition, liver kinase 1 (LKB1) is reported to be mutated in several tumors (i.e. Peutz-Jeghers syndrome) so that AMP-activated protein kinase is not able to inhibit mTOR pathway (Jenne et al., 1998).

Oncogenic Myc has been shown to collaborate with HIF in the activation of several glucose transporters and glycolytic enzymes (i.e. LDHA, PDK1) (Kim et al., 2007) and tumor suppressor 53 (Tp53) is mutated frequently, so that glycolysis is not inhibited by TP53-induced glycolysis and apoptosis regulator (TIGAR) (Bensaad et al., 2006).

Oncogenic K-RAS mutations are essential players in the development of many tumors by activating downstream signalling pathways that contribute to cell transformation. For instance, loss of oncogenic K-RAS

down regulates glucose uptake in pancreatic ductal adenocarcinoma (PDAC) cancer cells (Ying et al., 2012).

In our laboratory, it was highlighted the importance of glucose for cancer cell growth. Indeed, glucose deprivation reduces their survival (Chiaradonna et al., 2006b) by increasing reactive oxygen species (ROS), decreasing ATP cell content and reducing HBP flux. Latter effect leads to prolonged Unfolded Protein Response (UPR) activation that eventually induces to cell death (Palorini et al., 2013a) and makes hyper-glycolytic cancer cells more sensible to low doses of Complex I inhibitors (Palorini et al., 2013b).

Another important metabolite is glutamine, as the donor of γ-nitrogen group (for synthesis of nucleotides and for HBP) and α-nitrogen group and/or carbon skeleton. It is also converted into glutamate that is used for synthesis of non-essential amino acid, glutathione, respiratory substrates and reducing equivalents (DeBerardinis and Cheng, 2010) and can transfer nitrogen to essential amino acids (leucine, isoleucine an valine) probably through reversible activity of aminotrasferases (Hiller et al., 2010).

Cancer cells are able to positively modulate the production of two of the most important antioxidants, reduced nicotinamide adenine dinucleotide phosphate (NADPH) and glutathione (GSH), in order to defeat from ROS production (Nathan and Ding, 2010). This is possible by increasing SLC5A1 and SLC7A1 transporters (for glutamine uptake) and by activating enzymes involved in glutaminolysis (Wise et al., 2008), so that glutamine

can be converted to glutamate, that is then converted to a-ketoglutarate (a-KG) in order to sustain production of amino acids and fatty acids and to fuel the TCA cycle (DeBerardinis et al., 2007).

As reported in our laboratory, glucose and glutamine dependent cell growth is associated to increased expression of glycolytic genes and high level of lactate, increased glutamine utilization, altered mitochondria morphology and down-regulation of mitochondrial genes (Chiaradonna et al., 2006a) (Chiaradonna et al., 2006b).

Increased glucose and glutamine uptake cooperate to maximize also the HBP. Its main role is to produce UDP-N-acetylglucosamine (UDP-GlcNAc) for post-translational O-/N-glycosylation modifications of proteins involved in a wide range of cellular functions.

Furthermore, two important signal transduction pathways regulate HBP flux in response to nutrients availability: cAMP-dependent protein kinase A (PKA)(Palorini et al., 2016) and AMP-activated protein kinase (AMPK). Both kinases regulate Glucosamine-fructose amido transferase 1 (GFAT1) activity, the HBP rate-limiting enzyme, by phosphorylating specific residues in its aminoacidic sequence (Chang et al., 2000) (Hu et al., 2004). Indeed it has been shown that PKA and AMPK may induce GFAT1 activity inhibition by phosphorylation on Ser205 and Ser243, respectively; conversely PKA-dependent phosphorylation on Ser202 of GFAT2, induces its activity (Eguchi et al., 2009). From these findings it has been proposed that the two GFAT proteins are regulated differently in order to satisfy the

specific needs of the different tissue in which they are expressed (Hu et al., 2004).

Recently, many researchers have focused their attention on HBP because it has been shown that several oncogenes are glycosylated (N-/O-glycosylated). Such a post-translational modifications lead to their stabilization and hence to a stronger activation of downstream signalling able to induce several cellular processes among which increased nutrient uptake. In addition altered O-/N-glycosylation is reported to be associated to several diseases (see "Glycosylation disease" section).

All these evidences emphasize the importance of glycobiology field for tumor development and suggest to synthetize specific HBP inhibitors as possible anti-cancer drugs.

Hexosamine Biosytnthetic Pathway (HBP)

Many researchers focus the attention on the HBP, a metabolic pathway, that integrates the metabolism of glucose and glutamine from each other and with that of fat (acetyl-CoA) and nucleotides (uridine-diphosphate) and producing UDP-GlcNAc as the end product of HBP (Hanover et al., 2012).

HBP has the first two reactions in common with glycolysis. Indeed, about 2-5% of total glucose enters in this pathway and it is converted in glucose-6-P or Glc-6-P (that can undergo also into pentose phosphate pathway or

PPI) by Hexokinase (HK) enzyme, and so that fructose-6-P or Fru-6-P (that can fuel both PPI and glycolysis) is produced by Glucose-6-phosphate isomerase (GPI) action. Fru-6-P is the substrate of the HBP rate limiting enzyme GFAT1 that interconverts Fru-6-P to glucosamine-6-P using glutamine as amine donor (transfer of ammonia group from glutamine to Fru-6-P). The GFAT1 activity is under the control of UDP-GlcNAc amount, the HBP end product, through an allosteric feedback mechanism (Broschat et al., 2002).

Glucosamine-6-P is acetylated on nitrogen atom by Glucosamine-N-6-P acetyltransferase 1 (GNPNAT1) producing N-acetylglucosamine-6-P (GlcNAc-6-P), that is further isomerized into GlcNAc-1-P by Phospho acetyl-glucosamine mutase 3 (PGM3) through a *ping-pong* mechanism. Uridylation of PGM3 substrate by UDP-GlcNAc pyrophosphorilase (UAP1) results in formation of the end product UDP-GlcNAc. This is the substrate for the enzymes involved in O- and N-glycosylation (Dennis et al., 2009b). UDP-GlcNAc can be thought the “sensing molecule” of nutrients, because its level depends on the nutrient availability (Palorini et al., 2013a) (Wellen et al., 2010) **(Figure 1)**.

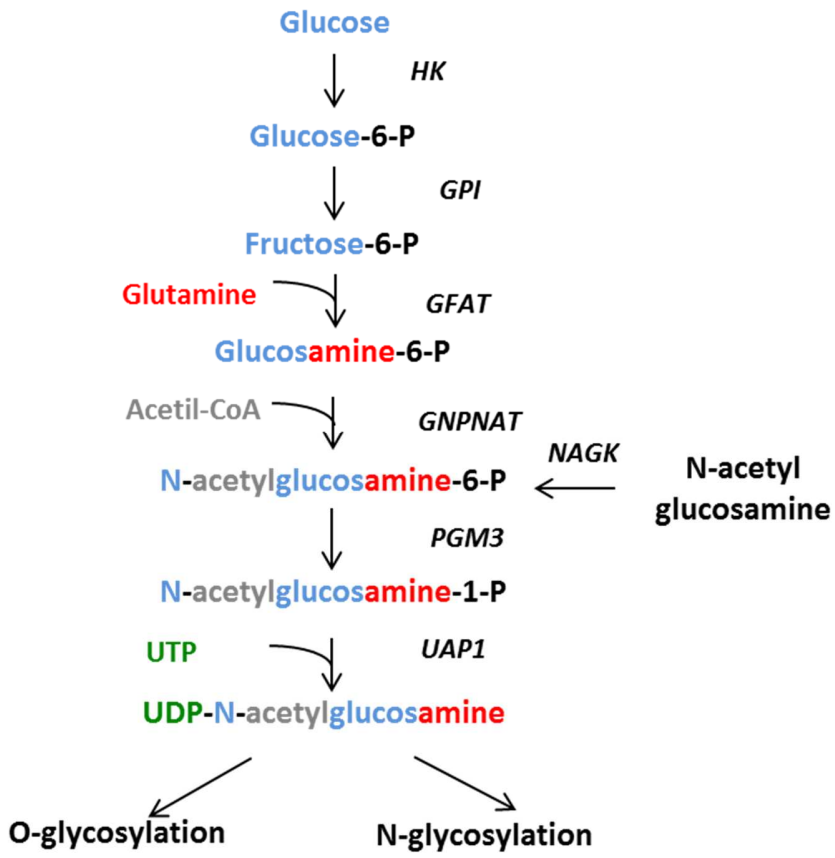

Figure 1: The biosynthetic pathway of UDP-GlcNAc in eukaryotes. All the reactions of HBP are showed with relative enzymes. **HK= H**exo**k**inase, **GPI= G**lucose-6-**p**hosphate **i**somerase , **GFAT1= G**lucosamine-**f**ructose **a**mido **t**ransferase **1**, **GPNAT1= G**lucosamine **N**-6-**P a**cetyl**t**ransferase **1**, **NAGK= N**-**a**cetyl **g**lucosamine **k**inase, **PGM3= P**hospho acetyl-**g**lucosamine **m**utase **3**, **UAP1= U**DP-GlcN**A**c **p**yrophosphorilase **1** .

Environmental GlcNAc recycling in the salvage pathway fuels canonical HBP. This is made possible through the action of the cytosolic enzyme N-acetylglucosamine Kinase (NAGK) that belongs to the sugar-

kinase/Hsp70/actin super family and shows homology sequence with hexokinase and glucokinase (Hinderlich et al., 2000). The enzyme is strictly specific for GlcNAc as phosphate acceptor derived from lysosomal degradation of oligosaccharide moieties or nutritional sources (Ligos et al., 2002). Upon sugar binding, a conformational change occurs and allows the binding of ATP, which is the phosphoryl group donor for the kinase. Catalytic cysteine residues, C131 and C143, seem to be directly involved in the transfer of the phosphate from ATP to the hydroxyl group at C6 of GlcNAc (Berger et al., 2002). Also Mg^{2+} is required for catalytic reaction and it may be replaced by other bivalent metal ions such as Mn^{2} and Co^{2+} with lesser degrees of effectiveness (Datta, 1970).

GlcNAc-6-P, NAGK product, may enter in *de novo* HBP and thus is used as substrate by PGM3. The presence of this branch suggests the relevant role of HBP in cell physiology.

Several papers report the importance of GlcNAc in a wide range of organisms, for synthesis of chitin (for the fungal wall), bacterial peptidoglycan and glycosaminoglycan in mammalian cells. In addition GlcNAc has a key role in cell signalling, for instance in fungi, after specific transport into the cells, the molecule can activate a cAMP-dependent or -independent cascade, leading to hypha morphogenesis or GlcNAc catabolic genes expression, respectively (Gunasekera et al., 2010). In bacteria, it can activate catabolic genes expression and can enhance the

biofilm formation, the adhesion and the internalization of *E.coli* by epithelial cells (Barnhart et al., 2006).

In mammalian cells, glycosylation regulates a huge number of proteins, affecting protein-protein interaction (Nf-kβ, STAT5a, CREB, YY1), transcription factor stability (p53, ER-α and β) and nucleo-cytoplasmic shuttling (NeuroD1, TORC2/CRTC2), transcriptional activity (c-Myc, FOXO1), regulation of DNA binding activity (PDX-1, C/EBP β) (Ozcan et al., 2010), cell to cell and cell to ECM interaction (Gu and Taniguchi, 2004), as well as the affinity between glucose transporter and substrates (Ahmed and Berridge, 1999).

A lot of surface proteins and growth factor receptors are targets for N-glycosylation, indeed surface localization and activity of important receptors (i.e. CTLA-4, GLUT4, EGFR, IGFR, HER2/ErbB2, FGFR), involved in cell differentiation and cell growth, are influenced by level of this post-translational modification (Lau et al., 2007).

N-linked glycosylation

N-glycosylation is a post-translational modification necessary for correct protein folding having a key role in protein maturation, protein stability and quality control. It plays a critical role for growth factor receptors and nutrient transporters, interaction between cells and cells with extracellular matrix (Goettig, 2016; Gwak et al., 2016; Lazniewska and Weiss, 2017). N-glycosylation is a well-conserved mechanism, however it

differs for some features between eukaryotes and prokaryotes. Indeed, Eukaryotic N-glycosylation occurs in endoplasmic reticulum (ER) while prokaryotic one at the plasma membrane. In addition, ranging from Archea to Eukaria, the heterogeneity of lipid-linked saccharides decreases: Archea exhibits higher heterogeneous glycan level, which decrease a little bit in Bacteria and then Eukarya shows a conserved lipid-linked oligosaccharide structure (Schwarz and Aebi, 2011).

Also prokaryotes have an oligosaccharyltransferase (OST)-like complex, which is the N-glycosyltransferase (NGT) whose main role is to transfer lipid-bound oligosaccharide to asparagine residue. NGT and OST have equal enzymatic activity although they share no homology sequence. In addition NGT is composed by a large number of the same subunit (due to duplication event) while OST is a complex of several proteins involved in different functions (i.e. maintaining protein in a glycosylation competent conformation, binding different proteins, having oxido-reductase activity, linking translocon etc.) (Chavan et al., 2005; Schulz et al., 2009).

In prokaryotes, in order to be glycosylated, N-X-S/T sequence need to adopt a specific conformation, as well as flexible region (secondary structure is not required), so glycosylation takes place after protein folding (Kowarik et al., 2006) while eukaryotic glycosylation occurs simultaneously to protein synthesis, reaching the correct protein folding (Schwarz and Aebi, 2011).

N-glycosylation mechanism can be divided into three principal steps:

- Synthesis of lipid-linked oligosaccharide (LLO) occurring at ER membrane towards cytosol
- LLO attachment to Asp residues of nascent protein target
- Flipping of glycosylated protein in the ER lumen

This type of modification requires a lipid intermediate, a dolichol phosphate (synthetized in cholesterol biosynthesis pathway) that is bound to UDP-GlcNAc (derived from HBP) producing GlcNAc-PP-Dol via N-acetylglucosaminephosphotransferase 1 (encoded by DPAGT1) activity. Thus, one molecule of GlcNAc and five mannoses are added, utilizing the nucleotide activated sugars, giving rise to $Man_5GlcNAc_2$-PP-Dol (this step is catalysed by DPAGT1 protein and two members of Asparagine–Linked Glycosylation family). Immediately, lipid-bound oligosaccharide is flipped on the ER membrane toward the lumen and then it is subjected to some other changes, indeed four mannose and three glucose are added obtaining $Glc_3Man_9GlcNAc_2$-PP-Dol (Aebi et al., 2010).

Upon formation of $Man_5GlcNAc_2$-PP-Dol, the carbohydrate portion is transferred covalently on the Asparagine (Asp) residue of nascent proteins by OST complex, which is associated to Sec61 translocon complex and ribosome near the ER membrane (Breitling and Aebi, 2013). Before the attachment, OST performs a protein scanning to evaluate if the Asp residue is surely inside to the consensus sequence (-N-X-T/S), necessary to have such modification. It is important to highlight that proline residue is not tolerable in the second position (Schwarz and Aebi, 2011). In this

context, dolichol phosphate acts as a carrier for carbohydrate **(Figure 2 upper panel)**.

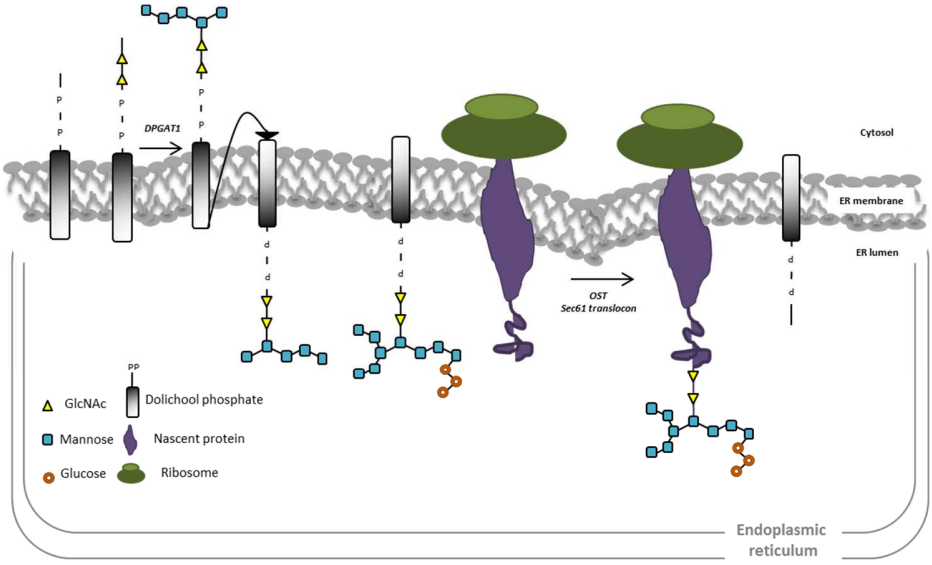

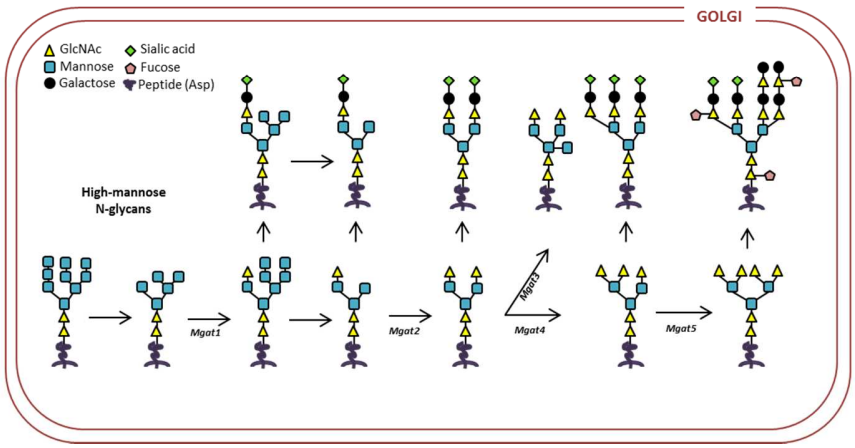

Figure 2: N-linked glycosylation mechanism. Schematic representation of the steps involved in the N-glycosylation process in endoplasmic reticulum **(upper panel)** and modifications of glycans in Golgi apparatus **(lower panel)**.

In order to obtain a functional protein, some residues have to be immediately removed. The outermost glucose (α 1-2) is removed as soon as possible by the enzyme glucosidase I (GI), followed by glucosidase II that removes the second glucose (α 1-3) molecule. Then, around the nascent protein, a chaperone complex is assembled that is composed by calnexin (a type I ER membrane lectin) and calreticulin (a soluble protein) (Ellgaard et al., 1999). The former interacts with the poly-peptide bound to monoglucosylated glycans, while the second one associates directly with glycans. This complex interacts with ERp75, a Protein Disulphide Isomerase (PDI) family member, which catalyses the formation of disulphide bonds leading to correct protein folding (Aebi et al., 2010). As following, protein is released from complex and its third glucose is removed by enzyme glucosidase II (GII), so that the folded protein can exit from ER.

Upon release, folded proteins can translocate in the final cellular compartment or can be transferred into Golgi organelle in order to be further modified **(Figure 2 lower panel)**.

In the Golgi, several N-acetylglucosaminyltransferases (Mgat) are found to add glucose, GlcNAc and galactose to elongate glycan antennae.

$Man_5GlcNAc_2$ glycan (or the high mannose structure) is firstly modified by Mgat1 that adding GlcNAc (using UDP-GlcNAc as donor), leads to the formation of N-glycan hybrid. The Mgat1 product loses α-mannose by α-mannosidase activity, producing the substrate for Mgat2. This enzyme adds GlcNAc to mono-antennary glycan leading to bi-antennary structure formation. They can be modified by Mgat3, which transfers a GlcNAc to the core to form a bisected N-glycan, or they can be the substrate of the Mgat4 and Mgat5 enzymes that increase the number of antennae (Dennis et al., 2009b). The relative affinity of the branching enzymes for UDP-GlcNAc decreases sequentially (k_m ranges from 0,04 mM to 10 mM) moving down the N-glycan branching pathway from Mgat1 to Mgat5. So the activity of the two first enzymes is limited by affinity for acceptors, while the activity of the other ones is limited by the amount of UDP-GlcNAc that reflects the availability of nutrients in the cells (Dennis et al., 2009b).

A lot of data show that hybrid mannose and bi-antennary glycans are associated to cell cycle arrest and cell apoptosis while tri- and tetra-antennary glycans to cell proliferation and cell survival. These associations are related to binding of glycan structure and specific galectins, whose affinities for N-glycans are proportional to GlcNAc branching. A cross-linked lattice is assembled on cell surface (Brewer et al., 2002), and it regulates cell surface residency and activity of receptors, of proteins involved in cell adhesion and of transporters (Dennis et al., 2009b).

Galectin family is made by members having both pro-/anti-apoptotic role. For instance mammalian infected cells expose N-glycans on cell surface and these are recognized and bound by galectin-8 that recruits nuclear dot protein 52KDa (NDP52) and microtubule-associated protein 1A/1B-light chain 3 (LC3) activating autophagy for the bacterium destruction in the autophagosomes (Thurston et al., 2012). Also galectin1 and 3 have pro-apoptotic role after binding with FAS in T and B cell, respectively. (Oka et al., 2005).

The Unfolded Protein Response (UPR) mechanism

In the case of misfolded proteins, the third glucose is re-bound to protein by UDP-glucose:glycoprotein glucosyltransferase (UGT1), a sensor of protein folding, leading to re-assembly of calreticulin-calnexin complex on the protein. If the uncorrect folding persists ER-associated degradation (ERAD) mechanism is activated. In particular, α1,2-linked mannose (the only one mannose that can be removed or reglucosylated) is removed from misfolded proteins by ER degradation enhancing α-mannosidase like proteins (EDEMs), major targets of ER-stress induced pathway (Olivari et al., 2005). In eukaryotes, before proteosomal degradation other mannose molecules are removed from $Man_8GlcNAc_2$ (Aebi et al., 2010).

Changes in N-glycosylation level as well as in redox state of Ca^{2+}, oxidizing environment (for disulphide bonds formation), cellular energy level (ATP)

are associated to UPR activation, a protective cellular strategy (Gaut and Hendershot, 1993) **(Figure 3)**.

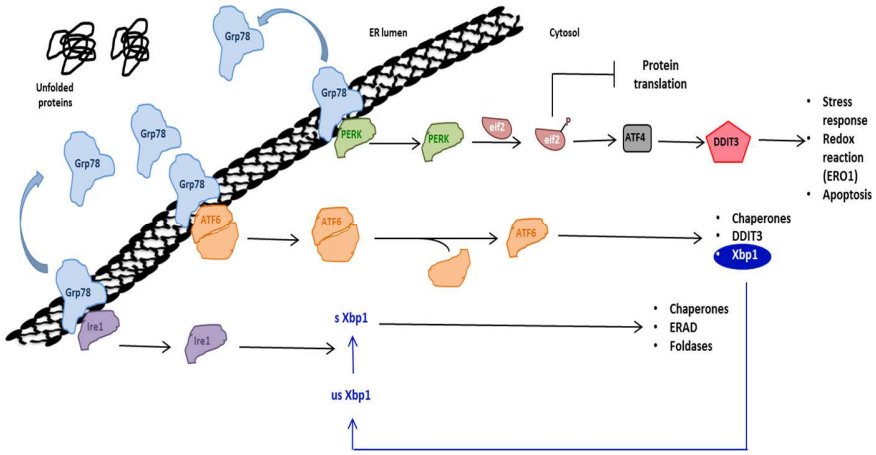

Figure 3: The Unfolded Protein Response mechanism. The three major stress sensors controlling UPR-dependent responses are shown: Pancreatic ER Kinase (PKR)-like ER Kinase (PERK), Activating Transcription Factor 6 (ATF6) and Inositol-Requiring Enzyme 1 (IRE1).

In resting cells UPR is not active, due to the binding of HSPA5/GRP78 (heat shock 70 kDa protein 5/78 kDa glucose-regulated protein) (ER chaperone) to the three ER transmembrane receptors namely protein kinase RNA-like endoplasmic reticulum kinase (PERK), activating transcription factor 6 (ATF6) and inositol-requiring enzyme 1 (IRE1). Upon unfolded proteins accumulation, for instance following a reduction of N-protein

glycosylation levels, GRP78 leaves them leading to UPR activation: type, intensity and duration of the stress define the specific activation of one or more UPR branches and the final effect of the UPR (DuRose et al., 2006). ATF6 is released from Grp78 for trafficking to the Golgi apparatus where it is cleaved by site 1 and site 2 proteases at the transmembrane site, yielding a cytosolic fragment known as ATF6 p50. It migrates to the nucleus activating transcription of target genes (encoding X-box-binding protein (Xbp1), ER chaperones).

Once released, Ire1 luminal domain activates itself by homo-dimerisation and trans-autophosphorylation and stimulating also its RNase activity. Removal of a 26 base intron from the mRNA Xbp1 occurs, and thus spliced form undergoes to nucleus where it recognizes and binds Unfolded Protein Response Element (UPRE) of target genes, leading to their expression (ER chaperones, ERAD, lipid synthesis).

After releasing from Grp78, Perk undergoes oligomerization and trans-autophophorylation and in turn phosphorylates Ser51 of eukaryotic initiation factor 2 (eif2α), inhibiting protein translation (and decreasing the load of nascent proteins arriving in ER), except for genes carrying internal ribosome entry sites (IRES) (i.e. activating transcription factor 4 (ATF4)), necessary to restore ER homeostasis. ATF4 improves cellular homeostasis and function by inducing amino acid biosynthesis and transport, promoting anti-oxidative stress responses, and stimulating the expression of autophagy genes. However if ER stress persists,

CCAAT/enhancer-binding protein homologous protein (CHOP), one of the main ATF4 target, is activated leading to cell death (Szegezdi et al., 2006).

O-linked glycosylation

O-glycosylation is a covalent binding of GlcNAc on Serine (Ser) or Threonine (Thr) residues of protein targets, in some case also on hydroxylysine (hLys) (i.e. collagens). Both eukaryotes and prokaryotes have several nuclear or cytoplasmic O-glycosylated proteins involved in a wide range of cellular functions.

Despite N-glycosylation, O-glycans are not further modified remaining a simple oligosaccharides (Spiro, 2002).

There are eight types of O-glycans in humans classified by the sugar residue that is attached to Ser/Thr or hLys (Spiro, 2002):

- O-linked GlcNAc is the binding of GlcNAc, which derives from activated nucleotide sugar, to target residue. The type of the binding can be α- or β-, the first is limited to eukaryotes while the second can be found also in prokaryotes. In addition GlcNAc- α -Ser/Thr is found to be associated to surface or secreted proteins (i.e. mucin), while the β- is typical of intracellular proteins.
- Gal- α -Ser/Thr occurs in the collagens.
- Man- α -Ser/Thr is synthetised in ER using a dolichol-linked monosaccharide as donor substrate. It is abundant in a-dstroglycan.

- Fuc- α -Ser/Thr is found on a wide range of proteins (urokinase, human coagulation factor VII, IX and XII). The related enzyme is localized into Golgi apparatus.
- Glc- α -Ser is limited to Ser residue that is in a consensus sequence, for example in the EGF domain the glucose is linked to Ser that is surrounded by two conserved cysteines.
- FucNAc- β -Ser/Thr attaches a trisaccharide containing a xylose and a pseudoaminic acid. This modification is found on proteins involved into pathological disease, after mammalian cell infection.
- Xyl- β -Ser is typical of first step of proteoglycan synthesis that can start in the Golgi apparatus in the case of rat liver or in the ER in chick chondrocytes.

O-glycosylation level depends on the activity of two enzymes, O-linked N-acetylglucosamine transferase (OGT) and N-acetyl-β-glucosaminidase (OGA) that adds and removes the glycan structure respectively (Slawson and Hart, 2011). OGT protein, encoded by X chromosome, consists of conserved catalytic domain (C-terminus), linker region, tetratricopeptide (TPR) and N-terminal domain. The alternative splicing produces three OGT variants with different cellular localization and number of TPR. The longest form, ncOGT is around 116KDa and is found in the nucleus and cytoplasm and contains 12 TPR. The mitochondrial OGT (mOGT), a 103KDa protein, is associated to inner membrane of mitochondria oriented toward intermembrane space (Love et al., 2003) due to a mitochondrial

targeting signal (MTS). sOGT, the shortest form (70KDa), shows only 3 TPR. All isoforms contain identical catalytic domains and the linker region **(Figure 4)** (Love and Hanover, 2005).

TPR domain has several functions. Indeed TPR modulates OGT trimerization, influencing its enzymatic activity, it is required for protein-protein interaction and mediates substrate specificity in a variety of peptide substrates (Kreppel and Hart, 1999). Furthermore, it has been shown that TPR is involved also in targeting OGT to mSin3A transcriptional complex leading to transcriptional repression of target genes (Yang et al., 2002). The mechanism with which TPR influences OGT is still unclear (Kreppel and Hart, 1999).

OGTs are also regulated by the availability of UDP-GlcNAc (substrate) that influences the affinity between the enzymes and the targets (high concentration of substrate increases the affinity) (Jínek et al., 2004). In addition, OGT is regulated by post-translational modifications, like auto-glycosylation in the catalytic and TPR domains as well as phosphorylation. For instance, phosphorylated OGT on Ser3 and Ser4 by Gsk3b shows higher enzymatic activity, while phosphorylation on Tyr444 by AMPK affects its ability to bind the substrates (Nagel and Ball, 2015).

The gene encoding OGA was initially identified as putative hyaluronidase expressed in human meningioma disease (MGEA5 or meningioma expressed antigen 5) (Comtesse et al., 2001). OGA protein is involved in the removing of O-glycans from proteins. It is composed of two domains,

the N- and C-terminal. The first one contains an N-acetyl- β -D-glucosaminidase domain and it has the ability to cleave the binding between glycans and protein target (Heckel et al., 1998), while the second one shares similarity with a Histone Acetyltransferase domain. Indeed OGA is able to acetylate protein target when is in a complex with accessory proteins (Toleman et al., 2004). This domain is present only in the longest form of the enzyme and not in the shortest one, in addition the former is localized in the cytoplasm and in the nucleus while the shortest is found only in the nucleus **(Figure 4)** (Comtesse et al., 2001).

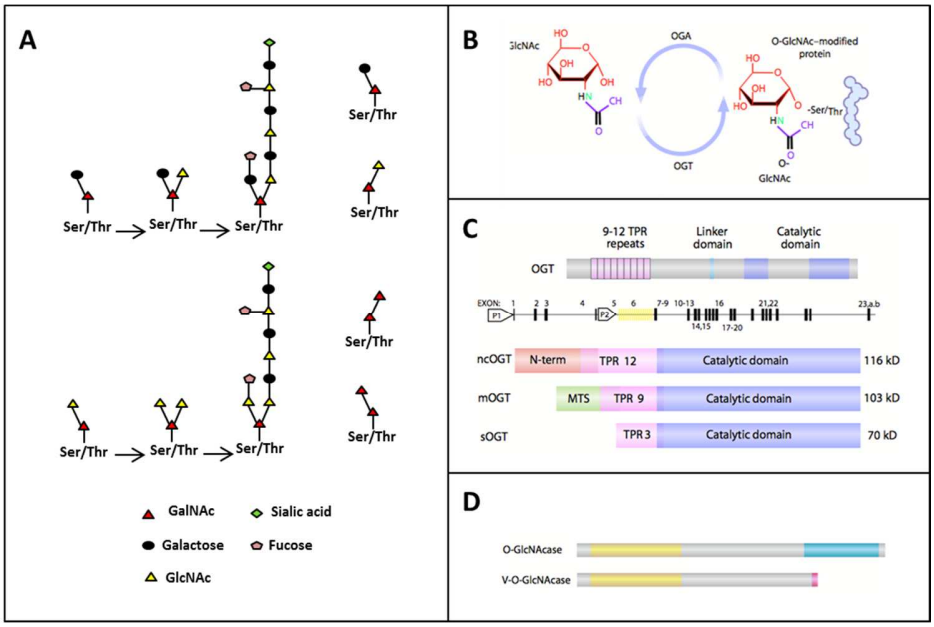

Figure 4: O-linked glycosylation. Schematic representation of **A.** the O-linked glycans. **B.** Addition and removal of O-GlcNAc is mediated by OGT and OGA, respectively. Domain structure of the **C.** OGT and **D.** OGA isoforms. (readaptation 0f Dona C. Love and John A. Hanover, 2005).

Also OGA is regulated by phosphorylation but how the activity is influenced by this modification is unknown (Khidekel et al., 2007). Moreover, it has been shown that during the apoptotic process OGA is cleaved by Caspase-3. This cleavage leads to recombination of the enzymatic sub-units without effect on its activity and leads to an increased specificity and affinity toward its targets (Butkinaree et al., 2008; Wells et al., 2002). Furthermore, OGA activity is regulated by interaction with other proteins, for example is found in complex with Histone Deacetylase1 (HDAC1) (Whisenhunt et al., 2006) and with Aurora B (Slawson et al., 2008).

It is well reported a dynamic interplay between O-glycosylation and phosphorylation on the same or adjacent amino acidic residues, influencing either the activity or the stability of the target proteins. For instance, O-glycosylated Myc is stabilized while phosphorylated Myc undergoes to degradation (Slawson and Hart, 2011). O-glycosylated carboxy terminal domain (CTD) of RNA pol II undergoes to conformational change that affects the specificity of the interaction with transcript elongation complex, while CTD phosphorylation is associated to gene transcription (Dahmus, 1996). In addition, these two post-translational modifications regulate also protein translation, targeting eif2α indirectly.

Indeed after glycosylation, p67 protein associates to eiF2α preventing its binding with kinase. As consequence, not-phosphorylated eiF2α permits protein translation. On the contrary, for example in serum starvation condition, un-glycosylated p67 does not interact with eiF2α that can be phosphorylated leading to inhibition of protein translation (Datta et al., 1989).

Glycosylation in disease

As anticipated in section about HBP, glycosylation influences stability, activity and also expression of several proteins involved in a wide range of functions. It is well reported the association between de-regulation of O-/N-linked GlcNAc level and various human diseases, including cardiovascular disease, neurodegenerative disorders, diabetes mellitus, and cancer. For instance, transgenic mice overexpressing GFPT in liver displayed obesity, enhanced glycogen storage, impaired glucose tolerance and insulin resistance (Veerababu et al., 2000).

Altered O-glycosylation level

As reviewed by Yann Fardini et al., O-glycosylated proteins can be grouped according to their function. In particular they can be grouped in proteins involved in regulation of transcription and translation (≈26%), proteins involved in cellular structure (≈14%), in metabolism (≈13%), in response

of cellular stress condition (≈11%), in protein processing (≈7%), in signalling (≈8%) and cell cycle progression (≈2%).
Recently, it is reported that O-glycosylation moiety on Thr58 prevents phosphorylation on same residue (mediated by GSK3b), leading to further stabilization of MYC protein, the main leading cause of cancer development (i.e. lymphomas) (Fardini et al., 2013; Oren and Rotter, 2010).

O-glycosylation on Ser733 prevents Ikkβ inhibition and leads to its stabilization, so that Nfkβ remained in activated state increasing glycolysis (Perkins, 2012), in addition the glycosylation on Nfkβ Thr322 and Thr352 residues is involved in cell anchorage in pancreatic cancer cells (Dajee et al., 2003). In some case, not direct O-glycosylation but interaction with OGT stabilizes protein preventing its degradation, as for FOXM1 (Caldwell et al., 2010) and β-catenin leading to bone metastasis and cell cycle progression(Olivier-Van Stichelen et al., 2012), respectively. Furthermore, in ER stress condition, O-glycosylation of three eif2α residues (Ser219, Thr239 and Thr241) hinders Ser51 preventing its phosphorylation, so that translation is not blocked and cancer cells survive (Jang et al., 2015). Also E-cadherin and its interaction with p120 and β-catenin are affected by O-glycosylation, stabilizing also transcriptional repressor Snail1. E-cadherin down-regulation supports cell detachment from matrix and release in bloodstream leading to metastasis (Zhu et al., 2012). In 2011 it is reported that OGT inhibition using shRNA down-regulates matrix

metalloproteinases (MMP) expression level affecting epithelial-mesenchymal transition (EMT), as well as invasion and metastasis (Gialeli et al., 2011).

Hyper-O-GlcNAcylation contributes to stress resistance, it negatively regulates phosphofructose kinase 1 (PFK1) in cancer cells, decreasing rate of glycolysis flux and increasing pentose phosphate pathway flux: this leads to high production of NAPDH, which is important for maintaining glutathione pool (Yi et al., 2012).

In order to pass from one phase to each other in the cell cycle, cyclins need to be expressed. For instance in *Xenopous Levis*, cyclin D1 and B1, involved in the regulation of the G1 and M phase respectively, decrease their expression in association to OGT inhibition (Slawson et al., 2005). Since O-glycosylation controls DNA replication through histone modification, its de-regulation leads to un-controlled proliferation and accumulation of DNA mutations, hallmarks of cancer (Fardini et al., 2013). According to the presence of OGT isoform in mitochondria, a lot of proteins localized in this organelle are O-glycosylated. Among these, we can find pyruvate dehydrogenase E1α (PDH E1α), NADH dehydrogenase [ubiquinone] iron-sulfur protein 3 (NDUFS3) (Burnham-Marusich and Berninsone, 2012), NADH dehydrogenase [ubiquinone] 1α complex (NDUFA5), mitochondrial membrane protein Metaxin-1 (MTX1), the β-oxidation protein ACADM, succinyl-CoA ligase GDP forming β (SUCLG2), aconitase (ACO2).

Furthermore, it has been shown the OGT/OGA overexpression leads to abnormal mitochondria, lack of cristae, error during fusion and fission mechanism, reduction of oxygen consumption rate, suggesting a key role of O-glycosylation for mitochondrial function and homeostasis (Tan et al., 2014).

O-glycosylation changes may impact also on cellular metabolism. In order to support proliferation and survival in unfavourable conditions, cancer cells undergo to metabolic reprogramming, which consists in an increase of aerobic glycolysis (Warburg effect), of pentose phosphate pathway (for nucleotide synthesis and NADPH production) and of HBP. At the same time, increase of HBP flux itself regulate cancer metabolism in a feedback manner. For example O-glycosylation of carbohydrate-responsive element binding protein (ChREBP) stabilizes the protein leading to inhibition of mitochondrial respiration and to stimulation of glycolysis, de novo lipogenesis and nucleotide biosynthesis (Tong et al., 2009). Another example derives from O-glycosylation of Sp1 transcription factor that activates a cholesterolgenic program (Penque et al., 2013), or of HIF1α that increases glycolytic rate (DeBerardinis et al., 2008). All these data are also supported by evidences revealing an increase of O-glycosylation level, due to down-regulation of OGA mRNA, in the breast cancer making cancer cells resistant to tamoxifen treatment (Hurvitz and Pietras, 2008), or to over-expression of OGT in colorectal cancer rather than adjacent normal tissues (Mi et al., 2011), in liver epatocarcinoma (Zhu et al., 2012) and in

bladder cancer (Rozanski et al., 2012).

Altered N-linked glycosylation

In recent years, the attention has been focused also on N-glycosylation and its involvement in metabolites uptake, responsiveness to growth factors, EMT, invasion, migration and tumor metastasis formation. Indeed, it has been shown that human leukemic cells have increased bi-antennary glycans on Glut-1 protein, enhancing transporter affinity for glucose (Ahmed and Berridge, 1999), or surface retention of Glut-2 and -4 depends on binding between their N-glycans and galectin (Lau et al., 2007).

Colorectal cancers, with higher level of N-glycosylation, show great ability of invasion, migration, anchorage-dependent colony formation and ability to resistant to radiotherapy (de-Freitas-Junior et al., 2012). Furthermore, Androgen Receptor (AR)-positive prostate cancer cell lines, expressing high level of GFPT1 and UAP1 enzymes as well as high level of N-glycosylation, show strong stabilization and membrane localization of insulin growth factor receptor 1 (IGFR-1) (Itkonen and Mills, 2013). EGFR has 12 sites that are reported to be N-glycosylated, a de-regulation of tri- and tetra-antennary glycans induces a cytoskeleton remodelling that makes MDA-MB-231 breast cancer cell line able to invade surrounding environment (Guo et al., 2007). In addition, increase of complex N-glycans levels, due to Mgat5 over expression, leads to lattice structure formation around EGFR precluding its binding to Caveolin-1, promoting receptor

interaction with the actin cytoskeleton (Lajoie et al., 2007).

Other proteins involved in EMT are reported to have one or more N-glycosylated sites. MGAT5 overexpression increases N-glycan branching on both E- and N-cadherin, which are epithelial and mesenchymal markers, respectively. High expression of glycans impairs E-cadherin localization and activity (Zhou et al., 2008) and promotes the binding between N-cadherin and galectin-3 (Boscher et al., 2012); this enhances EMT and cancer migration.

Lack of complex N-glycan on fibronectin receptor affects its dimerization and its localization leading to a decrease of migration ability (Isaji et al., 2006).

Complex N-glycans have key role in Wnt and Notch signalling, influencing ligand-receptor binding, lipid processing and β-catenin signal transduction in the first case (Komekado et al., 2007), cell proliferation, survival and differentiation in the second one (Kopan and Ilagan, 2009; Miele et al., 2006).

Also genetic background influences the expression of enzymes involved in N-linked glycosylation. For example oncogenic RAS proteins induce both Mgat4 and 5 gene expression leading to an increase of tri- and tetra-antennary glycans on surface receptors. Upon these modifications, receptors are well recognized and bound by galectin-3, that participate to

a reduction of their membrane turnover and hence to a prolonged signalling activation (Buckhaults et al., 1997; Stanley, 2007). ATP synthase subunits (i.e a subunit of ATP synthase (F_1F_0 complex) and subunit d) are reported to be N-glycosylated (Burnham-Marusich and Berninsone, 2012).

In recent years, it has been demonstrated the correlation of HBP and autoimmune diseases, a complex immunological alterations characterized by T cell proliferation, CTLA-4 endocytosis, T_H1 differentiation. The nutrient environment and metabolite supply regulate T-cell function and autoimmunity through GlcNAc branching that influences the binding to galectins at the cell surface of immune cells. Supplementation of HBP with GlcNAc, increasing complex N-glycans, regulates autoimmunity by modulating several T cell function. Authors compared GlcNAc versus GlcN effect on immune system. The latter is less powerful because, once phosphorylated, GlcN-6-P acts as HBP negative regulator, inhibiting GFAT1 (Grigorian et al., 2007).

Conversely, in the perspective of immune therapy, GlcNAc seems to be an interesting agent for restoring normal HBP flux. In 2000, 12 children with immunological diseases were oral administered with GlcNAc for around two years, and after the treatment they had a significant clinical improvement without significant side effects (Salvatore et al., 2000). In addition many evidences show the effectiveness of GlcNAc treatment in

mice affected by autoimmune diabetes (Grigorian et al., 2007) (Ryczko et al., 2016).

Commercial available HBP inhibitors

In the last decades, some modulators have been synthetized to restore normal level of glycosylation for cancer therapy, reducing the capacity of tumour cells to proliferate and metastasize. The commercial available inhibitors can be classified in two groups according to type of their target: the first group is composed by inhibitors of enzymes catalysing the early reaction of HBP and the second one is composed by inhibitors whose targets are enzymes directly involved in transferring of GlcNAc.
Here some commercial available inhibitors are briefly described.
6-Diazo-5-oxo-L-norleucine (DON) and *Azaserine (Aza)* belong to the first group indeed they are used as inhibitors of the HBP rate-limiting enzyme GFAT: both are reported to reduce O-GlcNAc under high glucose conditions. However, due to their chemical structure, which is similar to that of glutamine, is known that both may interfere with nucleotide and protein synthetic pathways, where glutamine acts as an important substrate. Therefore they lack of specificity, as they also inhibit other glutamine-utilising enzymes such as the amidotransferases and glutamine synthetase. In addition although they have anti-cancer activity, as shown

in different animal models, they are excluded from clinical trial due to their toxicity (Palorini et al., 2013b)

Tunicamycin (*Tun*) is a mixture of homologous nucleoside antibiotics and it has been originally synthetized as an inhibitor of bacterial and eukaryote N-acetylglucosamine transferases. It blocks the formation of protein N-glycosidic linkages by preventing the transfer of GlcNAc-1-P to dolichol monophosphate (Chatterjee et al., 1981). *Tun* resulted to be a therapeutic agent for multidrug-resistant human ovarian cystadenocarcinoma cells, in combination with *doxorubicin*, *epidoxorubicin* and *vincristine* (Donavon, 2007). In addition, it enhances *erlotinib*-induced cell growth inhibition in non-small cell lung cancer cells (Contessa, 2010)**.**

Other antibiotics as *amphomycin* (Kang et al., 1978) *tridecaptin*, *diumicyn*, *flavomicyn* and *tsushimycin* show the same action mechanism of *Tun* (Elbein, 1984).

Castanopermine, for instance, inhibiting GI prevents the formation of complex chains leading to glycoproteins containing mostly Glc3Man79GlcNAc2 structures (Saul et al., 1983); *swainsonine* that inhibits α-mannosidase II, blocks the formation of complex-type N-glycans (Elbein, 1984). In particular, *swainsonine* may be considered an interesting anticancer agent because it is able to inhibit tumor growth and metastasis, augmenting natural killer and stimulating bone marrow cell proliferation (Olden et al., 1991).

Since it was originally described as an inhibitor of mucin glycosylation in the Golgi, *benzyl-2-acetamido-2-deoxy-α-D-galactopyranoside* (*BAG*) prevents the O-GlcNAc modification. Several evidences report its low specificity (Fülöp et al., 2007). *Alloxan* interferes with the process of protein O-glycosylation by blocking OGT (Konrad et al., 2002), although its uptake is fast in pancreatic β cells it results to be very unstable.

In addition, given its role in cancer, poly-LacNAc inhibitors have been synthetized in order to inhibit or the binding with galectins or to block enzyme involved in LacNAc biosynthesis (Vasconcelos-Dos-Santos et al., 2015)

Summarizing, it is possible to distinguish molecules that inhibit enzymes involved in the canonical HBP from that ones that inhibit enzymes involved in one of the two branches of HBP. Since the first ones are low specific and the second ones are able to modulate just one branch of the HBP, the need to synthetize new specific modulators of HBP rises.

In order to inhibit both kinds of aforementioned post-translational modifications, we decide to focus the attention on upstream reactions of O-/N-linked glycosylation. Obviously it is important to consider the role of salvage pathway since through this pathway, HBP can be refuelled especially in nutrient depleted conditions. All these information lead us to select Phosphoacetyl glucosamine mutase 3 as good candidate. Indeed, its reaction is upstream of both glycosylation modifications, it occurs in *de*

novo HBP, it is downstream of NAGK catalysed reaction, and in addition, until now, no PGM3 inhibitors until now have been synthesized.
The purpose of my PhD project was the synthesis and the characterization of different compounds able to act as competitive inhibitors for PGM3, enzyme involved in the inter-conversion of GlcNAc-6-P and GlcNAc-1-P in HBP (for more information see following section).

Phospho acetyl-glucosamine mutase 3 (PGM3)

The human phosphoglucomutases (PGM), the phosphomannomutase (PMM) and N-acetyl-glucosamine phosphate mutase (AGM) belong to hexose phosphate mutase family. Although they show partially overlapping specificities for substrate, they have distinct role: PGM is involved in interconversion of Glc-1-P and Glc-6-P (essential for the synthesis of glycogen and carbohydrate chains), PMM into catalysis of mannose-1-P producing mannose-6-P and AGM produce GlcNAc-1-P from GlcNAc-6-P. In addition, AGM interconverts Glc-1-P and Glc-6-P, while PGM does not recognize AGM substrate. Due to its double specificity and according to H. Pang et al. (Pang et al., 2002), it is possible to consider human PGM3 as AGM1. For this reason, by now, we will refer to AGM1 as PGM3.
PGM3 gene, made by 13 exons, is located on human chromosome 6 (6q14.1) (Li et al., 2000) and encodes a protein with a predicted molecular

weight of about 60 kDa. Alternatively spliced transcript variants encoding multiple isoforms have been observed for this gene. This variant 1 (NM_001199917.1 → NP_001186846.1) represents the longest transcript and encodes the longest isoform (570 aa). The variant 2 (NM_015599.2 → NP_056414.1) differs in the 5' UTR, lacks a portion of the 5' coding region, and initiates translation at an alternative start codon, compared to variant 1. The encoded isoform 2 has a distinct N-terminus and is shorter (542 aa) than isoform 1. The variant 3 (NM_001199918.1 → NP_001186847.1) differs in the 5' UTR and has multiple coding region differences, compared to variant 1. These differences cause translation initiation at a downstream AUG and result in a shorter isoform 3 (441) with distinct N- and C-termini, compared to isoform 1. The variant 4 (NM_001199919.1 → NP_001186848.1) differs in the 5' and 3' UTRs and has multiple coding region differences, compared to variant 1. These differences cause translation initiation at a downstream AUG and result in a shorter isoform 4 (566 aa) with distinct N- and C-termini, compared to isoform 1 (https://www.ncbi.nlm.nih.gov/).

In the late sixties, Hopkins and Harris discovered PGM3 through genetic studies of human polymorphism (Hopkinson and Harris, 1968) and in 2000 human AGM1/PGM3 was cloned for the first time by complementation of yeast null mutant (Mio et al., 2000).

PGM3 is phylogenitically conserved and, until now, all information about it has been generated from the crystal structure of *Candida Albicans*

enzyme (Nishitani et al., 2006). PGM3 is a heart shape enzyme due to the arrangement of four domains; domain 1, 2 and 3 show the same fold (four b strands located between two a helices), while the fourth one, which contains two antiparallel b-sheets, is different.

The active site is composed by four loops, one from each domain **(Figure 5)**:

- The active serine loop (Thr-64 to Glu-71 in domain 1) contains Ser66, which has a key role during the catalysis.
- The metal-binding loop (Asp-290 to Arh-295 in domain 2) can bind Mg^{2+} (only in presence of substrate or product) enhancing PGM3 enzymatic catalysis, or Zn^{2+} inhibiting PGM3 enzymatic catalysis.
- The sugar-binding loop (Glu-387 to His-391 in domain 3) binds the hydroxyl groups of the substrate. Glu387 is hydrogen-bonded to the O-3 and O-4 atoms of the sugar ring both in substrate and product complexes. While a water molecule is bound to the O-4 atom in the substrate complex, the Asn389 interacts, through an hydrogen binding, with the O-3 atom only in the product complex.
- The phosphate-binding loop (Arg-512 to Ala-519 in domain 4) interacts with the phosphoryl group of the substrate, on the opposite side of the active serine loop.

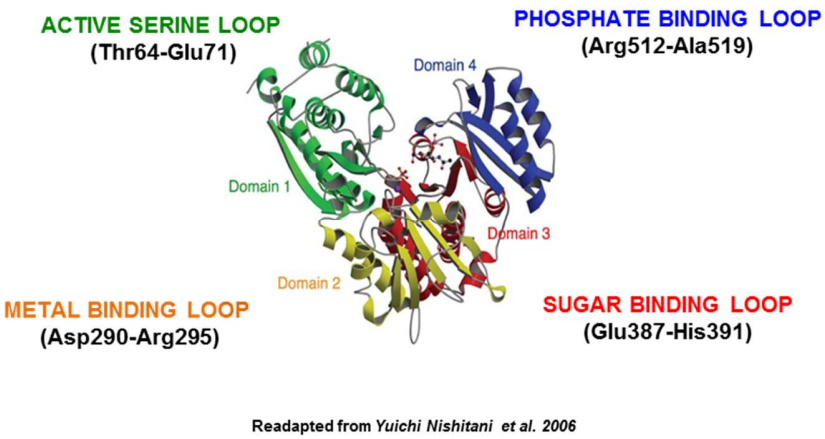

Figure 5: Structure of Phosphoacetyl glucosamine mutase of C. Albicans. Catalytic pocket of PGM3 enzyme is made by loops of four domains arranged in heart shape. Domain 1 contains the active serine loop, the second the loop for metal ion binding, the third the loop for sugar binding and the fourth the loop for phosphate binding.
Readapted from Yuichi Nishitani et al. 2006.

The substrate specificity is due to its N-acetyl group, whose carbonyl oxygen is hydrogen bounded to the N-atom of Lys371 through a water molecule. The distance between N-acetyl group and Val370 side chain (3.24 Å) is indispensible for enzyme-substrate recognition, which does not occur if distance is different. Many Authors reported key role of some amino acidic residues localized in the PGM3 domains and their mutation as leading cause of immunological diseases. Sassi A. et al. identified, in four consanguineous families with recurrent infection, different PGM3 mutations: 1) p.Leu83Ser in the N-terminal catalytic domain, 2)

p.Glu340Del in the central sugar binding and 3) p.Asp502Tyr in the phosphate-binding domain. The decrease in protein expression and the dysfunction of PGM3, suggest the important role of Glu340 residue in sugar binding domain (Sassi et al., 2014).

Pedersen et al., discovered that homozygous c.737A-G mutation , a nucleotide transition resulting in Asn246-to-ser substitution, c.737dupA mutation, a nucleotide frame shift resulting in a premature termination in the active site, and c.1352A-G mutation, a transition resulting in a Gln451-to-Arg substitution in the sugar binding domain lead to skeletal dysplasia resembling that on of Desbuquois (osteochondrodysplasia). Moreover, subject with heterozygous c.715G-C mutation (Asp239-to-His) a nucleotide transversion in the active site died from infection in infancy (Stray-Pedersen et al., 2014).

The catalytic mechanism is so called *ping-pong*, because a transfer of phosphoryl group happens from enzyme to substrate and *viceversa*. At the beginning of the reaction, the enzyme needs to be phosphorylated on Ser66, then the enzyme binds the substrate converting it into a bis-phosphorylated intermediate. Then, it rotates of 180° arranging the C-6 phosphoryl group near Ser66 and the metal ion. In this way, this group dissociates from C-6 and binds Ser66. At the end of the catalysis, GlcNAc is phosphorylated on C-1 and enzyme on Ser66 **(Figure 6)**.

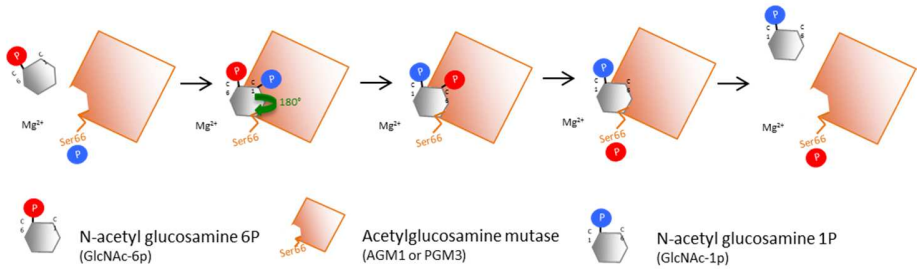

Figure 6: Schematic drawing of the proposed catalytic mechanism for the conversion of GlcNAc-6-P to GlcNAc-1-P by PGM3. Phosphoryl groups are indicated by *P* in a *shaded circle*. The phosphoryl group near Ser-66 first binds the substrate. The substrate is then converted into a bis-phosphorylated intermediate. Then, this intermediate rotates of 180°. Consequently, the phosphoryl group at C-6 changes positions with another phosphoryl group at C-1. Finally, the phosphoryl group near the metal ion dissociates from the intermediate and binds the Ser-66.

PGM3 expression is tissue specific according to different levels of production of glycosylated proteins. With the exception of lung, PGM3 is found to be expressed in many adult tissues, indeed the expression is elevated in the pancreas, heart, liver, placenta and is very low in skeletal muscle, brain and kidney (Li et al., 2000).

Little is known about up- or down-regulation of PGM3 enzyme and its association to cancer. According to Protein Atlas website (http://www.proteinatlas.org/) most cancer tissues display higher expression of PGM3 enzyme as compared to normal ones, that show very weak expression or no expression. For instance, in breast cancer PGM3 protein expression increases in lobular and duct trait; PGM3 level is higher

in cervix and endometrium adenocarcinoma and in low and high-grade prostatic adenocarcinoma. In this regard, a transcriptional analysis performed in prostate cancer upon androgens treatment, has identified a specific up-regulation of several enzymes involved in HBP (and also in O-/N-glycosylation mechanism) among which PGM3 protein (Munkley et al., 2017). In addition, as it is listed in Gene Expression Omnibus (GEO) website, PGM3 gene expression is modulated (up- or down-regulated) in different conditions. In particular PGM3 gene expression is up-regulated in human breast cancer brain metastases (positive to epidermal growth factor receptor 2), compared to non-metastatic ones (GEO Profile: GDS5306 / 210041_3p_s_at) suggesting a role of PGM3 during migration of cancer cells. PGM3 mRNA has been found down-regulated in time dependent manner upon treatment with insulin growth factor 1 (IGF1) (GEO GDS4063 / 221788_at) and in lung epithelial cancer cell line A549, glucose depletion increases PGM3 expression probably as consequence of adaptation to metabolic stress conditions (GEO Profile GDS5418 / 210041_s_at).

Many evidences highlighted the role of PGM3 in diseases associated to immune system. Defects in the synthesis of carbohydrate structures (glycans) and in the attachment of glycans result in Congenital Disorders of Glycosylation (CDG). It can be caused by mutations in the genes encoding proteins involved in the synthesis of sugar nucleotides or involved in different steps of the glycosylation processes. In addition, CDG

matches with primary immune-deficiencies (PID) when glycosylation defects lead to the alteration in immune system affecting IgE glycosylation pattern.

Several reports have shown the correlation between PGM3 mutations and PIDs, which are rare inherited diseases characterized by defects in immune system that may lead to an increased viral infection susceptibility (Wu et al., 2016). Recently, patients with mutated PGM3 (homozygous mutations), have marked high level of IgE associated to recurrent infections and atopic diseases (eczema, allergy, and asthma) (Yang et al., 2014). These clinical phenotypes are due to a significant low UDP-GlcNAc global level leading to a significant change of N-glycan profile.

Aim of Research

During my research activities, I attended to an experimental project in collaboration with the group of Prof. La Ferla, department of Biotechnology and Biosciences of Milano-Bicocca.

Aim of my PhD research project was to synthetize and evaluate the effect of a novel class of HBP inhibitors, on cancer cell proliferation and survival. Indeed, a lot of evidences suggest the key role of HBP in a wide range of cell functions and its involvement in several diseases among which cancer. Since the major part of the commercial available HBP inhibitors show low specificity and are able to inhibit enzymes involved only in one of the two glycosylation branches, during my PhD project we decided to focus our attention on the PGM3, one enzyme of the HBP. This enzyme has been chosen for different reasons: 1) it is higher expressed in several tumors as compared to normal tissue (http://www.proteinatlas.org/); 2) it is downstream the savage pathway, controlling also the fuelling of HBP by the lysosomial degradation of cellular glycoconjugates; 3) its modulation permit to control both N- and O-glycosylation; 4) no inhibitors for this protein are available.

Material and Methods

Cell culture

Human breast cancer MDA-MB-231 were routinely cultured in Dulbecco's modified Eagle's (DMEM) medium containing 25mM glucose, supplemented with 4mM L-glutamine, 100 U/mL penicillin, 100 mg/mL streptomycin (complete medium) and 5% fetal bovine serum.

The other breast cancer cell lines (SKBR-3, BT-474, Mcf7, T-47D, MDA-MB-361) were culture in the same medium, with exception for serum that was 10%.

Normal lung fibroblasts Wi38 were cultured in EMEM medium containing 25mM glucose and supplemented with 2mM L-glutamine, not essential amino acids, 1mM Sodium Pyruvate, 100 U/mL penicillin, 100 mg/mL streptomycin and 10% fetal bovine serum (complete medium).

Pancreatic ductal adenocarcinoma cancer (PDAC) cell lines (Mia Paca-2, Capan-1, BxPC-3) were cultured in different media. Mia Paca-2 cells were culture in DMEM medium supplemented with 10% North American fetal bovine serum, while Capan-1 and BxPc-3 in RPMI1640 medium supplemented with 20% of South American fetal bovine serum and 10% North American fetal bovine serum, respectively. All PDACs were cultured in 11.1mM glucose, 2mM L-glutamine, 100 U/mL penicillin and 100 mg/mL streptomycin (complete medium). All reagents for media were purchased from Life Technologies.

Cell treatment and reagents

Where not differently specified, for experiments cells were seeded in complete growth medium and after 24 hours washed twice with Phosphate Buffer Saline (PBS) and incubated in complete medium with or without the inhibitors.

All chemicals and inhibitors were purchased from Sigma-Aldrich, except for Erk inhibitor SCH772984 (Selleckchem) and ERO1 inhibitor EN460 (Calbiochem, Merck Millipore).

To measure cell proliferation, harvested cells were counted using the Burker chamber. Where indicated, cell viable count was performed using Trypan Blue Stain 0,4% (Life Technologies).

Computational analysis

All molecular docking calculations were performed using the PGM3 crystal structure of Candida Albicans (Protein Data bank [PDB], 2dkc) co-crystallized with the natural substrate (GlcNAc-6-P).

The docking scores were detected with the software Schrodinger 10.1 Maestro and the docking calculations were performed using Glide docking (Friesner et al., 2004) (Jorgensen et al., 1988).

The analysis of interaction between the new molecules and PGM3 protein were performed at cellular pH (7.00 ±0,3). In order to obtain the lowest conformational energy, the structures of the protein and the ligand

(substrate or new molecules) were minimized within the Protein Preparation Wizard, by applying a force field OPLS_2005 (addition of hydrogens atoms, assignment of atomic charges and bond orders, elimination of water molecules that are not involved in ligand binding).
Thus, to define the space of interaction ligand-protein with specific aminoacidic residues, the grid (15-18 Å) was generated around the binding site of the ligand. This grid identifies the pose of new molecules in the active site. All ligands were docked with extra precision (XP) method and ligand sampling flexible.

Cell Tox assay

Cytotoxicity was measured using CellTox Green Cytotoxicity assay (Promega) according to the manufacturer's protocol. Briefly, $1*10^4$ cells (breast and pancreatic cancer cells) were seeded into 100 µL of medium in 96 flat bottom multiwell. After 24h the cells were incubated with different concentrations of specific compound mixed with the CellTox Green dye in medium without phenol red. The emitted fluorescence was measured at different time points using an excitation wavelength of 512 nm and emission of 532 with Digi Read software using Cary Eclipse spectrofluorimeter (Varian).

Colony formation assay

After specific treatment, the cells were collected and then re-seeded at low density in complete medium. After 14 days, cells were washed twice with PBS, fixed in PBS-formaldehyde 5%, and stained with 0.1% crystal violet for 5 minutes. After colorant dissolving by acetic acid 10% the absorbance was analyzed at spectrophotometer.

Chemical synthesis

All reagents used for synthesis of FR051 and other tested compounds were purchased from Sigma Aldrich. For details about synthesis process refer to Results section.

The NMR spectra of the compounds were recorded at 25 °C on a Bruker Avance III-400 MHz using a 5-mm QCI cryoprobe.

Flow cytometric analysis

All flow cytometric analysis were performed using a FACScan flow cytometer (Becton-Dickinson, Franklin Lakes, NJ, USA) with CellQuest software (Becton-Dickinson).

Propidium Iodide (PI)/Annexin V-FITC staining was performed using Apoptosis assay kit from Immunological Sciences (Rome, Italy). In particular, $10x10^5$ cells were collected in 50 µL of binding buffer and

stained with 1 µL of Annexin V-FITC and 1 µL of PI, for 15 minutes at room temperature. After the incubation, samples were diluted in an appropriate volume of binding buffer and analyzed.

ROS levels were measured by staining cells with 5µM dichloro-dihydro-fluoresceine-diacetate (H_2-DCFDA, Life Technologies) for 30 minutes at 37°C. After staining, the cells were trypsinized, collected in PBS plus serum and analyzed.

To determinate cell surface expression of N-linked glycoproteins, cells were stained with Concanavalin A, Alexa Fluor 594 conjugate lectin, or Phaseulus Vulgaris, Alexa Fluor 488 conjugate lectin for 1 hour at 4ºC and then analyzed.

RNA extraction and semiquantitative RT-PCR analysis

RNA was extracted from cultured cells using Trizol reagent (Life Technologies). Total RNA was reverse-transcribed with oligo dT by using the QuantiTect Reverse Transcription Kit, Qiagen, according to the manufacturer' s protocol. 0.2 µ g of the product of reverse transcription was amplified by qPCR with an Applied Biosystem 7500 standard system (Thermo Fisher Scientific) using POWER SYBR GREEN PCR mix for qPCR (Life Technologies). Primers were designed using Primer3Plus software (http://www.bioinformatics.nl/cgi-bin/primer3plus/primer3plus.cgi) and used at 0.25µ M. The relative level of expression was calculated by the

2−ΔΔCT method β -actin was used as endogenous control. Primers are listed in the table below:

	Forward	Reverse
GFPT1	Gctgcaatctctctcgtgtg	gtccatccactactgctgca
OGT	Cagcatcccagctcactt	cagcttcacagctatgtcttc
OGA	Cctttgtacactgcggaacc	gccgagtgaacattcccatc
PGM3	Aggcagctggtgatgctatt	ggtcattgattgcctcctgt
ATF4	Ccagacggtgaacccaattg	tcactgcccagctctaaact
DDIT3	Ccactcttgaccctgcttct	tggttctcccttggtcttcc
HSPA5	Cggtctactatgaagcccgt	catctgggtttatgccacgg
Xbp1	Gagttaagacagcgcttggg	gatgttctggaggggtgaca
Actin	Gcctttattgcttccagcag	cgtggatgccacaggact

Western blot analysis

Cells were harvested and disrupted in a buffer containing 50mM HEPES pH 7.5, 150mM NaCl, 1% (v/v) glycerol; 1% (w/v) Triton X-100, 1.5mMMgCl2, 5mM EGTA, protease inhibitor cocktail (Sigma-Aldrich) and phosphatase inhibitors (Sigma-Aldrich). 10 to 30µg of total protein were resolved by SDS-PAGE and transferred to the nitrocellulose membrane, which was incubated overnight with specific antibodies: vinculin, Eif2α, Grp78, CHOP (GADD153) and OGT from Santa Cruz Biotechnology Inc.;

cleaved caspase 3, PARP, Total Erk (p44/42 MAP Kinase), phospho-Erk Thr202/Tyr204 and actin from Cell Signaling Technology Inc.; O-Linked N-Acetylglucosamine (Clone RL2) from Thermo Scientific; Glucosamine Fructose Amidotransferase 1 (GFPT1) and Phosphoglucomutase 3 (PGM3) from Proteintech; UAP1 from Sigma-Aldrich.

D-Glucose and L-Lactate measurement

D-Glucose and L-Lactate levels in culture medium were determined using spectrophotometric enzyme assay kits (R-Biopharm, Darmstadt, Germany) as specified by manufacturer's datasheet.

Statistics

Statistical analyses were performed using Microsoft Excel. Statistical significance (*p<0,5, **p<0,01) between the means of at least three groups was determined using Student's t test, and the results are presented as the mean value and SD unless stated otherwise.

Results

Hexosamine Biosynthetic Pathway inhibition affects cell proliferation and survival of a triple negative breast cancer cell model, MDA-MB-231

As reported in literature, alteration of glycosylation level is associated to several diseases, among which cancer (Ozcan et al., 2010) (Lau et al., 2007). Given that, we decided to analyze the relevance of the HBP, the metabolic pathway regulating cellular level of glycosylation, in a triple negative (ER^-, PgR^-, $Erbb^-$) breast cancer cell line, MDA-MB-231, carrying an oncogenic form of K-ras (K-ras G13D). This cell line has been chosen because we and other Authors well characterized their metabolism, and in particular the role of glucose metabolism in their ability to proliferate and survive (Baracca et al., 2010) (Palorini et al., 2013a) (Palorini et al., 2016).

MDA-MB-231 cells, grown at 25 mM glucose (high glucose or HG) were treated with different concentrations of one recognized HBP inhibitor, Aza, which blocks the GFAT1 enzyme, the limiting step of HBP. Moreover, since an alternative approach commonly used to mimic HBP inhibition is to block N-acetyl glucosaminyl 1-phosphate transferase activity in the ER and consequently the N-linked protein glycosylation, the cells were also treated with Tun (Rajapakse et al., 2009) (Chatterjee et al., 1981). As shown in **Figure 1A and 1C**, both inhibitors, in dose and time dependent

manner, induced a dramatic decrease of MDA-MB-231 proliferation as compared to untreated ones.

More specifically, they induced also cell death **(Figure 1B and 1D),** especially at higher doses used. These findings suggested us a pivotal role of HBP in MDA-MB-231 cell proliferation and survival, and therefore we moved to the designing and synthesis of novel HBP inhibitors.

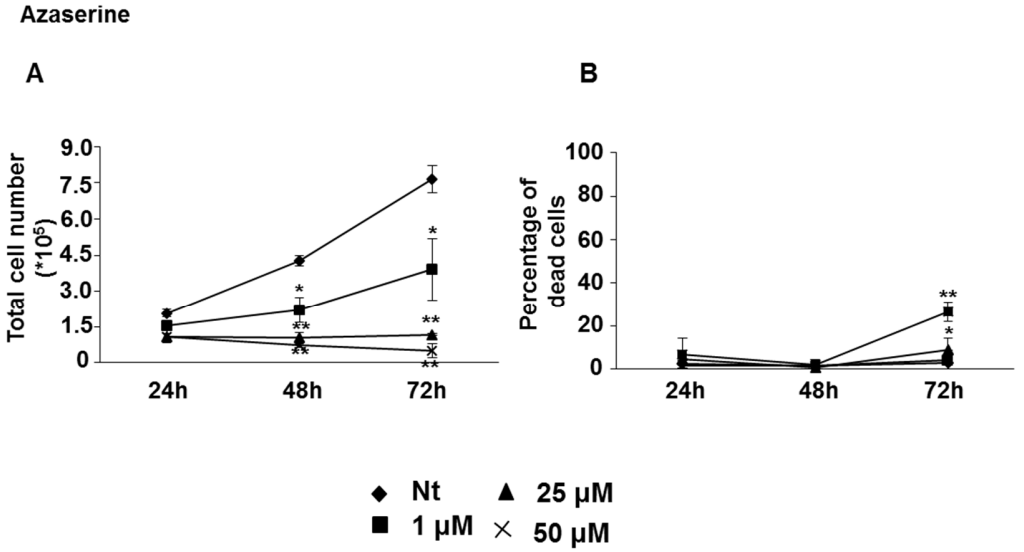
Azaserine
A
B
Total cell number (*10^5)
9.0
7.5
6.0
4.5
3.0
1.5
0
24h
48h
72h
Percentage of dead cells
100
80
60
40
20
0
Nt
25 µM
1 µM
50 µM

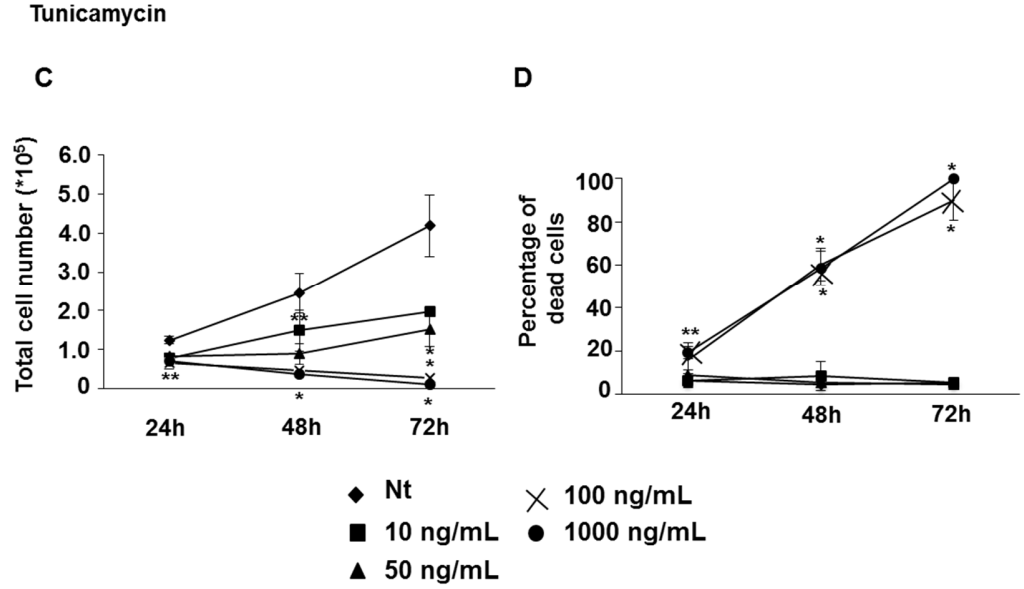
Tunicamycin
C
D
Total cell number (*10^5)
6.0
5.0
4.0
3.0
2.0
1.0
0
24h
48h
72h
Percentage of dead cells
100
80
60
40
20
0
Nt
100 ng/mL
10 ng/mL
1000 ng/mL
50 ng/mL

Figure 1. Hexosamine Biosynthetic Pathway inhibition in MDA-MB-231 cancer cells induces either cell growth arrest or cell death. MDA-MB231 cells were cultured in HG and treated, at indicated time points, with different concentrations of **A.** Azaserine and **C.** Tunicamycin. **B. and D.** Cell viability was analyzed by Trypan Blue (TB) staining after azaserine and tunicamycin treatment. All data represent the average of at least three independent experiments (± s.d.); *p<0,05 (Students's t-test).

Design of the structure of the novel molecules and computational analysis

Earlier studies demonstrated the relatively low specificity of available HBP inhibitors, such as Aza and DON. Indeed, both compounds are glutamine analogs, able to bind irreversibly to the active site of a number of glutamine-utilizing enzymes, including GFAT1. Clinical studies with these compounds showed limited antitumor activity but their development was restricted by severe toxicities, potentially due to the broad antagonism of multiple glutamine-utilizing enzymes and transporters (ELLISON et al., 1954).

For this reasons, the need to synthetize new modulators of HBP is a challenge (see introduction section). In order to find novel HBP inhibitors, we focus our attention on the enzyme PGM3, the mutase catalyzing the conversion of GlcNAc-6-P and GlcNAc-1-P in HBP.

To identify novel PGM3 inhibitors, a step-wise strategy of virtual screening and knowledge-driven designing was employed. We have designed and synthesized 8 compounds **(Table 1)**. This library of new compounds has been designed in way that their structures could be similar to the natural substrate of PGM3, GlcNAc-6-P, and to the final product GlcNAc-1-P, in order to compete for the catalytic pocket of the enzyme.

In the **Table 1** the chemical structure and formula of new molecules are shown.

Table 1: List of the new molecules, as putative PGM3 inhibitors

N° of the molecule	Chemical structure	Chemical formula
1	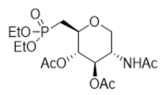	*N*-acetyl-3,4-di-*O*-acetyl-1-deoxy-6-diethylphosphonate-α-D-glucosamine
2	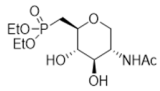	*N*-acetyl-1-deoxy-6-diethylphosphonate-α-D-glucosamine
3	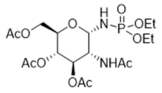	*N*-acetyl-3,4,6-tri-*O*-acetyl-1-deoxy-1-diethylphosphoramidate-6-phosphate-α-D-glucosamine
4	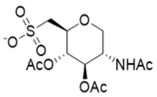	*N*-acetyl-3,4-di-*O*-acetyl-1-deoxy-α-D-glucosamine-6-sulphonate
5	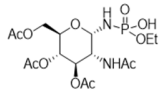	*N*-acetyl-3,4,6-tri-*O*-acetyl-1-deoxy-1-monoethylphosphoramidate-6-phosphate-α-D-glucosamine
6	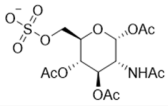	*N*-acetyl-3,4-di-*O*-acetyl-6-sulphate-α-D-glucosamine
7	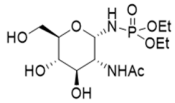	*N*-acetyl-1-deoxy-1-diethylphosphoramidate-6-phosphate-α-D-glucosamine
8	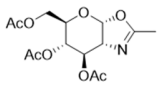	2-methyl-(3,4,6-tri-O-acetyl-1,2-dideoxy-α-D-glucopyrano)-[2,1-d]-2-oxazoline

Molecular modeling of all designed molecules, in their de-acetylated form, with the 3D-structure of the catalytic domain of PGM3, was performed by using Schrodinger 10.1 Maestro software. The tests were performed with high precision and flexibility parameters of both enzyme and putative ligands at pH 7.0 ± 0.3 (Glide Docking software).

In the **Figure 2,** new molecules were classified according to cLogP (logarithm of its partition coefficient between n-octanol and water log ($c_{octanol}/c_{water}$)), which measures the compound's hydrophilicity (black bars) and according to the scoring functions that predicts the strength of binding between target enzyme and new molecules (gray bars). The analysis has been performed at pH 7.0±0.3. As shown in **Figure 2** while the scoring function of the eight compounds was almost similar, molecule #8 showed the best value in terms of hydrophilicity (cLogP) and docking score.

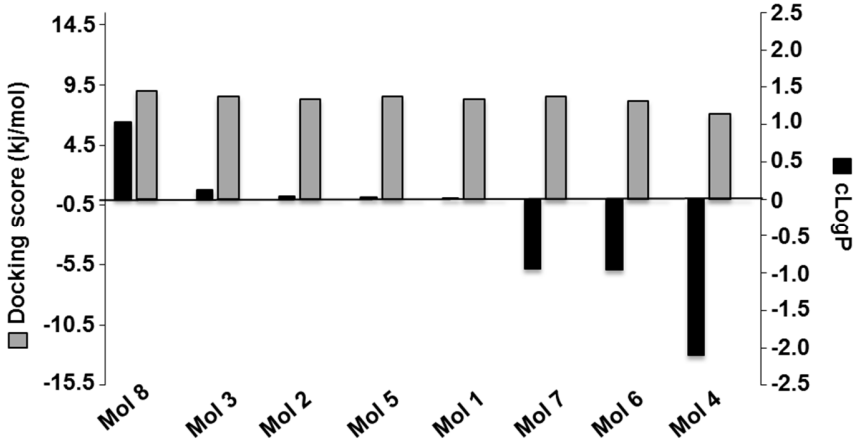

Figure 2. Computational analysis of new library. Docking score (Kj/mol) (grey bars), measuring the affinity between new molecules and pocket cleft of enzyme at pH 7.0, and the relative cLogP (black bars), or logarithm of partition coefficient, were analyzed using Schrodinger 10.1 Maestro software.

Chemical synthesis of the new compounds

According to computational analysis, molecules were synthesized and chemical structures were confirmed by Nuclear Magnetic Resonance (NMR) spectra.

During first part of my PhD 2-Methyl-(3,4,6-tri-O-acetyl-1,2-dideoxyα-D-glucopyrano)-[2,1-d-2]-oxazoline or molecule #8 was synthetized as described. Glucosamine hydrochloride (1.5 g, 6,95 mmol) was acetylated with acetic anhydride (10 equi, 69,50 mmol) and pyridine (35 equi, 243.25 mmol) for 4-5 hours. To neutralize pyridine we performed an extraction with AcOET: HCl (5%) for three times, thus organic phase was washed with brine and anhydrificated with sodium sulfate. The solvent was evaporated. 1,2,3,4-Penta-O-acetyl-α-D-glucopyranose was refluxed for 16h in dry CH_2Cl_2 (20mL) under argon in the presence of trimethylsilyl trifluoromethanesulfonate (TMDOTf) (0.85mL, 4.62mmol, 1.2equi.). The reaction mixture was then quenched with triethylamine (Et_3N), evaporated under reduced pressure, and the residue was purified by flash chromatography over silica gel (eluent: EtPet:AcOET-2:8) to yeld 1.03 g

(3.13 mmol, 81%) of 2-Methyl-(3,4,6-tri-O-acetyl-1,2-dideoxy-α-D-glucopyrano)-[2,1-d]-2-oxazoline as yellow/ brown oil.

The parameters about NMR spectra of molecule # 8 are summarized in **Figure 3**: ^{1}H NMR (400 MHz, Chloroform-*d*) δ 5.95 (d, *J* = 7.5, 1.9 Hz, 1H, **H1**), 5.30 – 5.21 (m, 1H, **H3**), 4.92 (d, *J* = 9.2, 1.8 Hz, 1H, **H4**), 4.20 – 4.08 (m, 3H, **H2**, **H6a**, **H6b**), 3.64 – 3.54 (m, 1H), 2.14 – 2.02 (m, 12H, 4 **CH$_3$**) (Haddoub et al., 2009).

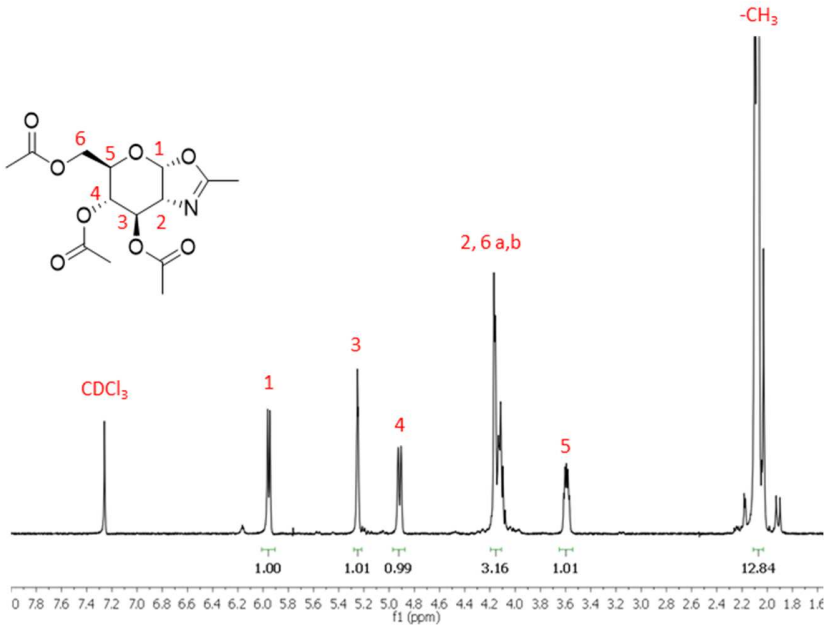

Molecule n°8 = 2-methyl-(3,4,6-tri-*O*-acetyl-1,2-dideoxy-α-D-glucopyrano)-[2,1-*d*]-2-oxazoline

Figure 3. 2-methyl-(3,4,6-tri-O-acetyl-1,2-dideoxy-α-D-glucopyrano)-[2,1-d]-2-oxazoline. 1H NMR (400 MHz, Chloroform-d) δ 5.95 (d, J = 7.5, 1.9 Hz, 1H, H1), 5.30 –

5.21 (m, 1H, H3), 4.92 (d, J = 9.2, 1.8 Hz, 1H, H4), 4.20 – 4.08 (m, 3H, H2, H6a, H6b), 3.64 – 3.54 (m, 1H), 2.14 – 2.02 (m, 12H, 4 CH3).

In vitro screening of new compounds

After synthesis and structural validation, new compounds were evaluated for cell viability in MDA-MB-231 cells grown in HG **(Figure 4)**. Cell viability assay was carried out as described in the Material and Method section, upon treatment with two different concentrations of all compounds, namely 500µM and 1mM.

Analysis of cell viability, performed after 48 hours of treatment, indicated that the molecule #8 had the stronger effect as compared to the others. This effect was in part expected, since the other compounds had a very low hydrophilicity (although they had a better docking score), suggesting different approaches for their dispensation. From now it will described the results obtained with compound # 8, which, hereafter will be referred as FR051.

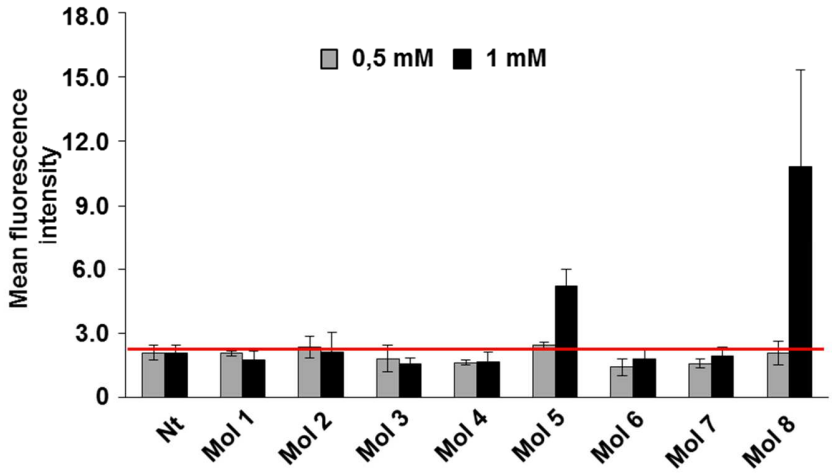

Figure 4. Screening of new compound on MDA-MB-231 breast cancer cell line. MDA-MB231 cells were cultured in HG and treated with different concentrations of new molecules and cell death was analyzed after 48 hours of treatment. Fluorescence intensity represents level of cell death. All data represent the average of at least three independent experiments (± s.d.).

In order to define FR051 action mechanisms, influencing cell survival, a deeper investigation was performed.

FR051 blocks cell proliferation and leads to cell death in dose and time dependent manner

MDA-MB-231 cell line was cultured in HG in presence of different concentrations of FR051, ranging from 100µM to 1mM concentration, as

suggested by our previous results **(Figure 4)** and from literature data (Gloster et al., 2011).

Cell proliferation and viability were analyzed after 24 and 48 hours of treatment **(Figure 5A)**.

As shown in **Figure 5B**, 500µM and 1mM of FR051 affected MDA-MB-231 cell proliferation and survival. In particular 1mM treatment induced an early effect, since the proliferation reduction was evident already at 24h of treatment (34.1% of reduction compared to untreated samples), while in 500µM the reduction was observed at later time point analyzed (48h) (34.4% of reduction compared to untreated samples). The **GI_{50}** value of FR051 was calculated as 474 µM **(Figure 5D)** using Prism6 software. In addition, specific analysis of cell death by using a vital staining (Trypan Blue or TB) indicated a four-fold increase in cell death only at 48h in 1mM treated samples **(Figure 5C)**. Importantly, cell death was preceded by the appearance of an altered cell morphology and an increased cell detachment **(Figure 5E)**. Notably, a dose of Aza of 25µM, normally used to induce cell death in other cancer cell models, induced similar effect on MDA-MB-231 cell proliferation but did not induced any cell death as compared to FR051.

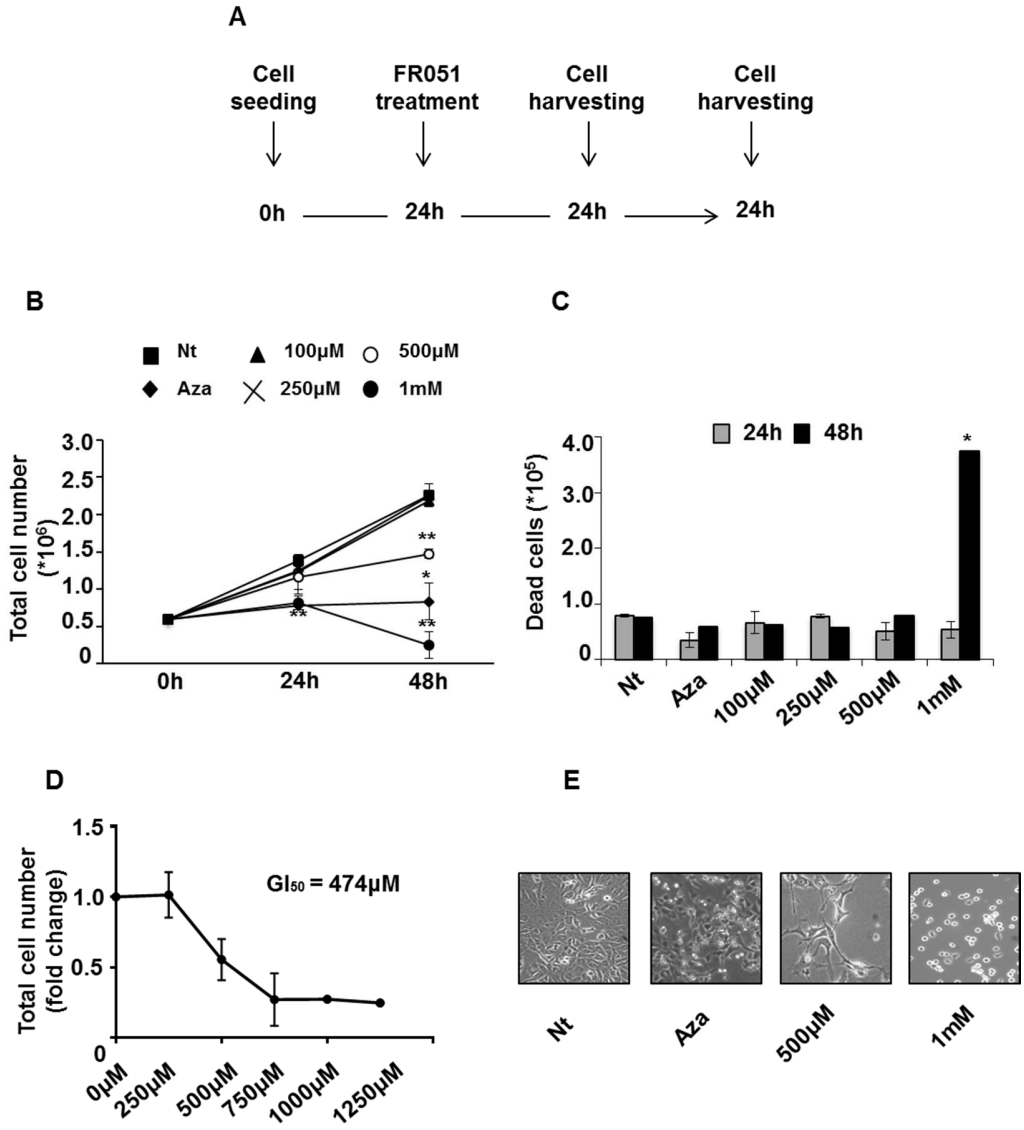

Figure 5. FR051 affects cell proliferation and viability. A. Schematic representation of the experiments workflow. MDA-MB231 cells were cultured in HG and treated with different concentrations of FR051. **B.** Proliferation curve was determined by cell counting

at indicated time points. Azaserine (Aza) was used as positive control. **C.** Cell viability was analyzed by TB staining and **D.** GI_{50} was calculated using Prism6 software. **E.** Phase contrast microscopy images were collected at 48 hours of cell culture. All data represent the average of at least three independent experiments (± s.d.); *p<0,05 (Students's *t-test*).

Cytotoxic effect of FR051 was further supported by a clonogenic assay **(Figure 6)**. In fact, 24h treated cells, re-plated in optimum condition, formed less colonies (around 80% and 90% of reduction, in 500µM and in 1mM of FR051 respectively) as compared to untreated cells.

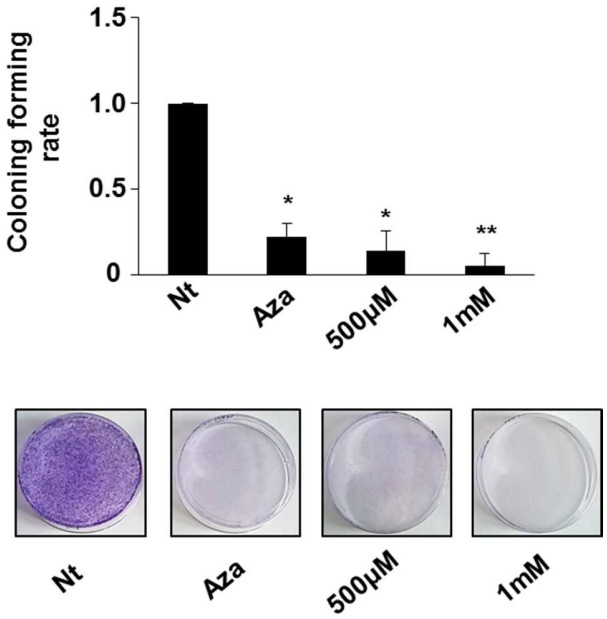

Figure 6. FR051 impairs clonogenic ability. After 24 hours of treatment with FR051, 3 x 10^3 cells were plated for clonogenic assay and colonies counted after 12 days. All data represent the average of at least three independent experiments (± s.d.); *p<0,05 (Students's *t-test*).

FR051 treatment did not induce cell death in primary cell line

To determine whether the cytotoxic effects of FR051 was selective for cancer cells in comparison to non-cancer cells, the normal human lung fibroblasts WI38 were exposed to the compound at varying concentrations in a similar fashion as the MDA-MB-231 cancer cells. These cells were less susceptible to the actions of the compound **(Figure 7)**, particularly using dosage different from 1 mM. According to these findings, additional investigations on the mechanisms of action of FR051 have been done. For the following experiments we decided to use the highest dose (1 mM) in order to obtain a strong and fast effect on cancer cells.

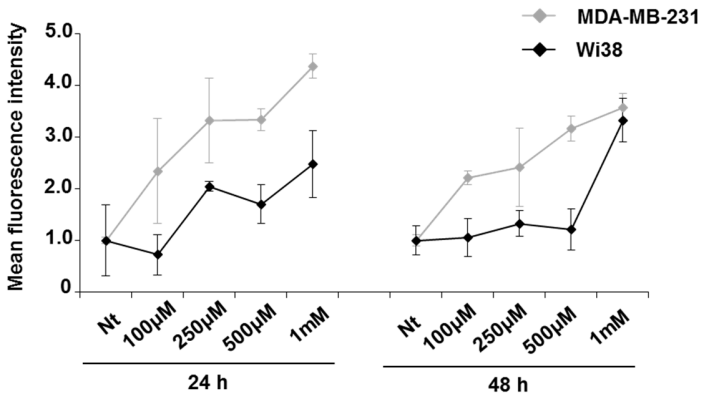

Figure 7. WI38 cells show a less sensitivity to FR051 treatment. MDA-MB-231 breast cancer cell line and WI38 lung normal cell line were plated in HG and treated with different concentrations of FR051. After 48h of treatment cell death (fluorescence intensity) was evaluated as described in experimental procedures. All data represent the

average of at least three independent experiments.

FR051 induces an apoptotic process in MDA-MB-231 cells

To further delineate the type of cell death induced by FR051 treatment (apoptosis or necrosis), a double staining with Propidium Iodide (PI) and Annexin V-FITC (AV) was performed. After 24 hours of treatment (1mM FR051), as shown also by TB staining **(Figure 5C)**, the percentage of AV-positive cells was almost similar to untreated cells (13% compared to 8%). However at 48h, the percentage increased dramatically (60,4% versus 7,2%) **(Figure 8A)**. Such data were further confirmed by a Western Blot analysis of caspase-3 and Poly ADP ribose polymerase (PARP) cleavage, both specific apoptotic markers. In fact as shown in **Figure 8B**, caspase 3 was activated at both 24 and 48h while PARP was present only at later time point of the analysis, in correlation with the apoptotic peak.

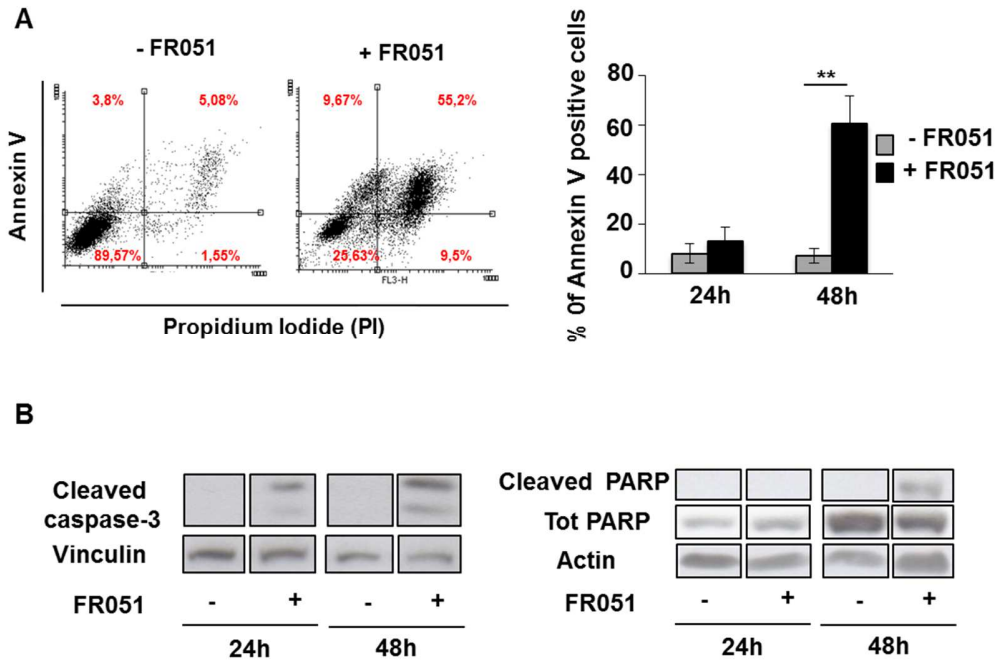

Figure 8. FR051 treatment induces an apoptotic process as shown by cleavage of Caspase-3 and Poli ADP-ribose polymerase. A. Cell death was evaluated by staining the cells with Propidium Iodide and Annexin V-FITC followed by FACS analysis. The apoptotic activation was confirmed by western blot analysis of **B.** cleaved caspase-3 and Poli ADP-ribose polymerase (PARP). Vinculin and actin were used as as loading control. All data represent the average of at least three independent experiments (± s.d.). *p<0,05 (Students's *t-test*).

FR051 affects both O- and N-glycosylation

As reported before, the UDP-GlcNAc, the final product of HBP, is the substrate for the enzymes involved in both O- and N-glycosylation modifications (Hanover et al., 2012).

To evaluate whether FR051 acts as HBP inhibitor, O- and N-glycosylation levels were assayed.

In particular, O-glycosylation level was detected by immuno-blot, using a specific antibody (RL2) against all O-glycosylated cellular proteins. After 24 hours of the treatment, MDA-MB-231 cells showed an increase of O-GlcNAc level, which strongly decreased after 48 hours **(Figure 9)**. Interestingly at both time-points the O-glycosylated protein pattern was rather different from untreated cells, suggesting a direct effect of FR051 on HBP and hence on protein O-glycosylation.

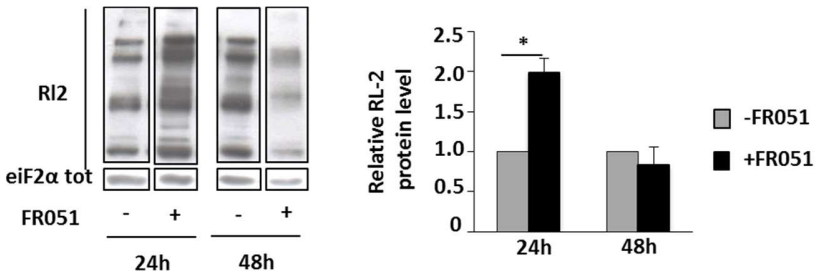

Figure 9. FR051 treatment influences O-glycosylation. MDA-MB-231 cells, grown at HG, were subjected to A) Western Blot analysis with a specific anti O-glycosylation antibody (O-GlcNAc). As loading control the expression of total eif2α was analyzed. B) Densitometric quantification of RL2 western blots. Image is representative of three

independent experiments. All data represent the average of at least three independent experiments (± s.d.); *p<0,05 (Students's *t-test*).

Since that O-glycosylation level depends on the presence of the UDP-GlcNAc as substrate and on the balance between the activities of two enzymes OGT and OGA, involved in addition and subtraction of the O-GlcNAc moiety to the protein respectively **(Figure 10A)**, mRNA and/or protein levels of both proteins were analyzed after FR051 treatment. As shown in **Figure 10B** and **C**, the 48h treatment induced OGT and OGA mRNA reduction, and a specific enhancement of OGT protein expression at early time point analyzed (24h) that strongly dropped at 48h **(Figure 10D)**. These results are completely in agreement with RL2 staining **(Figure 9)** and previous observations (Ngoh et al., 2009) in which has been suggested that inhibition of HBP pathway stimulates an early adaptive response to compensate for the reduction of protein glycosylation.

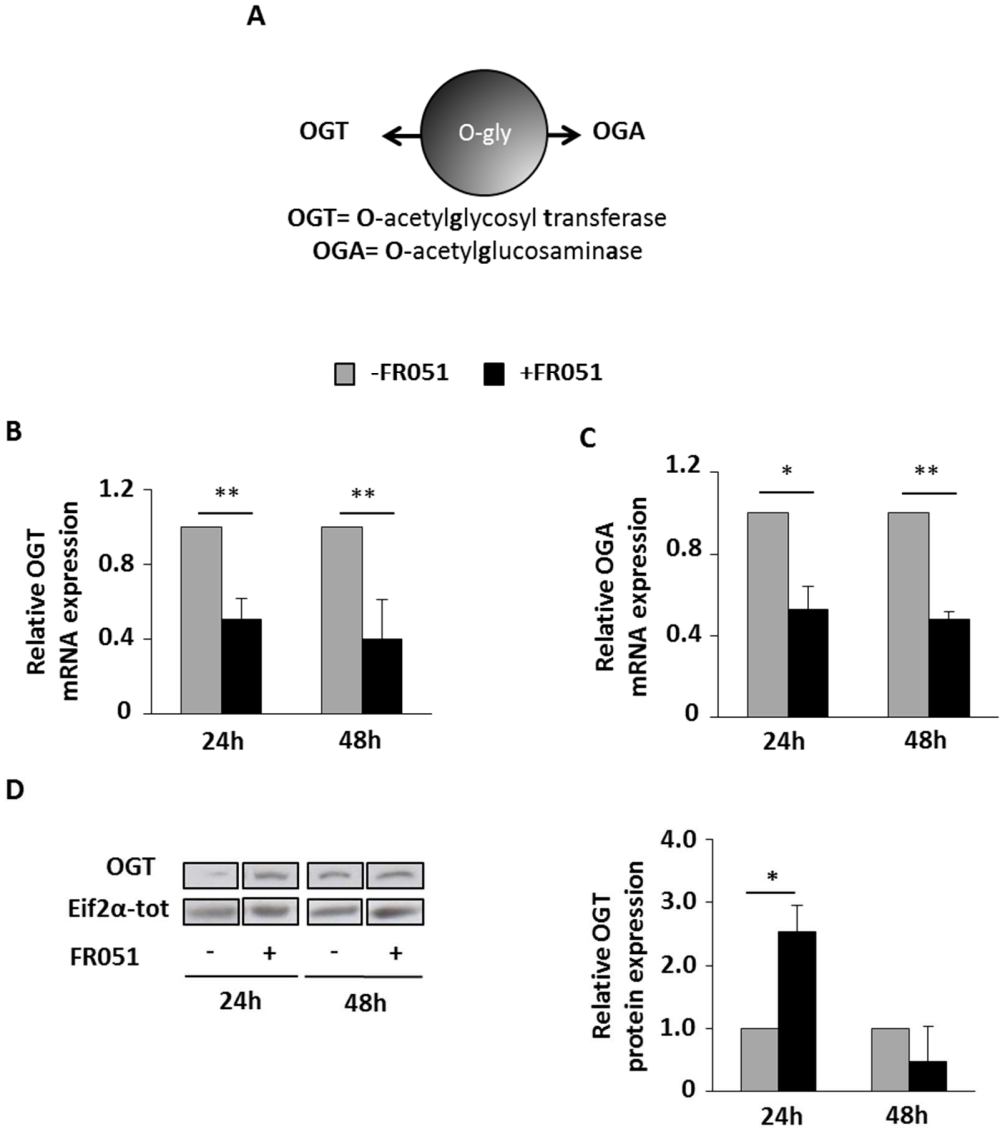

Figure 10. FR051 treatment influences O-glycosylation related genes and protein. A. O-glycosylation level depends on O-N acetyl glucosaminyl transferase (OGT) and O-N

acetylglucosaminidase (OGA) activity. **B.** The relative mRNA expression of the OGT and of **C.** OGA were analyzed after 24 and 48 hours of treatment with FR051 **D.** OGT protein expression was measured by using a specific antibody. Total eif2α was used as loading control. All data represent the average of at least three independent experiments (± s.d.); *p<0,05 (Students's *t-test*).

N-glycosylation level was detected by using specific lectins that selectively bind the carbohydrate moieties of the glycoprotein on cell surface. To distinguish the glycan structures (hybrid/high mannose and di-antennary from tri-/tetra-antennary glycans), lectins conjugated to different fluorochromes were used. Hybrid/high mannose and di-antennary glycans were recognized by Alexa Fuor594 *Concanavalin A* (ConA), while tri-/tetra-antennary structures were detected by Alexa Fluor488 *Phaseolus vulgaris* (PHA-L) **(Figure 11)**. Flow cytometric analysis of MDA-MB-231 cells, after FR051 treatment, indicated that the ConA reactivity of the cells remained almost similar to untreated cells at both time points **(Figure 11A)**. Conversely, at same time points, PHA-L reactivity of the cells significantly decreased **(Figure 11B)**. Our recent reports showed that glucose starvation induces a reduced HBP flux that impact lectin reactivity. In fact, as shown in **(Figure 11)**, either ConA reactivity or PHA-L reactivity was significantly reduced upon 1mM glucose cell growth (Palorini et al., 2013a) (Palorini et al., 2016). These data showed that inhibition of HBP by FR051 specifically altered cell surface lectin reactivity as previously observed in glucose starvation. Moreover this indicates that early N-glycosylation processing in the ER were not altered by FR051 (ConA

reactivity), whereas N-glycan branching was more sensitive to FR051 (PHA-L reactivity). These findings strongly suggest that FR051 interfere with in UDP-GlcNAc levels.

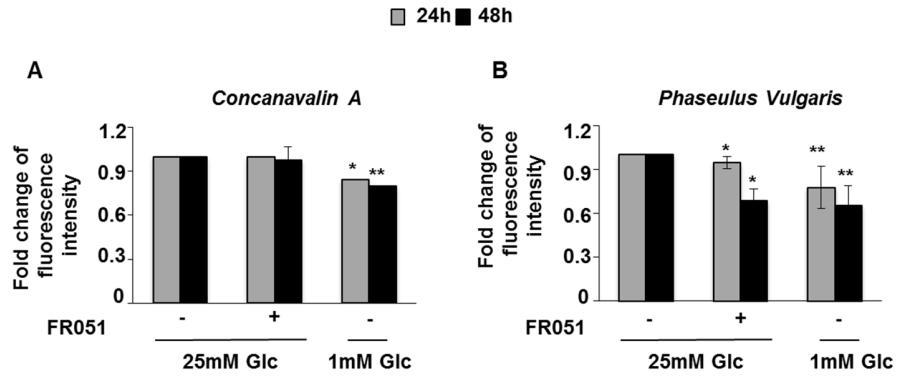

Figure 11. FR051 treatment decreases N-glycosylation level. MDA-MB-231 cells were cultured in HG and after 24 hours cells were treated with 1mM of FR051. After 24 hours of treatment FACS analysis of live cells was performed after staining with fluorochrome-conjugated **A.** *ConcanavalinA* and **B.** *Phaseulus Vulgaris* for detection of N-glycans. Cells grown in 1mM glucose were used as positive control for N-glycosylation level decrease. All data represent the average of at least three independent experiments (± s.d.); *p<0,05 (Students's *t-test*).

Exogenous treatment with GlcNAc does not rescue the FR051 effects

To further support a direct effect of FR051 on HBP pathway and

specifically on PGM3 enzyme, as suggested by previous findings and computational modeling **(Figure 2)**, we sought to treat the cells with GlcNAc, a PGM3 upstream substrate. In fact, NAGK, through the salvage pathway, recycles GlcNAc from the environment and introduce it in the HBP directly bypassing GFAT1 (Hinderlich et al., 2000), increasing endogenous levels of UDP-GlcNAc either in cell models or organisms. MDA-MB-231 cells were co-treated with FR051 and GlcNAc (10 mM) in HG and analyzed for their ability to proliferate. As control we used cells grown in low glucose, in which we have previously showed that GlcNAc addition is able to restore cell survival by increasing HBP flux (Furo et al., 2015). After 48 hours of co-treatment, cell survival was not rescued by GlcNAc addition as confirmed by cell number reduction, caspase-3 activation and cell morphology change **(Figure 12A, B and C)**, further suggesting that FR051 is able to inhibit HBP downstream to salvage pathway.

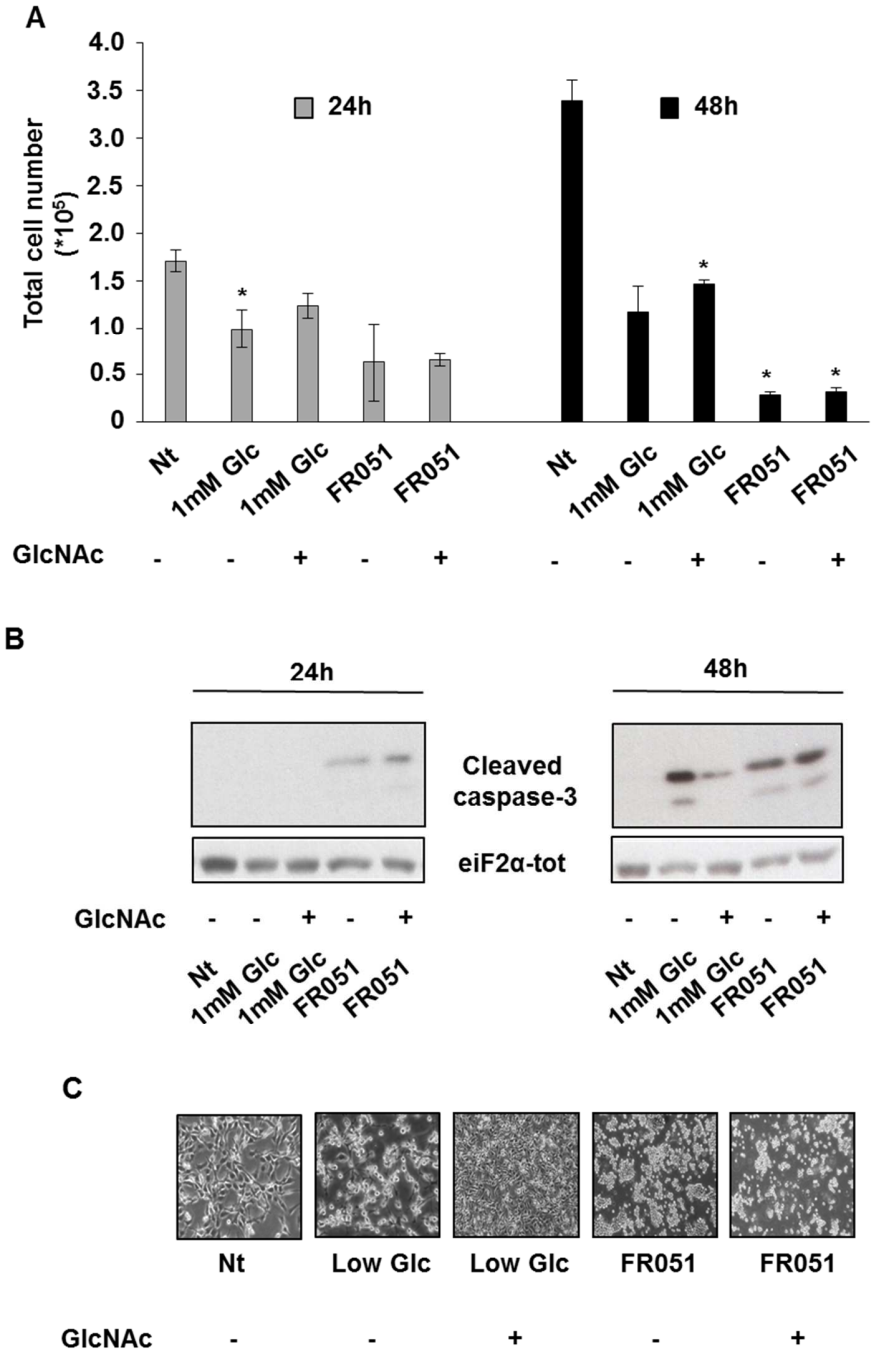
A
Total cell number (*10^5)
4.0
3.5
3.0
2.5
2.0
1.5
1.0
0.5
0
24h
48h
Nt
1mM Glc
1mM Glc
FR051
FR051
GlcNAc
B
24h
48h
Cleaved caspase-3
eiF2α-tot
C
Nt
Low Glc
Low Glc
FR051
FR051

Figure 12. N-Acetyl-D-glucosamine does not revert FR051 effect. A. Proliferation curve of MDA-MB-231 after the co-treatment with FR051 and N-Acetyl-D-glucosamine (10mM) and **B.** Analysis of cleaved caspase-3. eiF2α-tot protein level was used as loading control**. C.** Phase contrast microscopy images were collected at 48h to show the cell morphology**.** All data represent the average of at least three indipendent experiments (± s.d.); *p<0,05 (Students's *t-test*).

Unfolded Protein Response activation upon N-glycosylation reduction

UDP-GlcNAc, the end product of the HBP, provides not only the substrate for O-GlcNAc modifications, but also is a critical donor for protein N-glycosylation, which is necessary for proper protein folding. In fact, as reported in literature, N-glycosylation is necessary for the interactions between cell and its extracellular environment (Gu and Taniguchi, 2004) (Dennis et al., 2009a), and for the protein folding and stability (Ellgaard et al., 2016). When the N-glycosylation level decreases, many proteins with un-correct folding accumulate into ER leading to severe cellular stress. This condition activates the UPR (Gaut and Hendershot, 1993) (DuRose et al., 2006). These facts, combined with the realization that previous studies reported UPR activation during glucose starvation (Palorini et al., 2013a) (Palorini et al., 2016) led us to investigate a possible link between the HBP and the UPR.

Since FR051 treatment led to decrease of complex N-glycans, the status of some UPR-involved proteins, in terms of mRNA and protein levels were evaluated. Examination of mRNA and protein levels by q-PCR and immunoblotting revealed a decrease in HSPA5/GRP78 **(Figure 13A)**, an important pro-survival molecular chaperone associated to UPR. Conversely, other UPR target mRNAs, ATF4 **(Figure 13B)** and CHOP **(Figure 13C)**, were significantly up regulated (approximately 4-fold after 24h and 7,5-fold after 48h for ATF4, and around 7,5-fold after 24h and 34-fold after 48h for CHOP). Importantly, increases in mRNA levels were accompanied by a significant increase in the pro-apoptotic CHOP protein **(Figure 13D)**. Additionally, the transcription factor Xbp1, a driver of UPR gene expression, increased of two-fold at mRNA level, suggesting an activation of ATF6 sub-pathway **(Figure 13E)**. However, the ER-stress induced splicing of Xbp1 was not detectable, suggesting a lack of activation in Ire1 sub-pathway **(Figure 13F)**. Importantly, while FR051 significantly activated some UPR branches to a level comparable to that of classical ER stressor such as *Thapsgargin* (*Th*) or *Tun*, by contrast, FR051 did not induce XBP1 splicing, effect observed upon *Th* treatment. Thus, these results while confirmed that the FR051 is able to induce the UPR, as expected for an inhibitor of the HBP, by contrast suggested also a specific effect, since its behavior was partially different from other ER stressors.

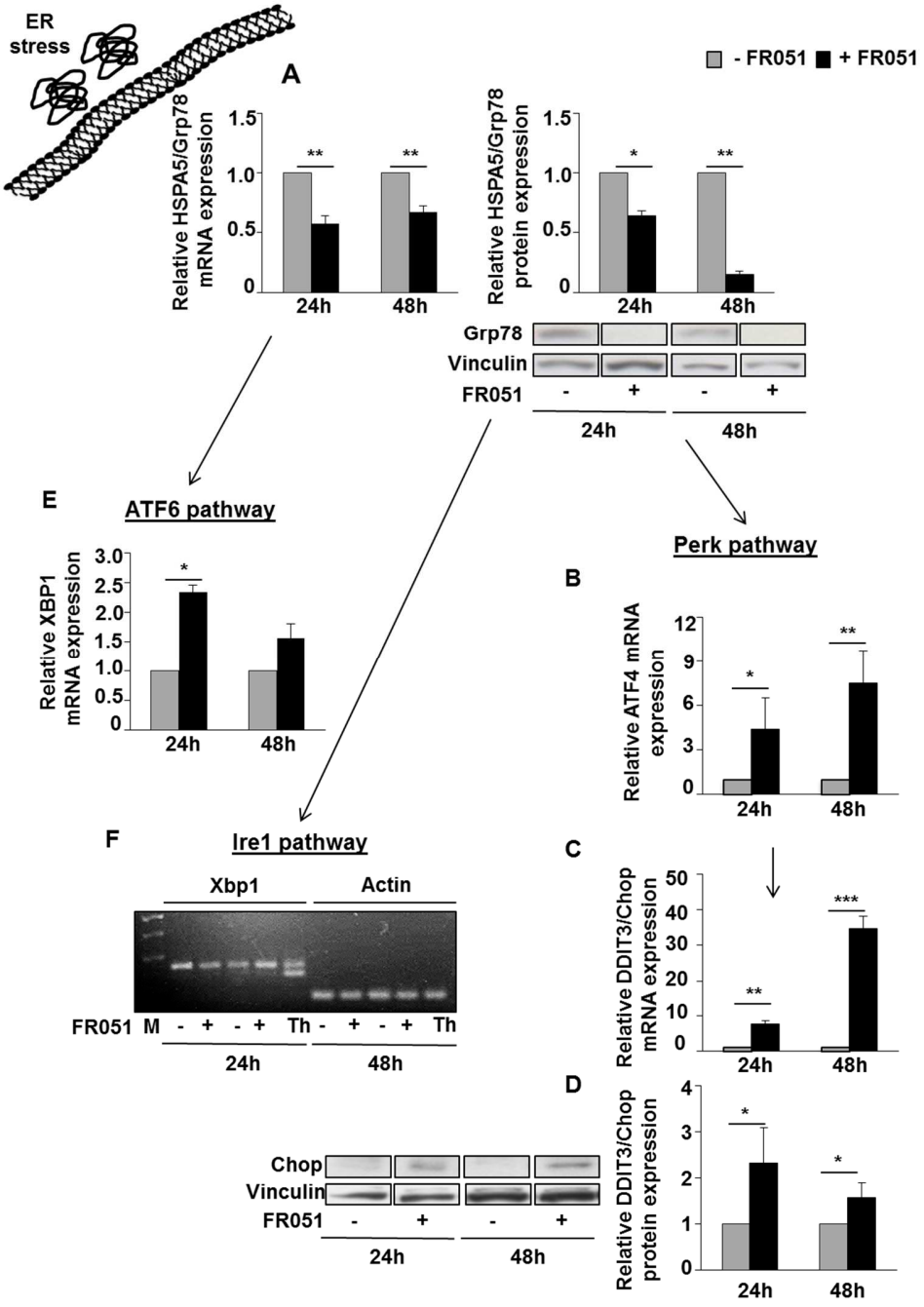
ER stress
A
- FR051 + FR051
Relative HSPA5/Grp78 mRNA expression
Relative HSPA5/Grp78 protein expression
24h
48h
Grp78
Vinculin
FR051
E
ATF6 pathway
Relative XBP1 mRNA expression
Perk pathway
B
Relative ATF4 mRNA expression
F
Ire1 pathway
Xbp1
Actin
M
Th
C
Relative DDIT3/Chop mRNA expression
D
Chop
Relative DDIT3/Chop protein expression

Figure 13. FR051 treatment activates Unfolded Protein Response by decreasing N-glycosylation. UPR activation was followed through the expression analysis of **A.** HSPA5/Grp78 mRNA and its relative protein, **B.** ATF4 mRNA, **C.** DDIT3/Chop mRNA and **D.** DDIT3/Chop protein, **E.** Xbp1 mRNA and **F.** its relative splicing status at 24 hours and 48 hours of FR051 and Th treatments. Protein and mRNA expression of Vinculin and Actin were analyzed, respectively, as loading control for mRNA and protein. All data represent the average of at least three independent experiments (± s.d.); *p<0,05 (Students's *t-test*).

Inhibition of Ire1 pathway affects the expression level of HBP enzymes

Previous data (Wang et al., 2014), demonstrated the spliced Xbp1 is able to bind a specific sequence, the UPRE, located in the promoters of some HBP genes, among which GFAT1 and PGM3 **(Figure 14)**.

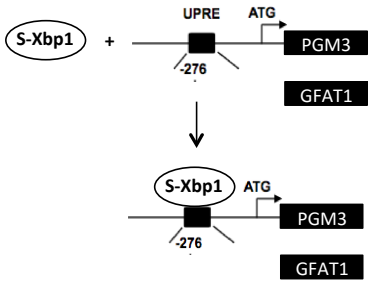

Figure 14. Spliced Xbp1 (S-Xbp1) interacts with unfolded protein response element (UPRE). Schematic representation of the interaction between spliced Xbp1 transcription factor and Unfolded Protein Response Element (UPRE) of some target genes, namely PGM3 and GFAT1.

Therefore, since FR051 did not induce XBP1 splicing, we sought to confirm this finding by measuring mRNA and protein levels of these two enzymes.

As shown in **Figure 15**, mRNAs for both enzymes decreased after 24 hours of FR051 treatment **(Figure 15A and B)**. However, while PGM3 mRNA decreased also at 48h, GFAT1 mRNA did not change compared to untreated samples. By contrast, PGM3 and GFAT1 protein levels, following FR051 treatment, were strongly increased at 24h and decreased at 48h **(Figure 15C and D)**. These findings suggested that while PGM3 and GFAT1 mRNA levels were correlated to the lack of XBP1 splicing, proteins regulation may also occur post-transcriptionally.

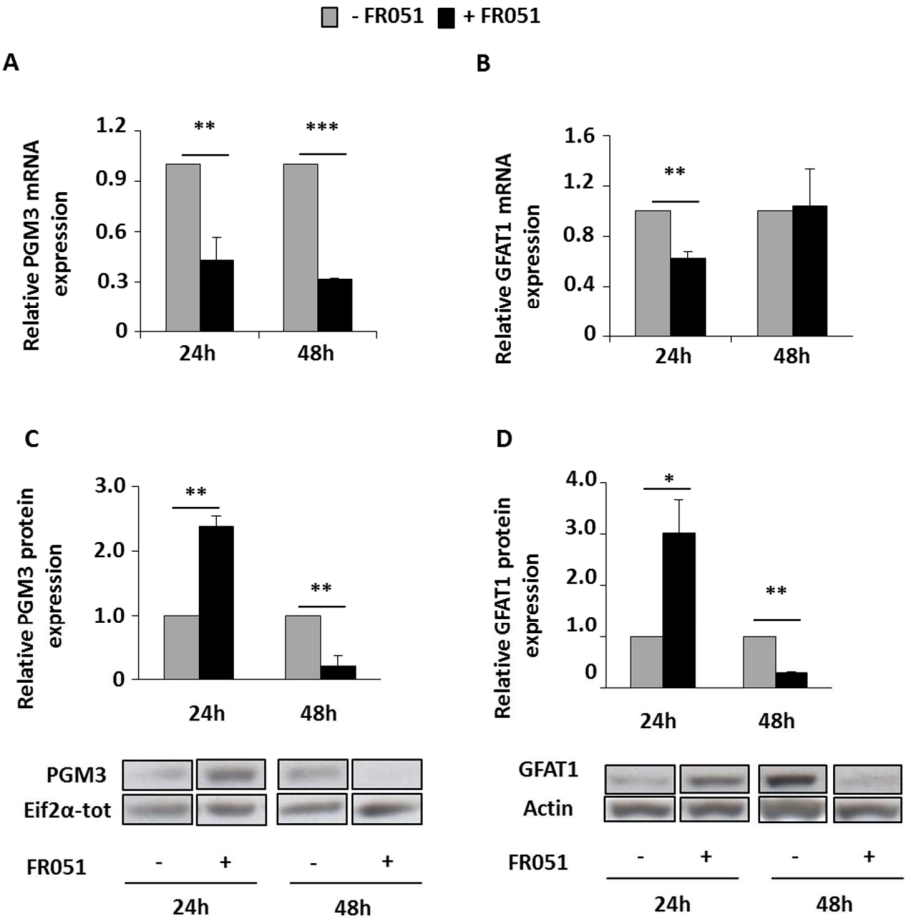

Figure 15. Ire1 controls mRNA expression of HBP enzymes. Relative mRNA and protein level of PGM3 (**A.** and **C.**) and GFAT1 (**B.** and **D.**) after 24 and 48 hours of treatment. All data represent the average of at least three independent experiments (± s.d.); *p<0,05 (Students's *t-test*).

FR051 treatment slightly influences glucose consumption as well as lactate production

As reviewed by Dona C. Love and John A. Hanover, about 13% of proteins involved in cell metabolic processes are influenced by glycosylation status (Love and Hanover, 2005). For instance, Yi et al. report that O-GlcNAcylation of a key Ser residue on PFK1 (Ser529) decreases enzyme activity and regulates central metabolism favoring glucose entering in PPP and hence increasing cell resistance to oxidative stress but reducing glycolysis (Yi et al., 2012). Since latter metabolic pathway is required for MDA-MB-231 cell survival, we sought to determine whether FR051 treatment could influence glucose metabolism reducing glucose uptake and thus participate to cell death observed. MDA-MB-231 cells were plated in HG, then, after 24 hours, the medium was replaced by fresh medium (25 mM glucose) supplemented with 1mM FR051. After 24 hours of treatment, as shown in **Figure 16A** and **B**, the amount of residual glucose and secreted lactate, as measured in the culture medium, were not significant different among FR051 treated and untreated samples. As consequence, also the glycolytic flux resulted to be only slightly decreased **(Figure 16C)**. These data suggested that FR051 treatment did not interfere with glycolysis (probably due to the fact high amount of glucose present in the experiments).

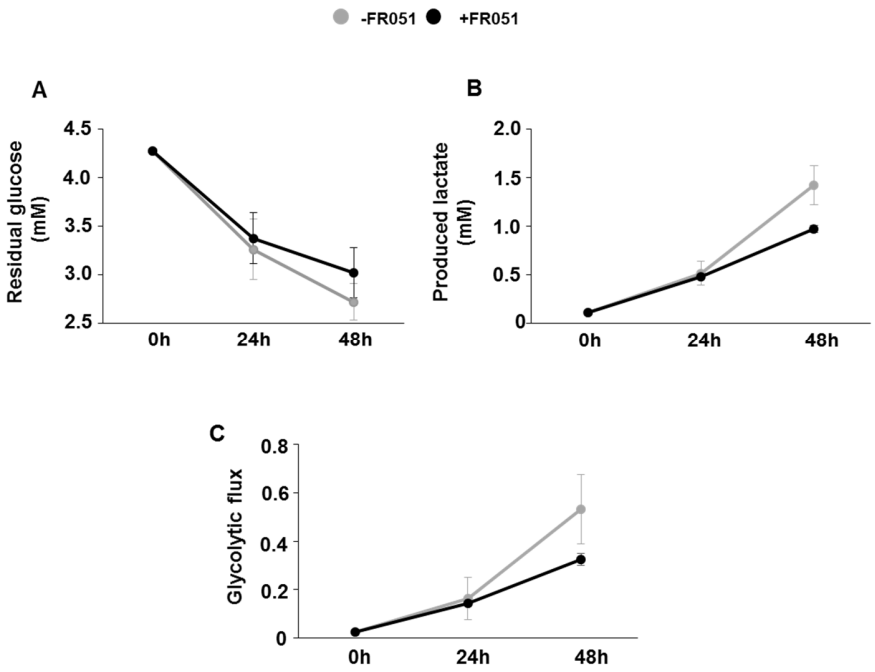

Figure 16. Measure of glucose consumption and of lactate secretion after FR051 treatment. A. Residual glucose per cell (calculated by measuring the residual glucose) and **B.** secreted lactate in the culture medium of MDA-MB.231 cells, grown at 25 mM initial glucose concentration, were measured by using specific enzymatic kits. **C.** Glycolytic flux was also evaluated according to **A.** and **B.** All data represent the average of at least three independent experiments (± s.d.); *p<0,05 (Students's *t-test*).

FR051-induced apoptosis is due to ROS production

Oxidizing conditions in ER lumen favor formation of disulphide bonds, necessary for correct protein folding, through the action of protein disulphide isomerase (PDI) and Endoplasmic Reticulum Oxidoreductin-1

(ERO1). Since oxygen molecules are final electron acceptors, ROS are normally produced into ER (Sevier and Kaiser, 2008). However, chronic unresolved accumulation of unfolded proteins in the ER, often leading to apoptosis, may significantly contribute to cell oxidative stress (Tu and Weissman, 2002). To determine whether accumulation of misfolded proteins in the ER lumen, upon FR051 treatment, could generate ROS, MDA-MB-231 cells were stained with dichlorofluorescein ($DCFH_2DA$), for which fluorescence requires production of the H_2O_2. $DCFH_2DA$ fluorescence strongly increased more than 3-fold upon 24h treatment with FR051 in MDA-MB-231 cells **(Figure 17)**.

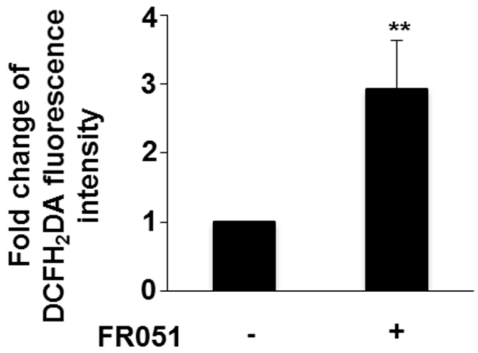

Figure 17. FR051 treatment increases ROS production. MDA-MB231 cells were treated with FR051 and Reactive Oxygen Species (ROS) production was analyzed after 24 hours from the treatment. Cells have been live-stained with $DCFH_2DA$ and then analysed by FACS. All data represent the average of at least three independent experiments (± s.d.); *p<0,05 (Students's *t-test*).

Ero1 activity contributes ROS production upon FR051 treatment

To understand whether ROS enhancement was due to increased Ero1 activity, upon prolonged UPR activation, MDA-MB-231 were treated for 24h with Ero1 inhibitor (EN460) before stimulation with FR051 (Blais et al., 2010). Percentage of cell death and ROS level were analyzed also in *Tun* (100 ng/mL) treated samples, as positive control (Li et al., 2009). Remarkably, the cells co-treated with FR051 and EN460 were partially protected from exposure to FR051 as well as to *Tun*, since both cell death and ROS levels were reduced in ERO1 inhibited samples **(Figure 18A and B)**. However, as shown by other Authors (Blais et al., 2010), the protection was relatively modest. Nonetheless, these observations suggest a potentially role of ERO1 in ROS accumulation and cell death.

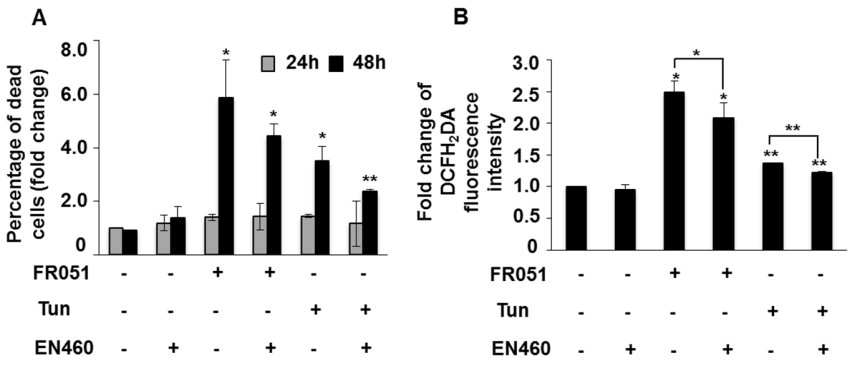

Figure 18. Ero1 inhibition slightly decreases ROS level. MDA-MB-231 cells grown in 25mM glucose were pre-treated with EN460 (1 µM) and then with FR051. **A.** Cell viability

was analyzed by TB staining after 24 and 48 hours from the treatment. **B.** Relative ROS level was detected by staining the cells with $DCFH_2DA$ after 24 hours of treatment with FR051, followed by FACS analysis. All data represent the average of at least three independent experiments (± s.d.); *p<0,05 (Students's *t-test*).

Mitochondrial ROS are not involved in ROS production upon FR051 treatment

According to the partial rescue of phenotype after treatment with Ero1 inhibitor we asked whether ROS could be derived also from mitochondria. This organelle represent a major source of endogenous ROS, which are produced during electron transfer from reduced metabolic intermediate to oxygen molecule (Panieri and Santoro, 2016). To understand this, we decide to pre-treat MDA-MB-231 cells with MitoTempo (50μM), a well-known inhibitor of mitochondrial ROS production mimicking SOD structure (Dikalova et al., 2010). Co-treated cells were not protected from cell death **(Figure 19A)** in association with a lack of reduction of ROS level in MitoTempo-FR051 co-treated samples **(Figure 19B)**. The effectiveness of the MitoTempo activity was confirmed by the observed decrease of ROS level in Antimicyn A samples, a known electron transport inhibitor able to increase mitochondrial ROS **(Figure 19B)** (Dairaku et al., 2004). According to evidences reporting the role of mitochondria in ER stress, we did not exclude completely mitochondrial role in the FR051 mediated mechanism (Szalai et al., 1999) (Tadic et al., 2014).

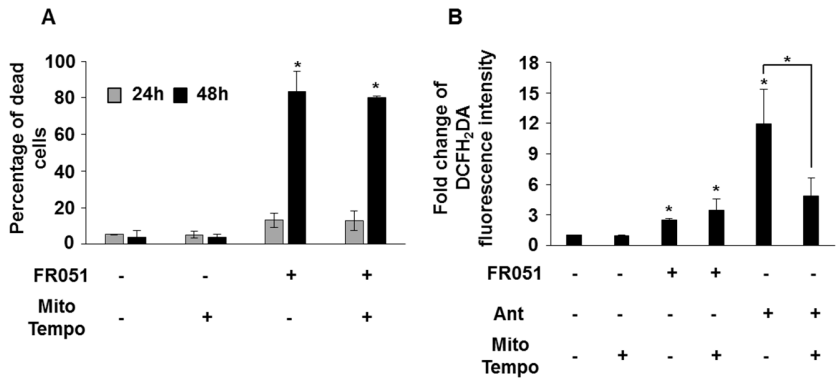

Figure 19. Inhibition of mitochondrial ROS production does not reduce FR051-dependent apoptosis . MDA-MB-231 cells grown in 25mM glucose were pre-treated with MitoTempo (50 µM) and then with FR051. **A.** Cell viability was analyzed by TB staining after 24 and 48 hours of treatment. **B.** Relative ROS levels were detected by staining the cells with $DCFH_2DA$ after 24 hours of treatment with FR051 followed by FACS analysis. All data represent the average of at least three independent experiments (± s.d.); *p<0,05 (Students's *t-test*).

Constitutively Erk1/2 phosphorylation is associated to cell death upon FR051 treatment

Several evidences have demonstrated the key role in controlling cell survival and death of Mitogen Activated Protein Kinases (MAPKs) activation in oxidative stress conditions (Guyton et al., 1996). For instance it has been reported that Erk1/2 phosphorylation may increase upon activation of UPR as consequence of an increase of ROS levels (Hung et al.,

2003). In addition it has been also shown that ERK-specific phosphatases are inhibited by high ROS, effect that leads to prolonged ERK activation (Kamata et al., 2005) (Levinthal and Defranco, 2005). Therefore, we examined the role of ERKs on FR051-induced apoptosis. Treatment of MDA-MB-231 cells with FR051 for 48h induced the phosphorylation of ERK1/2 **(Figure 20A)**. Considering previous data (Cagnol et al., 2006) a specific chemical inhibitor was utilized to investigate the potential involvement of ERK1/2 in mediating FR051-induced apoptosis (Manchado et al., 2016). A pre-treatment of MDA-MB-231 cells (24h) with the specific Erk1/2 inhibitor SCH772984 (50nM) strongly reduced the cell death, measured upon 24h and 48h of FR051 treatment **(Figure 20B and C)**. These data suggested that activation of ERK1/2 activity could participate to the induction of cell death upon FR051 treatment.

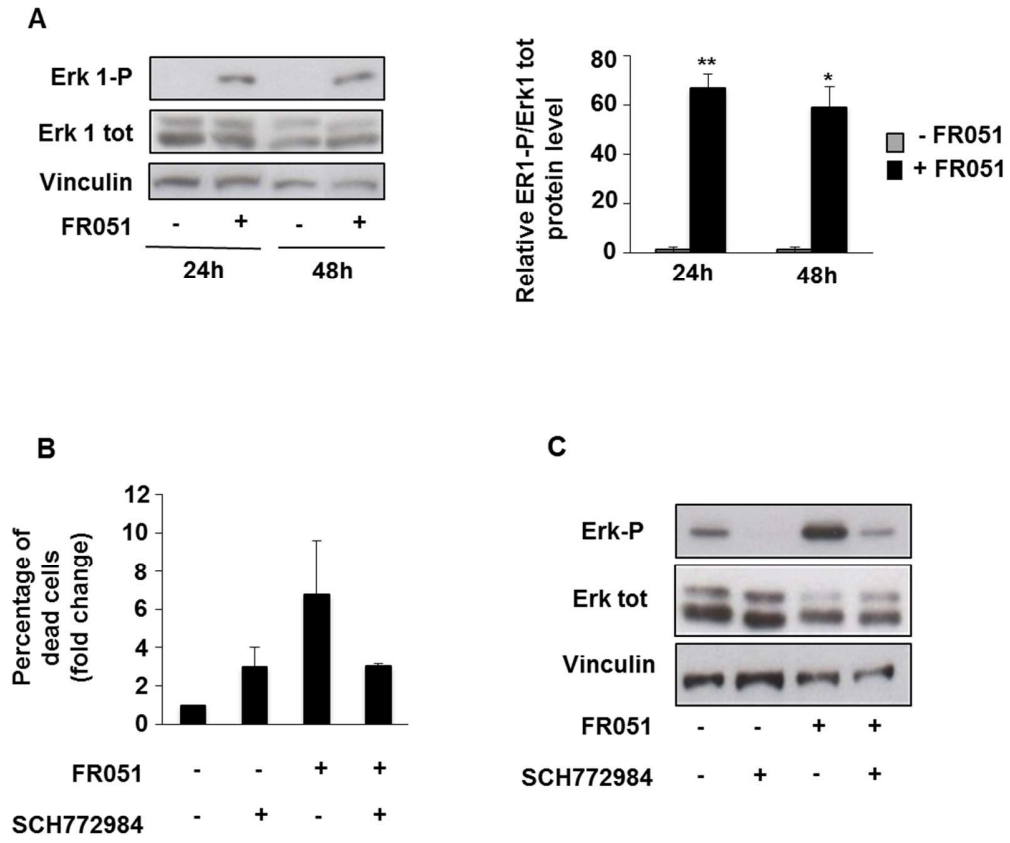

Figure 20. Apoptotic mechanism is mediated by activation of Erk1/2 signal transduction. A. MDA-MB231 cells were treated with FR051 (for 24 and 48 hours) and phosphorylation status of Erk Thr42/Tyr44 was analysed by a specific antibody. Vinculin was used as loading control. **B.** Cancer cells were pre-treated with Erk1/2 inhibitor (SCH772984) and then with FR051. Percentage of cell death was determined by TB staining after 24 and 48 hours of FR051 treatment. **C.** Western Blot analysis of ERK phosphorylation (Erk-P), total-Erk (Erk tot) and vinculin after FR051 and SCH772884 treatments.

All data represent the average of at least three indipendent experiments (± s.d.); *p<0,05 (Students's t-test).

Synthesis and characterization of FR053: the de-acetylated counterpart of FR051

In order to exclude any extracellular unspecific effect of the new molecules, all of them were initially synthetized in both acetylated and de-acetylated forms. In fact, as shown in several reports, de-acetylated compounds usually have a strong reduction of their ability to enter into the cells, preserving the same efficiency on the target *in vitro* assay (Wenling et al., 2005).

FR053, the deacetylated counterpart of FR051, synthesis followed the same procedure previously described for FR051, with the addition of de-acetylation step (on carbon 3, 4 and 6 of the ring) that was carried out in methanolic ammonia. NMR spectra of FR053 are summarized below: ^{1}H NMR (400 MHz, Methanol-*d*4) δ 6.03 (d, *J* = 7.3 Hz, 1H, **H1**), 3.99 (m, 1H, **H2**), 3.87 (t, *J* = 3.7 Hz, 1H, **H3**), 3.77 (dd, *J* = 12.0, 2.5 Hz, 1H, **H6a**), 3.67 – 3.61 (dd, *J* = 6.8 Hz, 1H, **H6b**), 3.55 – 3.50 (m, 1H, **H4**), 3.33 (ddd, *J* = 12.0 Hz, 2.4Hz, 6.4 Hz, 1H, **H5**), 2.03 (s, 3H, **CH_3**) **(Figure 21A)**.

cLogP and docking score of FR053 were compared to that one of FR051. As expected while the docking score of FR053 was equal to that of FR051, its cLogP resulted to be lower as compared to one calculated for FR051 **(Figure 21B)**. On the basis of these observations, MDA-MB-231 cancer cells were treated with increasing concentrations of FR053, as previously

performed with FR051. Cell proliferation and viability were analyzed after 24 and 48 hours from the treatment. As shown in **Figure 21C**, FR053 did not have any affect either on cell proliferation or cell viability. Importantly, FR053 did not have any effect also on membrane protein N-glycosylation levels, since live cells stained with PHA-L **(Figure 21D)** did not show any change as compared to untreated cells. All these data suggested that, for its action, FR051 have to enter into the cells since its de-acetylated form does not interfere with cell proliferation, survival and N-glycosylation protein.

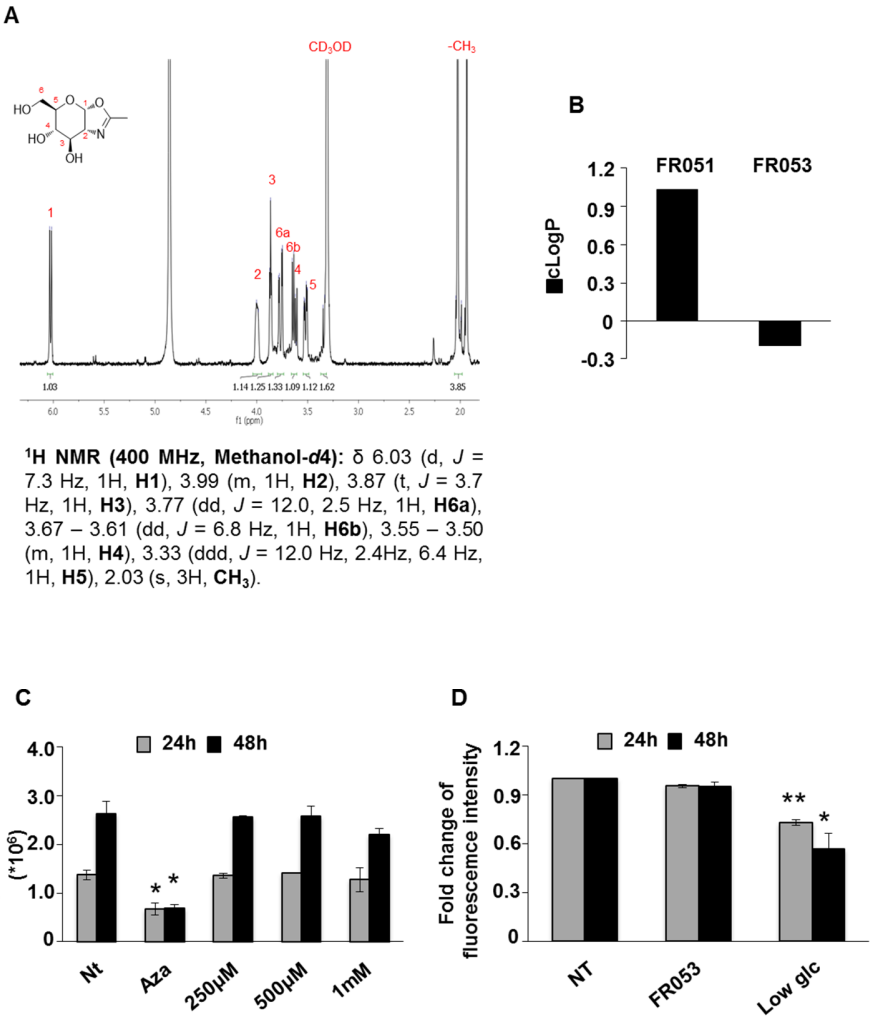

^{1}H NMR (400 MHz, Methanol-*d*4): δ 6.03 (d, *J* = 7.3 Hz, 1H, **H1**), 3.99 (m, 1H, **H2**), 3.87 (t, *J* = 3.7 Hz, 1H, **H3**), 3.77 (dd, *J* = 12.0, 2.5 Hz, 1H, **H6a**), 3.67 – 3.61 (dd, *J* = 6.8 Hz, 1H, **H6b**), 3.55 – 3.50 (m, 1H, **H4**), 3.33 (ddd, *J* = 12.0 Hz, 2.4Hz, 6.4 Hz, 1H, **H5**), 2.03 (s, 3H, **CH_3**).

Figure 21. Synthesis and characterization of FR053. **A.** Chemical structure and NMR spectra of N-acetyl-1-deoxy-α-D-glucosamine or FR053. **B.** clogP of FR053, compared to that one of FR051, were analyzed using Schrodinger 10.1 Maestro software. **C.** Cell proliferation was determined counting the cells at indicated time points. aza was used as the positive control. Cell viability was analyzed by TB staining. **D.** After 24 and 48 hours of treatment, FACS analysis of live cells was performed upon staining with PHA-L for detection of N-glycans. Cells grown in low glucose (low glc) were used as positive control

for N-glycosylation level decrease. All data represent the average of at least three indipendent experiments (± s.d.); *p<0,05 (Students's *t-test*).

FR051 treatment affects cell viability also in other breast cancer models

Considering histological type, tumour grade, lymph node status, presence of predictive markers (like estrogen receptor and human epidermal growth factor receptor 2 (HER2) and positivity to HER2-), breast cancer results a complex and heterogeneous disease (Holliday and Speirs, 2011). Indeed, breast cancer cell lines show a different genomic background especially regarding the Estrogen Receptor (ER), Progesterone Receptor (PrR) and Erb-B2 Receptor (ERBB) status: MDA-MB-361 (adenocarcinoma), Skbr-3 (adenocarcinoma), BT-474 (ductal carcinoma), Mcf7 (adenocarcinoma), T-47D (ductal carcinoma) **(Figure 22)**.

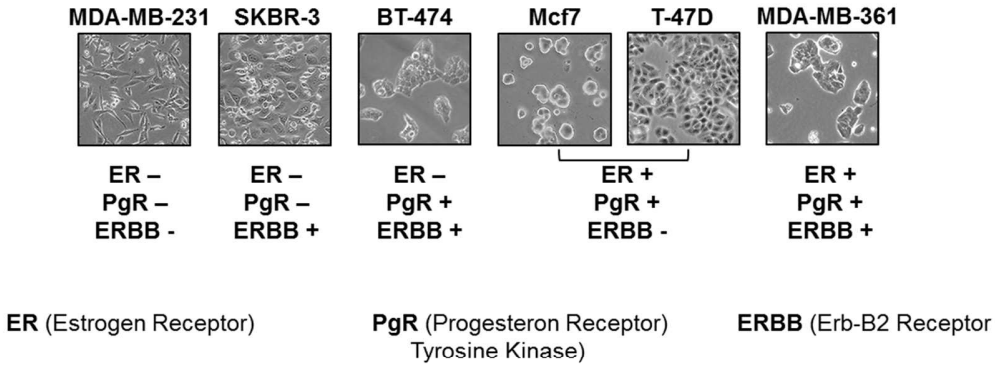

Name	Tissue	Cell type	Disease
MDA-MB-231	mammary gland; breast: pleural effusion	epithelial	adenocarcinoma
SKBR-3	mammary gland; breast: pleural effusion	epithelial	adenocarcinoma
BT-474	mammary gland; breast/duct	epithelial	ductal carcinoma
Mcf7	mammary gland; breast: pleural effusion	epithelial	adenocarcinoma
T-47D	mammary gland; breast/duct: pleural effusion	epithelial	ductal carcinoma
MDA-MB-361	mammary gland; breast: brain	epithelial	adenocarcinoma

Figure 22. Breast cancer cell lines and relative features. Phase contrast images of breast cancer cell lines with their positivity for the Estrogen receptor, Progesterone receptor and Erb-B2 receptor. Informations about breast cancer cell lines are summarized in the table.

After FR051 characterization in MDA-MB-231 cells (triple negative breast cancer model) we decided to test the effectiveness of the molecule on all breast cancer cell lines previously described. They were cultured in HG and then treated with different concentrations of FR051. Cell viability assay was carried out upon 48h of treatment. Notably, all the breast cancer cells resulted more sensitive to the FR051 treatment as compared to MDA-MB-231 cells. In particular, Skbr-3 and BT-474 cell survival was affected to a concentration of 100µM, which is 10 fold less of MDA-MB-231 cells **(Figure 23A-F)**.

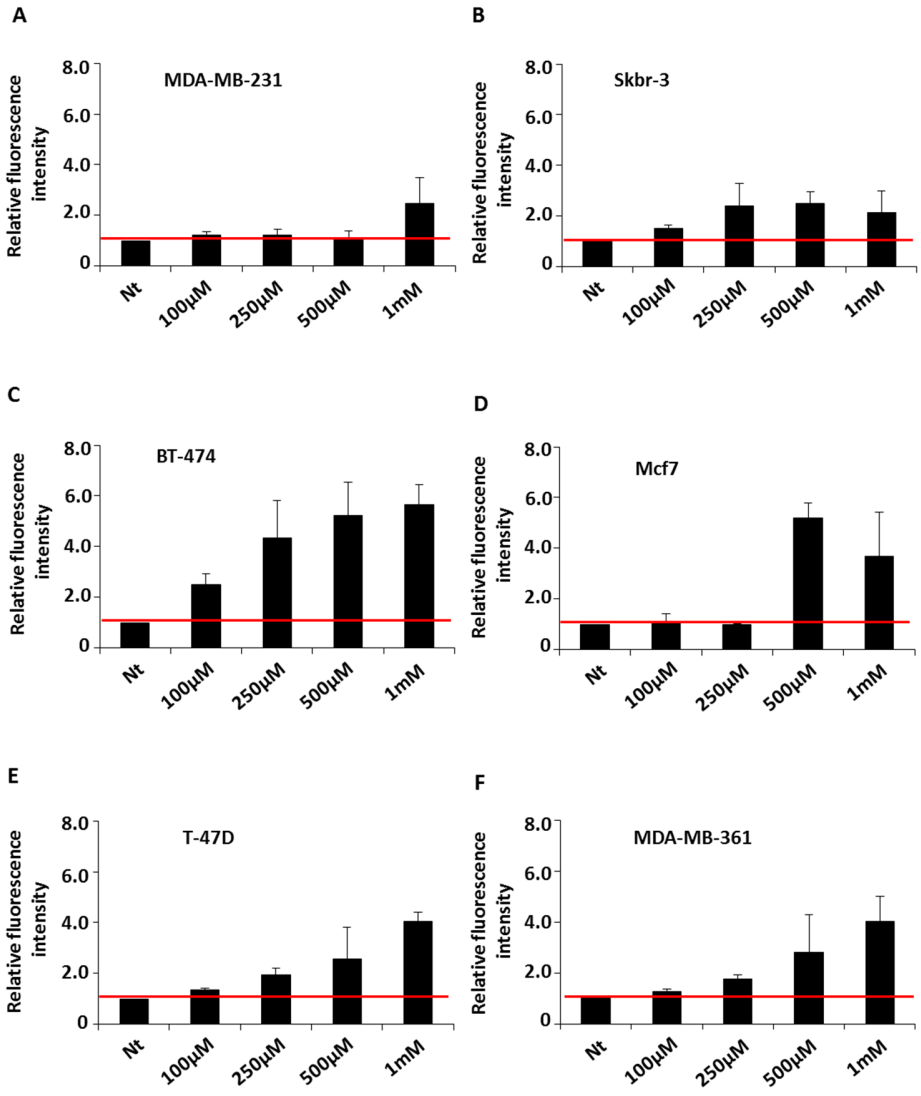

Figure 23. FR051 treatment increases cell death of breast cancer cell lines. A-F. Breast cancer cell lines were plated in HG and then treated with different concentrations of FR051. After 48h of treatment cell death (fold change of fluorescence intensity) was

evaluated by using a specific kit. All data represent the average of at least three independent experiments.

Analysis of protein expression of HBP involved enzymes, N- and O-glycosylation level

In order to define the relevance of HBP in the breast cancer cell lines previously described, some HBP related parameters including protein level of GFAT1 (first HBP enzyme), PGM3 (target of interest), UAP1 (last HBP enzyme), OGT and the basal status of the N- and O-glycosylation levels, were analyzed as possible readout of HBP flux. All the cell lines showed almost the same GFAT1 levels (except for BT-474) while UAP1 protein level decreased ranging from MDA-MB-231 to MDA-MB-361 **(Figure 24A and B)**. While the PGM3 mRNA level was almost similar in all the cell lines **(Figure 25)**, by contrast its protein levels were quite different. In fact MDA-MB-231 and T-47D showed the lower expression, BT-474, MDA-MB-361 and Skbr-3 an intermediate expression and Mcf7 the highest expression **(Figure 24A and B)**. Although the GFAT1, PGM3, UAP1 and OGT protein level were different among the different breast cancer cell lines analyzed, we were not able to correlate their different sensitivity to FR051 treatment with any specific HBP enzyme.

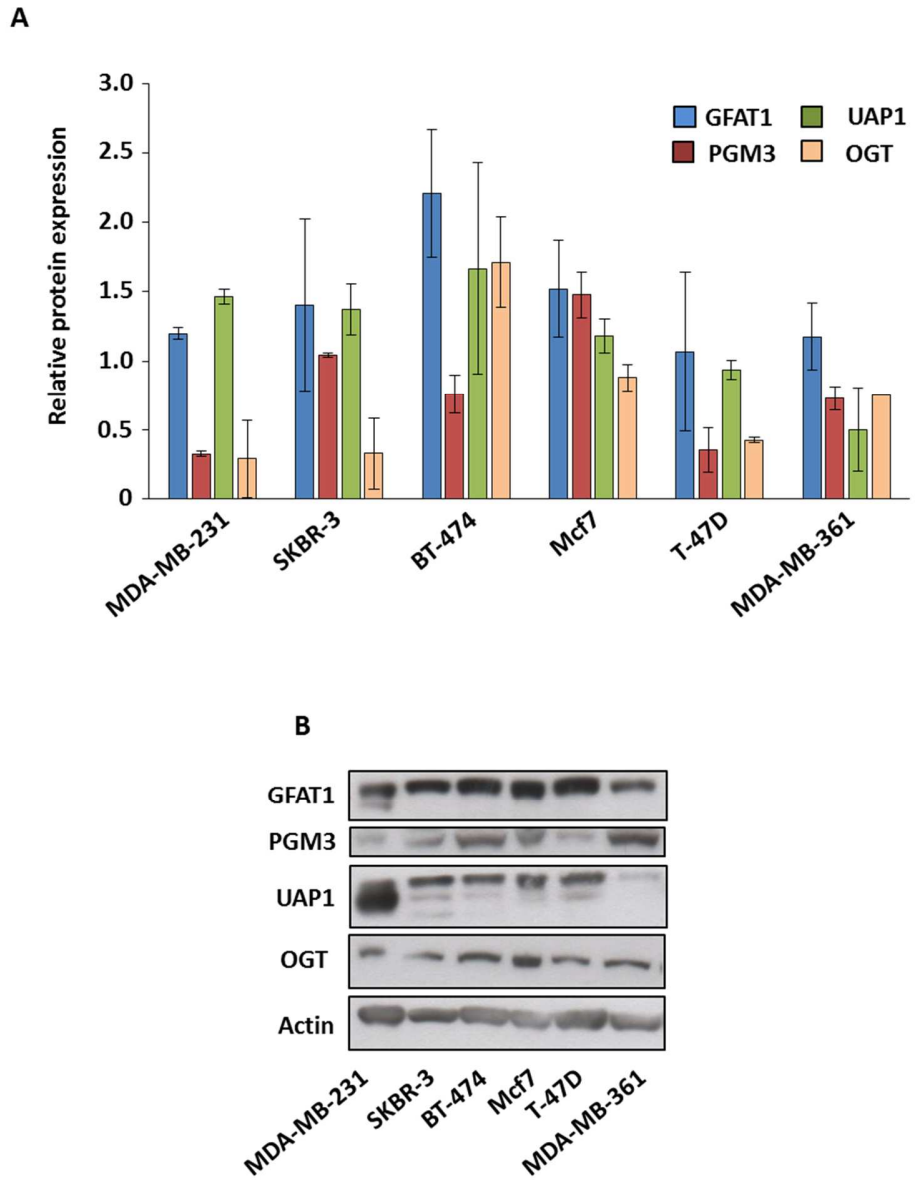

Figure 24. Basal levels of some HBP enzymes. A.-B. Analysis of GFAT1, PGM3, UAP1 and OGT protein level in all breast cancer cell lines, grown in HG. All data represent the

average of at least three independent experiments (± s.d.).

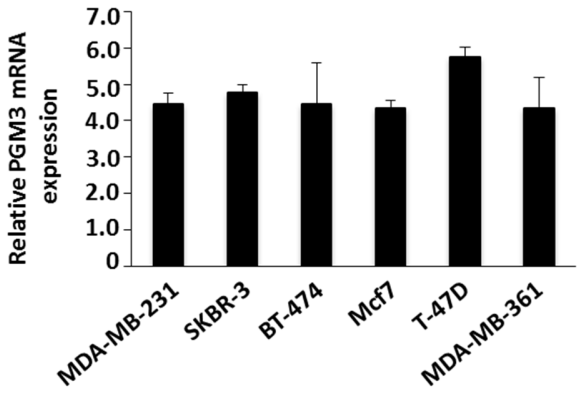

Figure 25. mRNA level of PGM3 in basal conditions. Analysis of mRNA level of PGM3 in all breast cancer cell lines, grown in HG. All data represent the average of at least three independent experiments (± s.d.).

A flow-cytometric analysis (using *P.vulgaris* lectin) displayed a low N-glycosylation level in Skbr-3, an intermediate level in T-47D, BT-474, Mcf7 and MDA-MB-361, and a high level in MDA-MB-231 **(Figure 26A).**

An immune-blot, for detection of the O-glycosylated proteins, revealed a different O-GlcNAc level among cancer cells (low level in Bt-474, T-47D and MDA-MB-361, intermediate level in MDA-MB-231 and Mcf7, higher level in Skbr-3) **(Figure 26B)**.

Correlation between some of the analyzed HBP parameters and FR051

sensitivity has been summarized in **Table 2.**

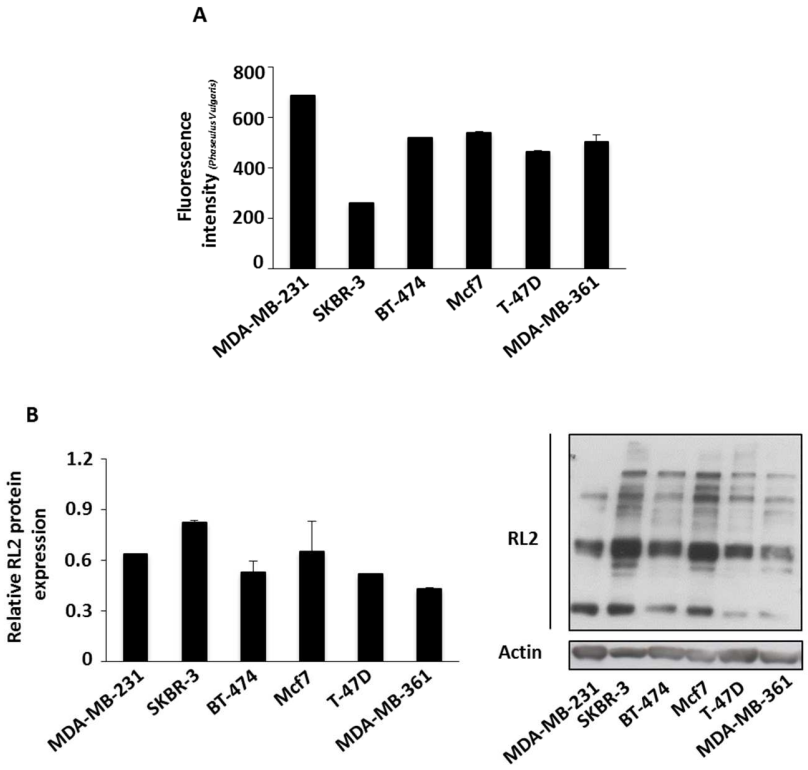

Figure 26. Basal level of N-/O-glycosylation. Analysis of **A.** N- and **B.** O-glycosylation level of in all breast cancer cell lines, grown in HG. All data represent the average of at least three independent experiments (± s.d.).

Table 2. Relative value of the HBP parameters and of FR051 sensitivity identified in the

different breast cancer cells (low (+), intermediate (++), high (+++) level).

Cell line	PGM3 protein level	O-gly level	N-gly level	FR051 sensitivity
MDA-MB-231	+	++	+++	+
SKBR-3	++	+++	+	+++
BT-474	++	+	++	+++
Mcf7	+++	++	++	++
T-47D	+	+	++	++
MDA-MB-361	++	+	++	++

Pancreatic Ductal Adeno Carcinoma (PDAC) cancer cell lines

Many evidences highlighted the key role of HBP in pancreatic cancers. For instance, Pancreatic Ductal Adeno Carcinoma (PDAC) cells exhibit high levels of O-GlcNAc glycosylated proteins due to up-regulation of GFPT1, GFPT2, and OGT, and low levels of OGA (Ma et al., 2013). In addition it has been shown that membrane expression of several Tyrosine Kinase Receptors (EGFR, ErbB2, ErbB3, and IGFR) is affected by *Tun* treatment in PDAC (Contessa et al., 2008). Since such metabolic pathway appears to be more important in pancreatic tumors as compared to breast tumors, we decided to test the effect of HBP inhibition in three different pancreatic cancer cell lines. In particular we used Mia Paca-2 (primary tumor carrying 12Cys K-ras mutation), BxPc-3 (primary tumor carrying no K-ras mutations) and Capan-1 (liver metastasis carrying 12Val mutation) (Deer et al., 2010).

In the first set of experiments, we used the two well-known inhibitors, *Aza* and *Tun*, previously described. All PDAC cell lines were plated in HG conditions (11,1 mM) and cell proliferation was analyzed after 24, 48 and 72 hours of treatment. As shown in **Figures 27A-C**, pancreatic cancer cells proliferation was impaired in dose and time dependent manner by *Aza* treatment. Importantly no appearance of cell death was observed along the 72 hours of treatment in Mia Paca-2 cell line. Conversely, at same time point (72h), high dose of treatment affected BxPC-3 and Capan 1 viability.

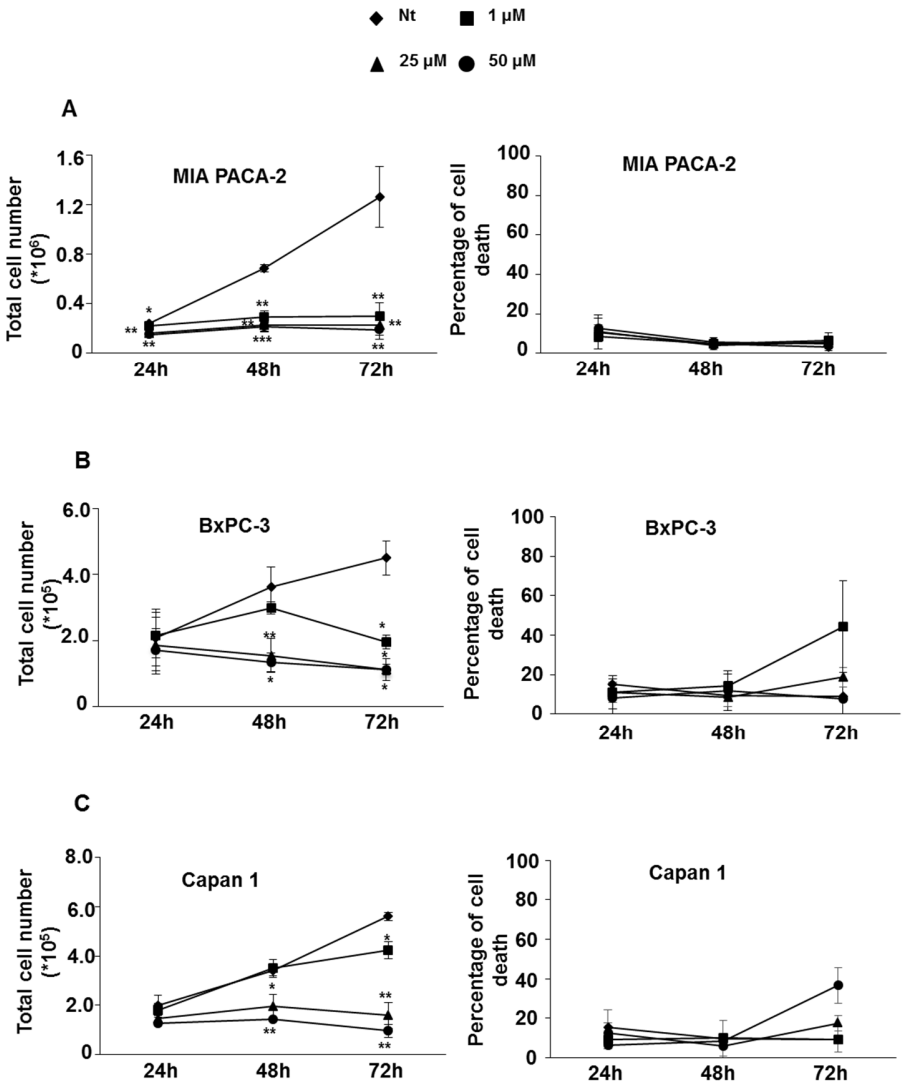

Figure 27. Proliferation of PDACs is affected by azaserine treatment. A. MIA PACA-2, **B.** BxPC-3 and **C.** Capan 1 were plated in high glucose conditions (11,1 mM) and then treated with different concentration of azaserine. Proliferation was analyzed after 24h, 48h and 72h of treatment. All data represent the average of at least three independent experiments (± s.d.); *p<0,05 (Students's *t-test*).

Conversely, *Tun* treatment, affected both cell proliferation and cell survival, in dose and time dependent manner **(Figure 28A-C)**. Altoghether these findings suggested an even more important role of HBP in pancreatic cancer cells as compared to breast cancer cells, since the same effects on cell proliferation and survival were observed at lower drug concentrations **(compare Fig. 1A-D to Fig. 28A-C)**.

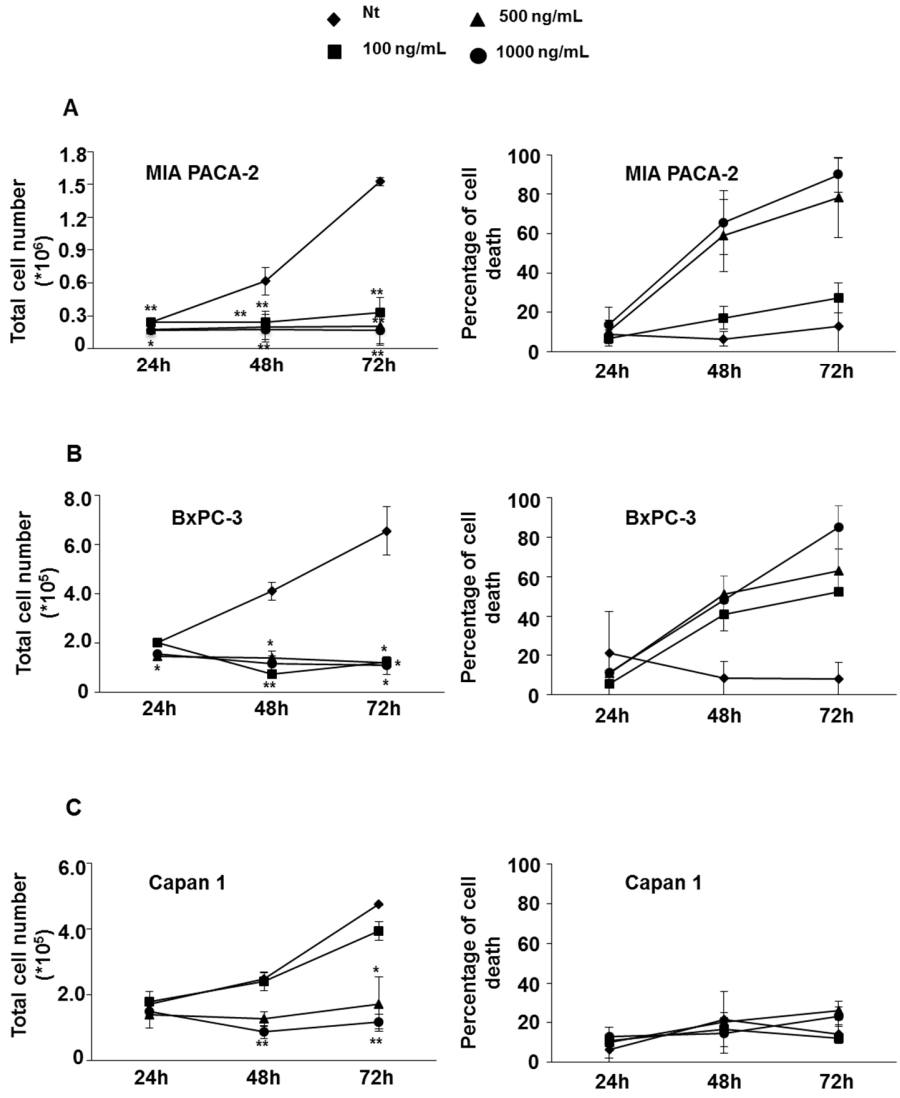

Figure 28. Tunicamycin blocks cell proliferation and increases cell death

A. MIA PACA-2, **B.** BxPC-3 and **C.** Capan 1 were plated in high glucose conditions (11,1 mM) and then treated with different concentration of tunicamycin. Proliferation analysis was performed after 24h, 48h and 72h from treatment. All data represent the average of at least three independent experiments (± s.d.); *p<0,05 (Students's *t-test*).

PDAC cancer cell lines are affected by FR051 treatment

Since previous data indicated an important role of HBP, the three pancreatic cancer cells, Mia Paca-2, BxPC-3 and Capan1 grown in HG, were treated with different concentrations of FR051.

Fluorescent intensity, indicating level of cell death, showed a high sensitivity to FR051 of pancreatic cancer cells as compared to breast cancer cells **(Figure 29A-C. left panels)**. In addition, caspase 3 analysis, indicated also in these cell lines a strong activation, confirming the ability of FR051 to induce apoptosis **(Fig. 29A-C. right panels).**

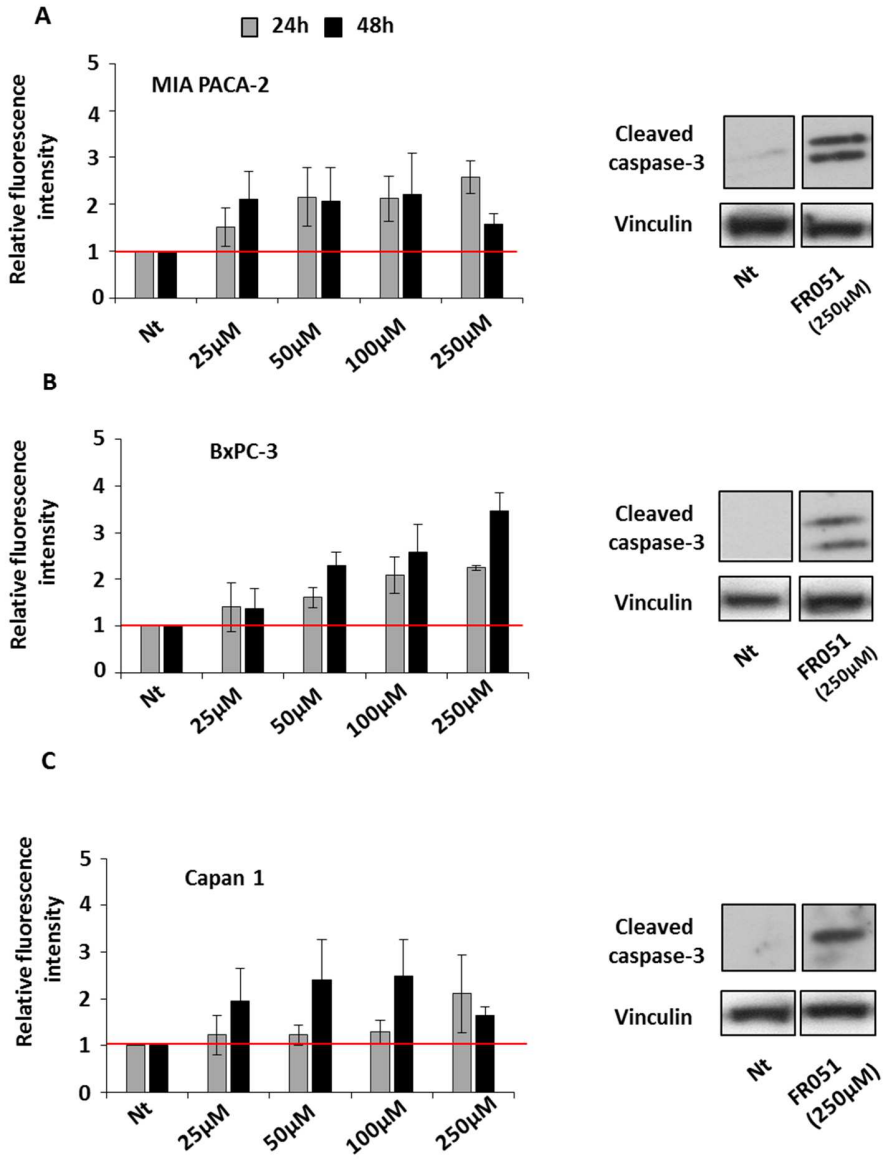

Figure 29. FR051 treatment increases cell death of PDACs. A-C. Pancreatic cancer cell lines were plated in HG and then treated with different concentrations of FR051. After

48h of treatment cell death (fold change of fluorescence intensity) was evaluated by using a specific kit. All data represent the average of at least three independent experiments.

Analysis of HBP related enzymes and glycosylation level

Analysis of some HBP parameters were performed also in pancreatic cancer cells as possible readout of HBP flux.

GFAT1 protein level was lower in Mia Paca-2, intermediate in Capan1 and high in BxPC-3; OGT and UAP1 showed the same different levels in PDACs cells (higher in Mia Paca-2, intermediate in BxPC-3 and lower in Capan1) **(Figure 30A and B)**.

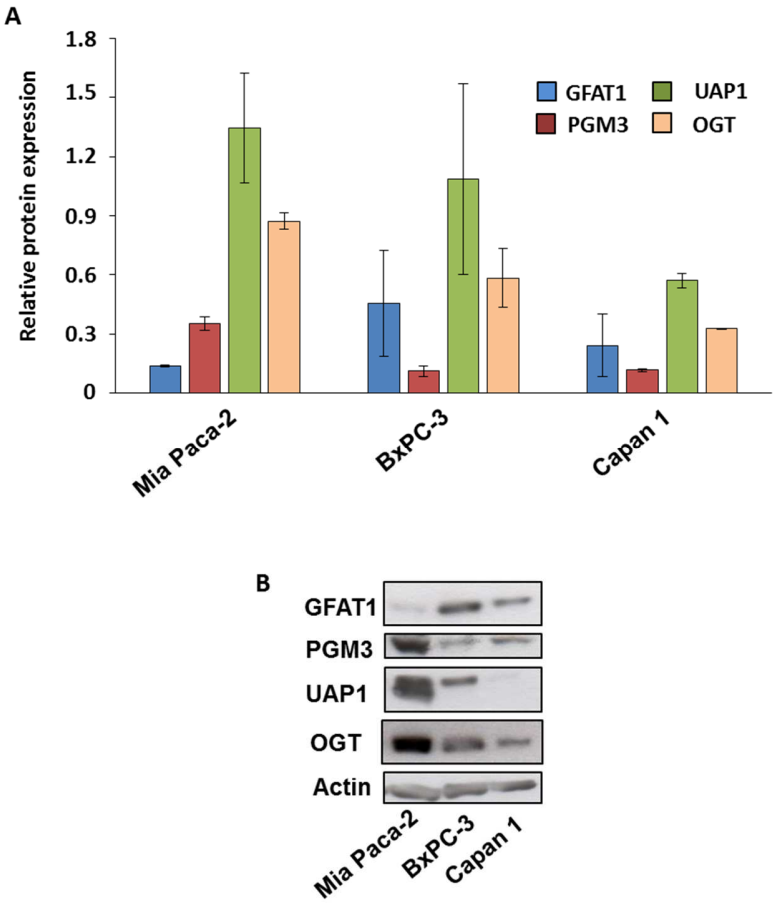

Figure 30. Basal level of HBP enzymes. A. B. Analysis of GFAT1, UAP1, PGM3 and OGT protein level in all PDAC cancer cell lines, grown in HG. All data represent the average of at least three independent experiments (± s.d.).

PGM3 protein levels were higher in Mia Paca-2 as compared to BxPC-3 and Capan1 (their protein level is similar) **(Figure 30)**, by contrast PGM3 mRNA level was equal in Mia Paca-2 and BxPC-3 cells, while it resulted higher in Capan1 **(Figure 31)**.

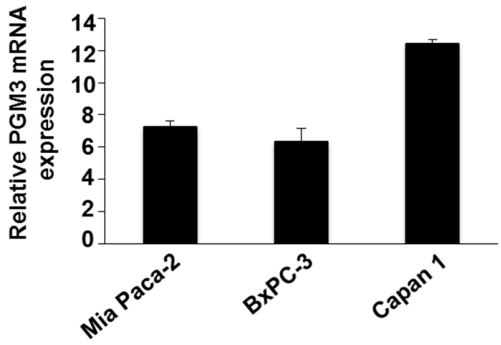

Figure 31. Basal level of PGM3 in Pancreatic Ductal Adenocarcinoma cell lines. Analysis of **A.** mRNA and **B.** protein level of PGM3 enzyme in all pancreatic ductal adenocarcinoma (PDAC) cell lines, grown in HG. All data represent the average of at least three independent experiments (± s.d.).

Finally, analysis of N-glycosylation did not reveal any differences among PDACs **(Figure 32A)** while O-glycosylation resulted to be lower in BxPC-3, intermediate in Mia paca-2 and higher in Capan1 **(Figure 32B)**. In the latter PDAC, O-glycosylation level did not correlate with OGT protein level, this can be due to the fact that Capan1 cells secrete high amount of mucin that is reported to be highly O-glycosylated (Lan et al., 1990).

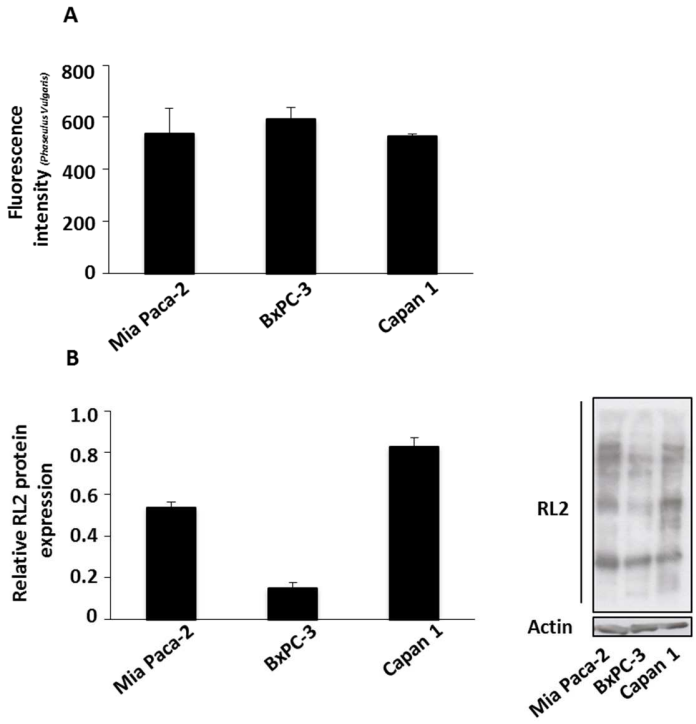

Figure 32. Basal level of N-/O-glycosylation. Analysis of **A.** N- and **B.** O-glycosylation level of in all pancreatic ductal adenocarcinoma cell lines, grown in HG.
All data represent the average of at least three independent experiments (± s.d.).

Analysis of some HBP parameters and sensitivity to FR051 treatment were summarized in **Table 3**.

Table 3. Relative value of the HBP parameters and of FR051 sensitivity identified in the different breast cancer cells (low (+), intermediate (++), high (+++) level).

Cell line	PGM3 protein level	O-gly level	N-gly level	FR051 sensitivity
Mia Paca-2	+++	++	+	+++
BxPC-3	++	+	+	++
Capan 1	++	+++	+	+

Discussion

It is well reported the ability of cancer cells to rewire their metabolism in order to support enhanced proliferation and survival especially in stress conditions (DeBerardinis and Cheng, 2010).

Among metabolites, glucose and glutamine are mostly used in cancer cells for several purposes like energy need, amino acid and fatty acid synthesis, redox balance through their utilization in several metabolic pathways (DeBerardinis and Cheng, 2010). Recently, several researchers have focused their attention also on the HBP. In fact this metabolic route is able to integrate the metabolism of glucose and glutamine with that of fatty acid (acetyl-CoA) and nucleotides (uridine-diphosphate). Hence, UDP-GlcNAc, the end product of the five reactions of HBP, can be identified as the "sensing molecule" of nutrients (Hanover et al., 2012).

UDP-GlcNAc is the substrate for enzymes involved into O-/N-glycosylation, two important post-translational modifications, identified in more than 50% of their possible targets, like lipids and proteins engaged in numerous cellular functions (Hanover et al., 2012). Thus alteration of O-/N-linked GlcNAc modifications have been linked to various human diseases, including cardiovascular disease, neurodegenerative disorders, diabetes mellitus, and cancer (Ozcan et al., 2010).

To understand a possible role of HBP, the precursor pathway involved in providing the substrate for these modifications, we used the triple negative breast cancer cell (TNBC) line MDA-MB-231 (Palorini et al., 2013a) (Palorini et al., 2016) (Palorini et al., 2013b). TNBCs, indeed, lacking

estrogen and progesterone receptors and the overactive HER2, that drive other forms of this disease, are largely treated with decades-old chemotherapies, surgeries and radiation techniques, since patients do not benefit from endocrine therapy or HER2-targeted therapy. Therefore, the identification of more targeted and/or efficient therapies in TNBC is an important need and a challenge. Moreover, recent studies performed in different breast cancer cells and tissues as compared to normal counterparts clearly reported an increase of complex glycans (i.e. tri- and tetra-antennary structures) on cell surface especially in metastatic cell lines and tissues as well as in TNBC (Christiansen et al., 2014). On the other hand, elevated *O*-GlcNAcylation has been described in breast cancer and reduction of protein *O*-GlcNAcylation inhibits cancer cell invasion *in vitro* and metastasis *in vivo* (Gu et al., 2010).

These cells have been initially treated with two well-known inhibitors of HBP: *Aza* and *Tun* (Rajapakse et al., 2009) (Chatterjee et al., 1981). MDA-MB-231 cells, grown in optimal growth conditions (HG), showed a reduction of both proliferation and cell survival in dose and time dependent manner after the treatments with the two inhibitors **(Figures 1A, B, C and D)**. These data confirmed a key role of HBP in MDA-MB-231 cancer cell survival and proliferation.

In the last decades, some HBP modulators have been synthesized in order to restore normal levels of glycosylation also in cancer. However, their low

specificity and their ability to target only one of the two HBP branches, has raised the necessity to synthesize new more specific and effective modulators (Vibjerg Jensen et al., 2013).

To inhibit the HBP flux we have decided to design and synthetize different compounds targeting PGM3 enzyme, a phospho acetyl-glucosamine mutase 3 involved in one of the final steps of HBP. Its relevance is confirmed by its evolutionary conservation (i.e. E.coli, S.cerevisiae, H.sapiens), and by the fact that gene knockdown in mouse model resulted lethal at early embryonic stage.

A library of new molecules, targeting PGM3, has been designed **(Table 1)** in collaboration with Prof. La Ferla using GlcNAc-6-P or GlcNAc-1-P as templates; in this way the new molecules putatively will compete with the natural substrate or product, for the catalytic binding site of enzyme.

In order to identify new useful molecules, in collaboration with chemists, a computational analysis was performed leading to classification of new compounds according to values of docking score (Kj/mol) and cLogP **(Figure 2)**. The first one represents the value of binding strength between target protein and molecule, while the second one is the logarithm of partition coefficient between n-octanol and water (log ($c_{octanol}/c_{water}$)) measuring the compound's hydrophilicity.

All molecules, with relevant docking score were synthetized. In particular,

during first part of my PhD, I synthetized 2-Methyl-(3,4,6-tri-O-acetyl-1,2-dideoxy-α-D-glucopyrano)-[2,1-d]-2-oxazoline or molecule #8 **(Figure 3)** (Haddoub et al., 2009), while the other ones were synthetized by our collaborators.

Once synthetized, new molecules were screened *in vitro*, in order to select only the best hit(s) able to have an effect on cancer cell proliferation and survival. For this purpose, we used MDA-MB-231 cancer cell line as model system. In the context of the library, only two molecules (molecules #6 and #8) increased cell death after 48 hours of treatment. We decide to focalize the attention on molecule #8, recalled FR051, because it resulted to be the most efficient **(Figure 4)**, since its cLogP was the lowest one as compared to the other molecules and it showed the best docking score value **(Figure 2).** Thus, we decide to better characterize the effects of this molecule on cell proliferation, cell death, glycosylation, in order to define its action mechanism.

For a deeper investigation, MDA-MB-231 cells were seeded in optimal growth conditions and then treated with different concentration (100µM-1mM) of FR051 **(Figure 5A)**. After 24 hours, it induced, in dose and in time dependent manner, a cell proliferation arrest, a pronounced cell detachment and an increase of cell death **(Figures 5B and C)**. Strikingly, after 72 hours of treatment all the cells were floating and almost all dead **(data not shown)**, suggesting that FR051 has stronger effect than *Aza* on

cell proliferation, cell morphology, cell survival and clonogenic ability **(Figures 5E and 6)**.

In the perspective of human therapy, new molecule needs to be also tested on normal cells. We compared cell death level, after FR051 treatment, of Wi38 cell line, a normal human lung fibroblast, to that of MDA-MB-231. We decided to use Wi38 because it is a primary cell line, without any kind of gene changes typical of immortalized cells. These cells were less susceptible to the actions of the compound **(Figure 7)**, particularly at doses lower than 1 mM. In this way we could exclude issues regarding FR051 toxicities against normal cells and we could move to further characterization of the new compound. In all the experiment we decided to use highest FR051 dose, in order to study its effects in a small time window.

According to data showed in **Figure 5C**, we revealed the ability of FR051 to drive cells toward an apoptotic cell death **(Figures 8A and B)**.

Since HBP inhibition reduces the UDP-GlcNAc amount, leading to decrease of both kind of glycosylation, we decided to analyze the O- and N-linked glycosylation status upon FR051 treatment, trying to understand whether this molecule really affects HBP. Surprisingly, the analysis of O-glycosylation variation, revealed an early increase of O-GlcNAc level and a change of protein pattern **(Figure 9).** In accordance to recent evidences, this phenomenon can be explained with the necessity of the cells to mitigate the reduced HBP flux by increasing, for instance, the OGT protein

level (Darley-Usmar et al., 2012; Ngoh et al., 2009) **(Figure 10D)**. However, prolonged inhibition of HBP flux, as observed at 48h of analysis for both O- and N-glycosylation **(Figure 9)**, resulted in cell death **(Figures 5C and 8)**.

In addition, since O-glycosylation level depends on the activity of OGT and OGA enzyme **(Figure 10A)** (Slawson and Hart, 2011), we investigated also about mRNA level of both enzymes, trying to obtain a correlation with O-glycosylation changes. A quantitative Real Time PCR analysis revealed a strong down-regulation of mRNA of both enzymes **(Figures 10B and C)**, while as it was mentioned before, OGT protein level increased until 24h. These data revealed a post-transcriptional mechanism of control of OGT. Indeed, it has been shown that OGT stability and activity also depend on its glycosylation status (Whelan et al., 2008).

Also N-glycosylation was investigated distinguishing the different types of N-glycans on cell surface, hybrid/bi-antennary from tri- and tetra-antennary glycans. FR051 treatment did not change hybrid and bi-antennary glycans level **(Figure 11A)**, while the level of tri- and tetra-antennary decreased especially after 48 hours of treatment **(Figure 11B)**. This can be explained referring to the different affinities of Alpha-1,3-mannosyl-glycoprotein 2-beta-N-acetylglucosaminyltransferases I, II, III, IV, V (GlcNAC-T-I, II, III, IV, V) enzymes for a common substrate (K_m for UDP-GlcNAc). Indeed, this affinity decreases from GlcNAC-T-I to -V enzymes, meaning that activity of last enzymes is impaired in presence of

small amount of substrate (Dennis et al., 2009a). The induction of cell death in FR051 treated cells may be also the consequence of the membrane reduction of pro-survival receptors like tyrosin kinase receptors. Indeed it has been demonstrated that, while simple glycan structures (high mannose, hybrid and mono-antennary glycans) are associated to proteins involved in cell death, the more complex structures (such as tri- and tetra-antennary) are associated to pro-proliferation and survival proteins (Dennis et al., 2009b).

As reported in the introduction section, glycoconjugates participate in many key physiological processes including cellular adhesion, migration, proliferation and receptor activation. Increased HBP flux leads to hyper N-glycosylation enhancing major aggressiveness, adhesion and invasion, typical hallmarks of cancer. Upon FR051 treatment, the morphological changes (i.e. reduction of length of filopodia) and the cell detachment **(Figure 5E)** were associated to the reduction of membrane N-glycans **(Figure 11A and B)**. Importantly, this effect is also associated to a strong reduction of cancer cells adhesion and migration **(data not shown)**, confirming previous findings. It has been demonstrated a relation between a reduction of protein N-glycosylation and a reduction of both adhesion and migration (Zheng et al., 1994) (Gu and Taniguchi, 2008).

As it is well known, HBP flux is refuelled of GlcNAc by NAGK activity. This enzyme is involved in the salvage pathway and its main action is to recycle

GlcNAc from the environment producing GlcNAc-6-P. Since PGM3 reaction is downstream the salvage pathway, we decide to co-treat cells with FR051 and GlcNAc focusing the attention on cell proliferation and cell death. Also in this condition, FR051 was able to block cell proliferation **(Figure 12A)** and to lead to apoptosis as confirmed by cleaved caspase-3 detection **(Figure 12B)**. GlcNAc effectiveness was ensured by the rescue of phenotype in low glucose (1 mM glc) treated samples.

Altogether these findings strongly suggest a direct inhibition of FR051 on PGM3 activity.

As I mentioned before, N-glycosylation is an important post-translational modification involved in protein folding, mechanism that occurs into ER. Indeed, about one-third of newly synthetized proteins are translocated into ER where they fold and assemble with the assistance of several chaperones. When proteins do not fold correctly, their accumulation leads to alteration of ER homeostasis, and according to the intensity and duration of this stress condition, different pathways (pro-survival or pro-death) of UPR are activated (Minamino et al., 2010). The decrease of N-glycosylation level led us to investigate in more detail UPR activation. HSPA5 mRNA and its relative protein level (Grp78) were down regulated **(Figure 13A)**, probably due to the prolonged stressful conditions induced by FR051 treatment. Analysis of mRNA revealed an up-regulation of ATF4 (one of the few transcribed and translated gene during ER stress) **(Figure**

13B) and its direct pro-apoptotic target DDIT3/Chop, which increased at both mRNA and protein levels **(Figure 13C and D)**. This result suggests that the activation of PERK sub-pathway, involved in UPR-dependent cell death, may be the main mechanism involved in FR051 effect. Conversely, the ATF6 and Ire1 pathways, both involved in the prosurvival response upon ER stress, appeared less active. In fact while ATF6 is the main regulator of Xbp1 mRNA expression (Mimura et al., 2012) (Margariti et al., 2013), Ire 1 is directly involved in its splicing. Analysis of mRNA level and splicing clearly indicated that Xbp1 was transcribed at higher level than untreated samples **(Figure 13E)**, but it was not spliced upon FR051 treatment **(Figure 13F)** revealing the ATF6 activation and Ire1 inhibition. This is extremely interesting since unspliced Xbp1 has been associated with IRE1-dependent mRNA decay (RIDD) activation. This activity, often associated to cell death, is another important RNase activity whose role is to degrade mRNAs at consensus site, generating mRNA fragments that will be completely degraded by cellular exoribonucleases (Hiramatsu et al., 2015). Unlike to Xbp1 splicing that has a cytoprotective effect during acute ER stress, increased RIDD level is associated to cell death under chronic stress conditions (Maurel et al., 2014).

In 2014, Zhao V.Wang et al. demonstrated a direct link between enzymes involved in HBP and UPR activation. According to the presence of UPRE in their promoter region, some HBP genes (i.e. GFAT1, PGM3, GNPNAT1, GalE) are transcribed only after the binding of active and spliced form of

Xbp1 to the UPRE sequence **(Figure 14)** (Wang et al., 2014). In correlation with the presence of only the unspliced form of Xbp1 in FR051 treated samples, both PGM3 and GFAT1 mRNAs resulted to be lower as compared to untreated samples **(Figures 15A and B)**. This was completely in agreement with data reported by Zhao V. Wang, suggesting that FR051 has a mechanism of action partially different from the normal UPR inducers such as *Th*, *Tun*, glucose starvation. On the contrary, protein level increased after 24h, probably due to a post-translational modification mechanism, and declined after 48h **(Figures 15C and D)**.

In order to avoid reduction of HBP flux, cancer cell reprogram their metabolism (Chiaradonna et al., 2012). Experimental observations support the link between the glycosylation status (especially O-glycosylation) and stability/activity of proteins involved in several metabolic pathways (Fardini et al., 2013) (Yi et al., 2012) (Tan et al., 2014). Given the HBP and metabolism relationship, residual glucose and produced lactate were measured. The data revealed only a slightly variation in glucose consumption **(Figure 16)** and lactate production **(Figure 16B)**, suggesting that FR051 treatment did not affect glucose consumption.

Conversely, upon 24h treatment, $DCFH_2DA$ signal increased in treated samples revealing the production of ROS in presence of FR051 **(Figure 17)**. This result is in part expected since UPR activation has been linked to an accumulation of ROS either in ER or in the cytoplasm, accumulation that

may lead to cell death (Malhotra et al., 2008). In particular, ROS levels increase during formation of disulphide bonds as a product of electron transport from thiol groups in proteins through PDI and Ero1 activity, leading to reduction of molecular oxygen (Sevier and Kaiser, 2008). To elucidate the relationship between ROS production and activity of Ero1, cells were treated with EN460 (Ero1 inhibitor) for 24 hours (Blais et al., 2010; Zito, 2015) and then treated with FR051 for further 24 hours. EN460 treatment slightly decreased both ROS level and the percentage of cell death as compared to sample treated with only FR051 **(Figure 18A and 18B)**. Other Authors have linked Ero1 to Chop activity and cell death (ERO1 is a transcriptional target of CHOP (Blais et al., 2010; Zito, 2015)).
The slightly reduction of cell death, upon Ero1 inhibition, suggested that FR051 treatment affects the cellular redox state through other mechanisms, which contribute to the increase of intracellular ROS level. In this regard, it is well known that mitochondrial electron transport chain is the main source of ROS (Panieri E. and Santoro MM., 2016). According to that, cells were co-treated with mitochondria-targeted antioxidant (MitoTempo) and FR051. As shown in **Figure 19A** MitoTempo treatment did not reversed the effect of FR051 on cell survival and ROS accumulation **(Figure 19B)**. However, the ROS increased (H_2O_2) level, and thus cell death, can be explained as the consequence of H_2O_2 accumulation (derived from O_2^- conversion performed by MitoTempo) in the cells. For this reason, we cannot still exclude an involvement of mitochondria-generated ROS in

FR051 effect. On the other hand, it is reported that in severe ER stress conditions, released Ca^{2+} from ER is taken up by mitochondria (Tadic et al., 2014), yielding to mitochondrial permeability transition pore (mPTP) opening, cytochrome C release and activation of caspase-mediated apoptosis. Caspase-dependent dismantling of the cell requires ATP whose amount is sustained by increased mitochondrial respiration, leading to ROS production (Szalai et al., 1999). In the future could be interesting a more detailed analysis of mitochondria activity, since it is strictly linked to ROS generation.

Since mitogen activated protein (MAP) kinases represent highly conserved signal transduction pathways for mediating cellular stress, we analysed the activation status of Erk1/2 protein by analyzing its phosphorylation levels upon FR051 treatment. As shown in **Figure 20A**, FR051 induced a strong increase of Thr42/Tyr44 phosphorylation, suggesting activation. Although traditionally Erk1/2 is thought to have a pivotal role in promoting cell survival, previously results **(Figure 8)** showing activation of apoptosis after FR051 treatment, made us to speculate whether Erk1/2 activation was associated to cell death. To further corroborate this observation, we pre-treated MDA-MB-231 with a specific Erk1/2 inhibitor SCH772984 (50nM) and then with FR051. Erk inhibition strongly reduced the percentage of cell death as compared to FR051 single treatment, revealing the pro-apoptotic role of Erk1/2 in our cell model **(Figure 20B and C)**. This result is in part supported also by some published

observations in which, it has been highlighted the association between Erk1/2 phosphorylation and the activation of UPR, after *Th* treatment (Arai et al., 2004; Futami et al., 2005).

To exclude that observed effects could be due to an unspecific effect of FR051 on cell membrane structure and to understand whether acetyl groups have a key role for molecule uptake, FR053 (the de-acetylated counterpart of FR051) was synthetized **(Figure 21A)**. This molecule, when added to MDA-MB-231 cells, did not affect their cell viability **(Figure 21C)** and their N-glycosylation level **(Figure 21D)**. These results (that can be explained by negative value of cLogP compared to that of FR051) revealed the role of acetylated groups on driving molecule into cells **(Figure 21B)**, as previously shown (Wenling et al., 2005) and furter underlined the specificity on HBP of FR051.

In order to understand whether FR051 could have affect also in other cancer models, we tested the molecule on other breast cancer cell lines: each of them representative of a subtype according to gene expression profiling and the immune-histochemical expression of ERα, PR and HER2 **(Figure 22)** (Holliday and Speirs, 2011).

We tested different concentrations of FR051 on MDA-MB-361 (ER^+, PgR^+, $ERBB^+$), T-47D and Mcf-7 (ER^+, PgR^+, $ERBB^-$), BT-474 (ER^-, PgR^+, $ERBB^+$), SKBR-3 (ER^-, PgR^-, $ERBB^+$) and on MDA-MB-231 (ER^-, PgR^-, $ERBB^-$), as positive control. All the mentioned cancer cell lines resulted to be more sensitive to the treatment as compared to MDA-MB-231 cells **(Figure 23A-**

F). For instance, BT-474 cells died using 100µM concentration that had no effect on MDA-MB-231.

To explain the reason of major sensibility, we analysed mRNA and protein level of our target of interest (PGM3). Although mRNA expression was similar from each other **(Figure 25A)**, PGM3 protein levels appeared to be slightly different in the different cell lines **(Figure 25B)**. Ranging from low to high expression level we found the following classification: (MDA-MB-231=T-47D)<(MDA-MB-361=BT-474)<(SKBR-3)<(Mcf7).

Then we analysed the protein level of some HBP enzymes (GFPT1, UAP1 and OGT) and basal O- and N-glycosylation level. Since both proteins level and glycosylation levels were highly variable among the different cell lines we were unable to find a direct correlation between sensitivity to FR051 and HBP pathway status. In the future will be interesting to measure UDP-GlcNAc or HBP flux to see if there is any a relation between sensitivity and rate of HBP.

PDAC is an aggressive disease, characterized by invasiveness, rapid progression and profound resistance to treatment, due to reduced vasculature and to surrounding stroma that protects cancer cells (Bardeesy and DePinho, 2002). Also PDAC show a strong metabolic reprogramming. Indeed, hypoxic regions display higher level of glycolysis as a consequence of glucose uptake (associated to aggressiveness) and lactate production in order to sustain proliferation (Guillaumond et al., 2013). Pancreatic cancer cell lines are also sensitive to glutamine

deprivation, suggesting its critical role for cancer growth (Son et al., 2013). By withdrawing high amount of glucose and glutamine, PDAC cells sustain also HBP flux, which results to be higher as compared to normal tissues. For instance, oncogenic Kras, the predominant mutated oncogene found in PDAC, increases flux of glucose into the HBP via up-regulation of GLUT1, glycolytic enzymes (HK1/2, Gpi1) and GFAT1. Hyper-O-GlcNAcylation increases cell proliferation, anchorage-independent growth, cell survival in pancreatic cancer cells and in orthotopic xenograft mice (Ma et al., 2013).

For this purpose, three PDAC cell lines were used for in vitro test: two of them are primary tumors (Mia Paca-2 and BxPC-3) and the third one derived from liver metastatic site (Capan1). All of them carry K-ras mutation, except for BxPC-3 (Deer et al., 2010).

Firstly, Mia Paca-2, BxPC-3 and Capan1 were tested for their sensibility to HBP inhibition in high glucose conditions, using *Aza* and *Tun* molecules. Like to MDA-MB-231 cells, both inhibitors affected cell proliferation at early time point of treatment, in dose dependent manner **(Figures 27A-C and 28A-C)**. However, only *Tun* treatment affected also cell survival inducing cell death in all three pancreatic cancer models **(Figures 28A-C)**. Mia Paca-2 was affected more than other two PDACs in both treatments, while Capan1 were less sensitive. We hypothesize that Capan1 sensitivity is influenced by the secretion of a high amount of mucin (Lan et al., 1990), which forming an envelope blocks drug entry. On the other hand

pancreatic cancer treatment is in part difficult because this tumor is higly fibrotic; therefore form an external barrier for drug diffusion (Klöppel et al., 2004). According to these results PDAC cell lines result an interesting model for testing new molecule, so we proceeded to test different concentrations of FR051 and to analyse level of cell death after 24 and 48 hours from the treatment.

Viability assay of pancreatic cancer cell lines revealed a strong, intermediate and less sensitivity to FR051 treatment in Mia Paca-2, BxPC-3 and Capan1, respectively **(Figures 29A-C)**. The different sensitivity to FR051 was similar to that observed after *Aza*/*Tun* treatment **(Figures 27 and 28)**, suggesting that our molecule is targeting HBP.

In addition, also in these pancreatic cancer cell models, FR051 induced apoptosis and caspase-3 activation **(Figures 29A-C)**. According to these data, we hypothesized that FR051 is able to activate the same mechanism in different cancer cell lines leading to apoptosis.

Also in these cancer models, we analysed protein level of PGM3 **(Figures 31 A and B)**, GFPT1, UAP1 and OGT protein level **(Figures 30 A-C)** and thus N-/O-glycosylation **(Figures 32 A and B)**. Also in this case, we were not able to correlate sensitivity to one of the aforementioned HBP parameters.

In conclusion, FR051 is able to induce either a cell proliferation arrest and an apoptotic process. These effects are consequence of a reduction of both type of glycosylation that may lead, at least upon N-glycosylation

reduction, to the activation of UPR, in particular of the Perk and ATF6 branches. In order to mitigate ER stress, Ero1 protein participates to proteins refolding by producing higher amount of ROS. This stress conditions may led to activation of an apoptotic mechanism, which is mediated also by activation of Erk1/2. We hypothesized that also mitochondria are involved in apoptotic mechanism but further investigations need to be done **(Figure 33)**.

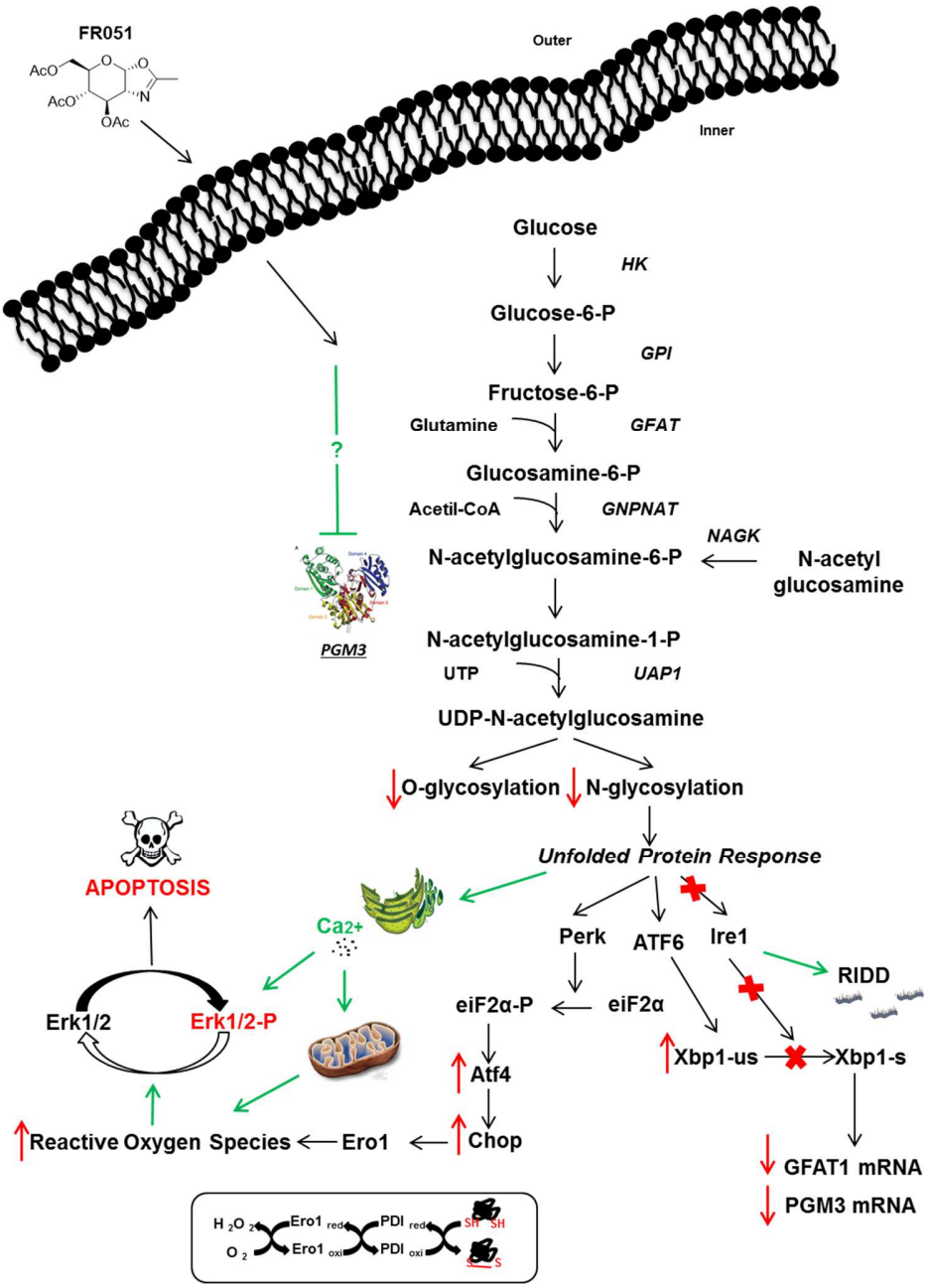
FR051
Outer
Inner
Glucose
HK
Glucose-6-P
GPI
Fructose-6-P
Glutamine
GFAT
Glucosamine-6-P
Acetil-CoA
GNPNAT
NAGK
N-acetylglucosamine-6-P
N-acetyl glucosamine
PGM3
N-acetylglucosamine-1-P
UTP
UAP1
UDP-N-acetylglucosamine
O-glycosylation
N-glycosylation
Unfolded Protein Response
APOPTOSIS
Ca2+
Perk
ATF6
Ire1
RIDD
Erk1/2
Erk1/2-P
eiF2α-P
eiF2α
Xbp1-us
Xbp1-s
Atf4
Reactive Oxygen Species
Ero1
Chop
GFAT1 mRNA
PGM3 mRNA

Figure 33. Representation of FR051-mediated effects. Schematic representation of the main pathways affected by FR051 treatment in MDA-MB-231 breast cancer cell line. The significant changes are depicted by red colour while green colour is referred to not yet experimental validated mechanisms.

In order to understand if FR051 is targeting really PGM3 enzyme, according to Atfa Sassi et al. (Sassi et al., 2014) we performed enzymatic assay combining PGM3 reaction with that of UAP1 and of inorganic phosphatase based on the idea that PGM3 product is converted by UAP1 to UDP-GlcNAc releasing pyrophosphate, which then is hydrolyzed to two phosphate ions by inorganic pyrophosphatases. The detection of phosphate ions occurs after their binding with malachite green molybdate, which is quantified at 620nm under acid conditions: inorganic phosphate derived from the pyrophosphate corresponds to PGM3 activity. Firstly, we performed the assay adding natural substrate (GlcNAc-6P) to the enzymatic reaction, but unfortunately, we did not obtain any results. So we tried also to perform *in vitro* test in other conditions according to other reports, but again, no results were obtained. Until now, we were not able to define the issues.

Now we are evaluating other procedures, reported in literature, that could be useful in order to understand whether FR051 is acting on target of interest as well as the analysis of the transition from the molecular ion (m/z 300) to a fragment of GlcNAc-6-P (m/z 138) (Stray-Pedersen et al., 2014), the measuring of the amount of PGM3 product (GlcNAc-1-P) by using gas chromatography/mass spectrometry (GC/MS) (Zhang et al., 2014) or of UDP-GlcNAc (HBP end product) as readout of PGM3 activity.

Until now, since we had not direct proof about selectivity for PGM3 enzyme, except for docking based virtual analysis, considering altogether these observations, all aforementioned effects make FR051 an interesting molecule in the HBP panorama; it might serve as a starting point for rational design of other inhibitors that could be more stable and efficient. These preliminary data confirmed that FR051 is able to activate the same mechanism in different cancer models, whose common feature was the dependence from an altered HBP. Synthesis and characterization of new inhibitors will make us able to deeper understand the role of HBP in cancer and, so that, to target this pathway for cancer therapy, also in combination with other chemotherapeutic agents, in order to completely eradicate the tumors.

References

Aebi, M., Bernasconi, R., Clerc, S., and Molinari, M. (2010). N-glycan structures: recognition and processing in the ER. Trends Biochem Sci *35*, 74-82.

Ahmed, N., and Berridge, M.V. (1999). N-glycosylation of glucose transporter-1 (Glut-1) is associated with increased transporter affinity for glucose in human leukemic cells. Leuk Res *23*, 395-401.

Arai, K., Lee, S.R., van Leyen, K., Kurose, H., and Lo, E.H. (2004). Involvement of ERK MAP kinase in endoplasmic reticulum stress in SH-SY5Y human neuroblastoma cells. J Neurochem *89*, 232-239.

Baracca, A., Chiaradonna, F., Sgarbi, G., Solaini, G., Alberghina, L., and Lenaz, G. (2010). Mitochondrial Complex I decrease is responsible for bioenergetic dysfunction in K-ras transformed cells. Biochim Biophys Acta *1797*, 314-323.

Bardeesy, N., and DePinho, R.A. (2002). Pancreatic cancer biology and genetics. Nat Rev Cancer *2*, 897-909.

Barnhart, M.M., Lynem, J., and Chapman, M.R. (2006). GlcNAc-6P levels modulate the expression of Curli fibers by Escherichia coli. J Bacteriol *188*, 5212-5219.

Bensaad, K., Tsuruta, A., Selak, M.A., Vidal, M.N., Nakano, K., Bartrons, R., Gottlieb, E., and Vousden, K.H. (2006). TIGAR, a p53-inducible regulator of glycolysis and apoptosis. Cell *126*, 107-120.

Berger, M., Chen, H., Reutter, W., and Hinderlich, S. (2002). Structure and function of N-acetylglucosamine kinase. Identification of two active site cysteines. Eur J Biochem *269*, 4212-4218.

Blais, J.D., Chin, K.T., Zito, E., Zhang, Y., Heldman, N., Harding, H.P., Fass, D., Thorpe, C., and Ron, D. (2010). A small molecule inhibitor of

endoplasmic reticulum oxidation 1 (ERO1) with selectively reversible thiol reactivity. J Biol Chem *285*, 20993-21003.

Boscher, C., Zheng, Y.Z., Lakshminarayan, R., Johannes, L., Dennis, J.W., Foster, L.J., and Nabi, I.R. (2012). Galectin-3 protein regulates mobility of N-cadherin and GM1 ganglioside at cell-cell junctions of mammary carcinoma cells. J Biol Chem *287*, 32940-32952.

Breitling, J., and Aebi, M. (2013). N-linked protein glycosylation in the endoplasmic reticulum. Cold Spring Harb Perspect Biol *5*, a013359.

Brewer, C.F., Miceli, M.C., and Baum, L.G. (2002). Clusters, bundles, arrays and lattices: novel mechanisms for lectin-saccharide-mediated cellular interactions. Curr Opin Struct Biol *12*, 616-623.

Broschat, K.O., Gorka, C., Page, J.D., Martin-Berger, C.L., Davies, M.S., Huang Hc, H.C., Gulve, E.A., Salsgiver, W.J., and Kasten, T.P. (2002). Kinetic characterization of human glutamine-fructose-6-phosphate amidotransferase I: potent feedback inhibition by glucosamine 6-phosphate. J Biol Chem *277*, 14764-14770.

Buckhaults, P., Chen, L., Fregien, N., and Pierce, M. (1997). Transcriptional regulation of N-acetylglucosaminyltransferase V by the src oncogene. J Biol Chem *272*, 19575-19581.

Burnham-Marusich, A.R., and Berninsone, P.M. (2012). Multiple proteins with essential mitochondrial functions have glycosylated isoforms. Mitochondrion *12*, 423-427.

Butkinaree, C., Cheung, W.D., Park, S., Park, K., Barber, M., and Hart, G.W. (2008). Characterization of beta-N-acetylglucosaminidase cleavage by caspase-3 during apoptosis. J Biol Chem *283*, 23557-23566.

Cagnol, S., Van Obberghen-Schilling, E., and Chambard, J.C. (2006). Prolonged activation of ERK1,2 induces FADD-independent caspase 8 activation and cell death. Apoptosis *11*, 337-346.

Caldwell, S.A., Jackson, S.R., Shahriari, K.S., Lynch, T.P., Sethi, G., Walker, S., Vosseller, K., and Reginato, M.J. (2010). Nutrient sensor O-GlcNAc transferase regulates breast cancer tumorigenesis through targeting of the oncogenic transcription factor FoxM1. Oncogene *29*, 2831-2842.

Chang, Q., Su, K., Baker, J.R., Yang, X., Paterson, A.J., and Kudlow, J.E. (2000). Phosphorylation of human glutamine:fructose-6-phosphate amidotransferase by cAMP-dependent protein kinase at serine 205 blocks the enzyme activity. J Biol Chem *275*, 21981-21987.

Chatterjee, S., Sekerke, C.S., and Kwiterovich, P.O. (1981). Effects of tunicamycin on the cell-surface binding, internalization and degradation of low-density lipoproteins in human fibroblasts. Eur J Biochem *120*, 435-441.

Chavan, M., Yan, A., and Lennarz, W.J. (2005). Subunits of the translocon interact with components of the oligosaccharyl transferase complex. J Biol Chem *280*, 22917-22924.

Chiaradonna, F., Gaglio, D., Vanoni, M., and Alberghina, L. (2006a). Expression of transforming K-Ras oncogene affects mitochondrial function and morphology in mouse fibroblasts. Biochim Biophys Acta *1757*, 1338-1356.

Chiaradonna, F., Moresco, R.M., Airoldi, C., Gaglio, D., Palorini, R., Nicotra, F., Messa, C., and Alberghina, L. (2012). From cancer metabolism to new biomarkers and drug targets. Biotechnol Adv *30*, 30-51.

Chiaradonna, F., Sacco, E., Manzoni, R., Giorgio, M., Vanoni, M., and Alberghina, L. (2006b). Ras-dependent carbon metabolism and transformation in mouse fibroblasts. Oncogene *25*, 5391-5404.

Christiansen MN1, Chik J, Lee L, Anugraham M, Abrahams JL, Packer NH. (2014). Cell surface protein glycosylation in cancer. Proteomics 14(4-5):525-46.

Comtesse, N., Maldener, E., and Meese, E. (2001). Identification of a nuclear variant of MGEA5, a cytoplasmic hyaluronidase and a beta-N-acetylglucosaminidase. Biochem Biophys Res Commun *283*, 634-640.

Contessa, J.N., Bhojani, M.S., Freeze, H.H., Rehemtulla, A., and Lawrence, T.S. (2008). Inhibition of N-linked glycosylation disrupts receptor tyrosine kinase signaling in tumor cells. Cancer Res *68*, 3803-3809.

Dahmus, M.E. (1996). Reversible phosphorylation of the C-terminal domain of RNA polymerase II. J Biol Chem *271*, 19009-19012.

Dairaku, N., Kato, K., Honda, K., Koike, T., Iijima, K., Imatani, A., Sekine, H., Ohara, S., Matsui, H., and Shimosegawa, T. (2004). Oligomycin and antimycin A prevent nitric oxide-induced apoptosis by blocking cytochrome C leakage. J Lab Clin Med *143*, 143-151.

Dajee, M., Lazarov, M., Zhang, J.Y., Cai, T., Green, C.L., Russell, A.J., Marinkovich, M.P., Tao, S., Lin, Q., Kubo, Y.*, et al.* (2003). NF-kappaB blockade and oncogenic Ras trigger invasive human epidermal neoplasia. Nature *421*, 639-643.

Darley-Usmar, V.M., Ball, L.E., and Chatham, J.C. (2012). Protein O-linked β-N-acetylglucosamine: a novel effector of cardiomyocyte metabolism and function. J Mol Cell Cardiol *52*, 538-549.

Datta, A. (1970). Studies on hog spleen N-acetylglucosamine kinase. I. Purification and properties of N-acetylglucosamine kinase. Biochim Biophys Acta *220*, 51-60.

Datta, B., Ray, M.K., Chakrabarti, D., Wylie, D.E., and Gupta, N.K. (1989). Glycosylation of eukaryotic peptide chain initiation factor 2 (eIF-2)-associated 67-kDa polypeptide (p67) and its possible role in the inhibition of eIF-2 kinase-catalyzed phosphorylation of the eIF-2 alpha-subunit. J Biol Chem *264*, 20620-20624.

de-Freitas-Junior, J.C., Bastos, L.G., Freire-Neto, C.A., Rocher, B.D., Abdelhay, E.S., and Morgado-Díaz, J.A. (2012). N-glycan biosynthesis inhibitors induce in vitro anticancer activity in colorectal cancer cells. J Cell Biochem *113*, 2957-2966.

DeBerardinis, R.J., and Cheng, T. (2010). Q's next: the diverse functions of glutamine in metabolism, cell biology and cancer. Oncogene *29*, 313-324.

DeBerardinis, R.J., Lum, J.J., Hatzivassiliou, G., and Thompson, C.B. (2008). The biology of cancer: metabolic reprogramming fuels cell growth and proliferation. Cell Metab *7*, 11-20.

DeBerardinis, R.J., Mancuso, A., Daikhin, E., Nissim, I., Yudkoff, M., Wehrli, S., and Thompson, C.B. (2007). Beyond aerobic glycolysis: transformed cells can engage in glutamine metabolism that exceeds the requirement for protein and nucleotide synthesis. Proc Natl Acad Sci U S A *104*, 19345-19350.

Deer, E.L., González-Hernández, J., Coursen, J.D., Shea, J.E., Ngatia, J., Scaife, C.L., Firpo, M.A., and Mulvihill, S.J. (2010). Phenotype and genotype of pancreatic cancer cell lines. Pancreas *39*, 425-435.

Dennis, J.W., Lau, K.S., Demetriou, M., and Nabi, I.R. (2009a). Adaptive regulation at the cell surface by N-glycosylation. Traffic *10*, 1569-1578.

Dennis, J.W., Nabi, I.R., and Demetriou, M. (2009b). Metabolism, cell surface organization, and disease. Cell *139*, 1229-1241.

Dikalova, A.E., Bikineyeva, A.T., Budzyn, K., Nazarewicz, R.R., McCann, L., Lewis, W., Harrison, D.G., and Dikalov, S.I. (2010). Therapeutic targeting of mitochondrial superoxide in hypertension. Circ Res *107*, 106-116.

Hiss DC1, Gabriels GA, Folb PI. (2007). Combination of tunicamycin with anticancer drugs synergistically enhances their toxicity in multidrug-resistant human ovarian cystadenocarcinoma cells. Cancer Cell Int. 18;7:5.

DuRose, J.B., Tam, A.B., and Niwa, M. (2006). Intrinsic capacities of molecular sensors of the unfolded protein response to sense alternate forms of endoplasmic reticulum stress. Mol Biol Cell *17*, 3095-3107.

Eguchi, S., Oshiro, N., Miyamoto, T., Yoshino, K., Okamoto, S., Ono, T., Kikkawa, U., and Yonezawa, K. (2009). AMP-activated protein kinase phosphorylates glutamine : fructose-6-phosphate amidotransferase 1 at Ser243 to modulate its enzymatic activity. Genes Cells *14*, 179-189.

Elbein, A.D. (1984). Inhibitors of the biosynthesis and processing of N-linked oligosaccharides. CRC Crit Rev Biochem *16*, 21-49.

Ellgaard, L., McCaul, N., Chatsisvili, A., and Braakman, I. (2016). Co- and Post-Translational Protein Folding in the ER. Traffic *17*, 615-638.

Ellgaard, L., Molinari, M., and Helenius, A. (1999). Setting the standards: quality control in the secretory pathway. Science *286*, 1882-1888.

ELLISON, R.R., KARNOFSKY, D.A., STERNBERG, S.S., MURPHY, M.L., and BURCHENAL, J.H. (1954). Clinical trials of O-diazoacetyl-L-serine (azaserine) in neoplastic disease. Cancer *7*, 801-814.

Elstrom, R.L., Bauer, D.E., Buzzai, M., Karnauskas, R., Harris, M.H., Plas, D.R., Zhuang, H., Cinalli, R.M., Alavi, A., Rudin, C.M*., et al.* (2004). Akt stimulates aerobic glycolysis in cancer cells. Cancer Res *64*, 3892-3899.

Fang, M., Shen, Z., Huang, S., Zhao, L., Chen, S., Mak, T.W., and Wang, X. (2010). The ER UDPase ENTPD5 promotes protein N-glycosylation, the Warburg effect, and proliferation in the PTEN pathway. Cell *143*, 711-724.

Fardini, Y., Dehennaut, V., Lefebvre, T., and Issad, T. (2013). O-GlcNAcylation: A New Cancer Hallmark? Front Endocrinol (Lausanne) *4*, 99.

Freeman, A.F., and Holland, S.M. (2009). Clinical manifestations, etiology, and pathogenesis of the hyper-IgE syndromes. Pediatr Res *65*, 32R-37R.

Friesner RA, Banks JL, Murphy RB, Halgren TA, Klicic JJ, et al. (2004) Glide: A new approach for rapid, accurate docking and scoring. 1. Method and assessment of docking accuracy. J Med Chem 25;47(7):1739-49.

Furo, K., Nozaki, M., Murashige, H., and Sato, Y. (2015). Identification of an N-acetylglucosamine kinase essential for UDP-N-acetylglucosamine salvage synthesis in Arabidopsis. FEBS Lett *589*, 3258-3262.

Futami, T., Miyagishi, M., and Taira, K. (2005). Identification of a network involved in thapsigargin-induced apoptosis using a library of small interfering RNA expression vectors. J Biol Chem *280*, 826-831.

Fülöp, N., Marchase, R.B., and Chatham, J.C. (2007). Role of protein O-linked N-acetyl-glucosamine in mediating cell function and survival in the cardiovascular system. Cardiovasc Res *73*, 288-297.

Gaut, J.R., and Hendershot, L.M. (1993). The modification and assembly of proteins in the endoplasmic reticulum. Curr Opin Cell Biol *5*, 589-595.

Gialeli, C., Theocharis, A.D., and Karamanos, N.K. (2011). Roles of matrix metalloproteinases in cancer progression and their pharmacological targeting. FEBS J *278*, 16-27.

Gloster, T.M., Zandberg, W.F., Heinonen, J.E., Shen, D.L., Deng, L., and Vocadlo, D.J. (2011). Hijacking a biosynthetic pathway yields a glycosyltransferase inhibitor within cells. Nat Chem Biol *7*, 174-181.

Goettig, P. (2016). Effects of Glycosylation on the Enzymatic Activity and Mechanisms of Proteases. Int J Mol Sci *17*.

Grigorian, A., Lee, S.U., Tian, W., Chen, I.J., Gao, G., Mendelsohn, R., Dennis, J.W., and Demetriou, M. (2007). Control of T Cell-mediated autoimmunity by metabolite flux to N-glycan biosynthesis. J Biol Chem *282*, 20027-20035.

Gu, J., and Taniguchi, N. (2004). Regulation of integrin functions by N-glycans. Glycoconj J *21*, 9-15.

Gu Y, Mi W, Ge Y, Liu H, Fan Q, Han C, Yang J, Han F, Lu X, Yu W. GlcNAcylation plays an essential role in breast cancer metastasis. (2010). Cancer Res. 1;70(15):6344-51.

Guillaumond, F., Leca, J., Olivares, O., Lavaut, M.N., Vidal, N., Berthezène, P., Dusetti, N.J., Loncle, C., Calvo, E., Turrini, O*., et al.* (2013). Strengthened glycolysis under hypoxia supports tumor symbiosis and hexosamine biosynthesis in pancreatic adenocarcinoma. Proc Natl Acad Sci U S A *110*, 3919-3924.

Gunasekera, A., Alvarez, F.J., Douglas, L.M., Wang, H.X., Rosebrock, A.P., and Konopka, J.B. (2010). Identification of GIG1, a GlcNAc-induced gene in Candida albicans needed for normal sensitivity to the chitin synthase inhibitor nikkomycin Z. Eukaryot Cell *9*, 1476-1483.

Guo, H.B., Randolph, M., and Pierce, M. (2007). Inhibition of a specific N-glycosylation activity results in attenuation of breast carcinoma cell invasiveness-related phenotypes: inhibition of epidermal growth factor-induced dephosphorylation of focal adhesion kinase. J Biol Chem *282*, 22150-22162.

Guyton, K.Z., Liu, Y., Gorospe, M., Xu, Q., and Holbrook, N.J. (1996). Activation of mitogen-activated protein kinase by H2O2. Role in cell survival following oxidant injury. J Biol Chem *271*, 4138-4142.

Gwak, H., Kim, S., Dhanasekaran, D.N., and Song, Y.S. (2016). Resveratrol triggers ER stress-mediated apoptosis by disrupting N-linked glycosylation of proteins in ovarian cancer cells. Cancer Lett *371*, 347-353.

Haddoub, R., Laurent, N., Meloni, M.M., and Flitsch, S.L. (2009). Straightforward Synthesis of 2-Acetamido-2-deoxy-β-*D*-glucopyranosyl Esters under Microwave Conditions (Synlett), pp. 3328-3332.

Hanover, J.A., Krause, M.W., and Love, D.C. (2012). Bittersweet memories: linking metabolism to epigenetics through O-GlcNAcylation. Nat Rev Mol Cell Biol *13*, 312-321.

Heckel, D., Comtesse, N., Brass, N., Blin, N., Zang, K.D., and Meese, E. (1998). Novel immunogenic antigen homologous to hyaluronidase in meningioma. Hum Mol Genet *7*, 1859-1872.

Hiller, K., Metallo, C.M., Kelleher, J.K., and Stephanopoulos, G. (2010). Nontargeted elucidation of metabolic pathways using stable-isotope tracers and mass spectrometry. Anal Chem *82*, 6621-6628.

Hinderlich, S., Berger, M., Schwarzkopf, M., Effertz, K., and Reutter, W. (2000). Molecular cloning and characterization of murine and human N-acetylglucosamine kinase. Eur J Biochem *267*, 3301-3308.

Hiramatsu, N., Chiang, W.C., Kurt, T.D., Sigurdson, C.J., and Lin, J.H. (2015). Multiple Mechanisms of Unfolded Protein Response-Induced Cell Death. Am J Pathol *185*, 1800-1808.

Holland, S.M., DeLeo, F.R., Elloumi, H.Z., Hsu, A.P., Uzel, G., Brodsky, N., Freeman, A.F., Demidowich, A., Davis, J., Turner, M.L.*, et al.* (2007). STAT3 mutations in the hyper-IgE syndrome. N Engl J Med *357*, 1608-1619.

Holliday, D.L., and Speirs, V. (2011). Choosing the right cell line for breast cancer research. Breast Cancer Res *13*, 215.

Hopkinson, D.A., and Harris, H. (1968). A third phosphoglucomutase locus in man. Ann Hum Genet *31*, 359-367.

Hu, Y., Riesland, L., Paterson, A.J., and Kudlow, J.E. (2004). Phosphorylation of mouse glutamine-fructose-6-phosphate amidotransferase 2 (GFAT2) by cAMP-dependent protein kinase increases the enzyme activity. J Biol Chem *279*, 29988-29993.

Hung, C.C., Ichimura, T., Stevens, J.L., and Bonventre, J.V. (2003). Protection of renal epithelial cells against oxidative injury by endoplasmic reticulum stress preconditioning is mediated by ERK1/2 activation. J Biol Chem *278*, 29317-29326.

Hurvitz, S.A., and Pietras, R.J. (2008). Rational management of endocrine resistance in breast cancer: a comprehensive review of estrogen receptor biology, treatment options, and future directions. Cancer *113*, 2385-2397.

Isaji, T., Sato, Y., Zhao, Y., Miyoshi, E., Wada, Y., Taniguchi, N., and Gu, J. (2006). N-glycosylation of the beta-propeller domain of the integrin alpha5 subunit is essential for alpha5beta1 heterodimerization, expression on the cell surface, and its biological function. J Biol Chem *281*, 33258-33267.

Itkonen, H.M., and Mills, I.G. (2013). N-linked glycosylation supports cross-talk between receptor tyrosine kinases and androgen receptor. PLoS One *8*, e65016.

Jang, I., Kim, H.B., Seo, H., Kim, J.Y., Choi, H., Yoo, J.S., Kim, J.W., and Cho, J.W. (2015). O-GlcNAcylation of eIF2α regulates the phospho-eIF2α-mediated ER stress response. Biochim Biophys Acta *1853*, 1860-1869.

Jenne, D.E., Reimann, H., Nezu, J., Friedel, W., Loff, S., Jeschke, R., Müller, O., Back, W., and Zimmer, M. (1998). Peutz-Jeghers syndrome is caused by mutations in a novel serine threonine kinase. Nat Genet *18*, 38-43.

Jínek, M., Rehwinkel, J., Lazarus, B.D., Izaurralde, E., Hanover, J.A., and Conti, E. (2004). The superhelical TPR-repeat domain of O-linked GlcNAc transferase exhibits structural similarities to importin alpha. Nat Struct Mol Biol *11*, 1001-1007.

Jorgensen WL, Tiradorives J (1988). The Opls Potential Functions for Proteins - Energy Minimizations for Crystals of Cyclic-Peptides and Crambin. J Am Chem Soc. 1 10 (6), pp 1657–1666.

Kamata, H., Honda, S., Maeda, S., Chang, L., Hirata, H., and Karin, M. (2005). Reactive oxygen species promote TNFalpha-induced death and sustained JNK activation by inhibiting MAP kinase phosphatases. Cell *120*, 649-661.

Kang, M.S., Spencer, J.P., and Elbein, A.D. (1978). Amphomycin inhibition of mannose and GlcNAc incorporation into lipid-linked saccharides. J Biol Chem *253*, 8860-8866.

Khidekel, N., Ficarro, S.B., Clark, P.M., Bryan, M.C., Swaney, D.L., Rexach, J.E., Sun, Y.E., Coon, J.J., Peters, E.C., and Hsieh-Wilson, L.C. (2007). Probing the dynamics of O-GlcNAc glycosylation in the brain using quantitative proteomics. Nat Chem Biol *3*, 339-348.

Kim, J.W., Gao, P., Liu, Y.C., Semenza, G.L., and Dang, C.V. (2007). Hypoxia-inducible factor 1 and dysregulated c-Myc cooperatively induce vascular endothelial growth factor and metabolic switches hexokinase 2 and pyruvate dehydrogenase kinase 1. Mol Cell Biol *27*, 7381-7393.

Klöppel, G., Detlefsen, S., and Feyerabend, B. (2004). Fibrosis of the pancreas: the initial tissue damage and the resulting pattern. Virchows Arch *445*, 1-8.

Komekado, H., Yamamoto, H., Chiba, T., and Kikuchi, A. (2007). Glycosylation and palmitoylation of Wnt-3a are coupled to produce an active form of Wnt-3a. Genes Cells *12*, 521-534.

Konrad, R.J., Zhang, F., Hale, J.E., Knierman, M.D., Becker, G.W., and Kudlow, J.E. (2002). Alloxan is an inhibitor of the enzyme O-linked N-acetylglucosamine transferase. Biochem Biophys Res Commun *293*, 207-212.

Kopan, R., and Ilagan, M.X. (2009). The canonical Notch signaling pathway: unfolding the activation mechanism. Cell *137*, 216-233.

Kowarik, M., Numao, S., Feldman, M.F., Schulz, B.L., Callewaert, N., Kiermaier, E., Catrein, I., and Aebi, M. (2006). N-linked glycosylation of folded proteins by the bacterial oligosaccharyltransferase. Science *314*, 1148-1150.

Kreppel, L.K., and Hart, G.W. (1999). Regulation of a cytosolic and nuclear O-GlcNAc transferase. Role of the tetratricopeptide repeats. J Biol Chem *274*, 32015-32022.

Lajoie, P., Partridge, E.A., Guay, G., Goetz, J.G., Pawling, J., Lagana, A., Joshi, B., Dennis, J.W., and Nabi, I.R. (2007). Plasma membrane domain organization regulates EGFR signaling in tumor cells. J Cell Biol *179*, 341-356.

Lan, M.S., Hollingsworth, M.A., and Metzgar, R.S. (1990). Polypeptide core of a human pancreatic tumor mucin antigen. Cancer Res *50*, 2997-3001.

Lau, K.S., Partridge, E.A., Grigorian, A., Silvescu, C.I., Reinhold, V.N., Demetriou, M., and Dennis, J.W. (2007). Complex N-glycan number and degree of branching cooperate to regulate cell proliferation and differentiation. Cell *129*, 123-134.

Lazniewska, J., and Weiss, N. (2017). Glycosylation of voltage-gated calcium channels in health and disease. Biochim Biophys Acta.

Levinthal, D.J., and Defranco, D.B. (2005). Reversible oxidation of ERK-directed protein phosphatases drives oxidative toxicity in neurons. J Biol Chem *280*, 5875-5883.

Li, C., Rodriguez, M., and Banerjee, D. (2000). Cloning and characterization of complementary DNA encoding human N-acetylglucosamine-phosphate mutase protein. Gene *242*, 97-103.

Li, G., Mongillo, M., Chin, K.T., Harding, H., Ron, D., Marks, A.R., and Tabas, I. (2009). Role of ERO1-alpha-mediated stimulation of inositol 1,4,5-triphosphate receptor activity in endoplasmic reticulum stress-induced apoptosis. J Cell Biol *186*, 783-792.

Ligos, J.M., de Lera, T.L., Hinderlich, S., Guinea, B., Sv°nchez, L., Roca, R., Valencia, A., and Bernad, A. (2002). Functional interaction between the Ser/Thr kinase PKL12 and N-acetylglucosamine kinase, a prominent enzyme implicated in the salvage pathway for GlcNAc recycling. J Biol Chem *277*, 6333-6343.

Love, D.C., and Hanover, J.A. (2005). The hexosamine signaling pathway: deciphering the "O-GlcNAc code". Sci STKE *2005*, re13.

Love, D.C., Kochan, J., Cathey, R.L., Shin, S.H., Hanover, J.A., and Kochran, J. (2003). Mitochondrial and nucleocytoplasmic targeting of O-linked GlcNAc transferase. J Cell Sci *116*, 647-654.

Ma, Z., Vocadlo, D.J., and Vosseller, K. (2013). Hyper-O-GlcNAcylation is anti-apoptotic and maintains constitutive NF-κB activity in pancreatic cancer cells. J Biol Chem *288*, 15121-15130.

Malhotra, J.D., Miao, H., Zhang, K., Wolfson, A., Pennathur, S., Pipe, S.W., and Kaufman, R.J. (2008). Antioxidants reduce endoplasmic reticulum stress and improve protein secretion. Proc Natl Acad Sci U S A *105*, 18525-18530.

Manchado, E., Weissmueller, S., Morris, J.P., Chen, C.C., Wullenkord, R., Lujambio, A., de Stanchina, E., Poirier, J.T., Gainor, J.F., Corcoran, R.B.*, et al.* (2016). A combinatorial strategy for treating KRAS-mutant lung cancer. Nature *534*, 647-651.

Margariti, A., Li, H., Chen, T., Martin, D., Vizcay-Barrena, G., Alam, S., Karamariti, E., Xiao, Q., Zampetaki, A., Zhang, Z.*, et al.* (2013). XBP1 mRNA splicing triggers an autophagic response in endothelial cells through BECLIN-1 transcriptional activation. J Biol Chem *288*, 859-872.

Maurel, M., Chevet, E., Tavernier, J., and Gerlo, S. (2014). Getting RIDD of RNA: IRE1 in cell fate regulation. Trends Biochem Sci *39*, 245-254.

Mengin-Lecreulx, D., and van Heijenoort, J. (1996). Characterization of the essential gene glmM encoding phosphoglucosamine mutase in Escherichia coli. J Biol Chem *271*, 32-39.

Mi, W., Gu, Y., Han, C., Liu, H., Fan, Q., Zhang, X., Cong, Q., and Yu, W. (2011). O-GlcNAcylation is a novel regulator of lung and colon cancer malignancy. Biochim Biophys Acta *1812*, 514-519.

Miele, L., Golde, T., and Osborne, B. (2006). Notch signaling in cancer. Curr Mol Med *6*, 905-918.

Mimura, N., Fulciniti, M., Gorgun, G., Tai, Y.T., Cirstea, D., Santo, L., Hu, Y., Fabre, C., Minami, J., Ohguchi, H.*, et al.* (2012). Blockade of XBP1 splicing by inhibition of IRE1Œ± is a promising therapeutic option in multiple myeloma. Blood *119*, 5772-5781.

Minamino, T., Komuro, I., and Kitakaze, M. (2010). Endoplasmic reticulum stress as a therapeutic target in cardiovascular disease. Circ Res *107*, 1071-1082.

Minegishi, Y., Saito, M., Morio, T., Watanabe, K., Agematsu, K., Tsuchiya, S., Takada, H., Hara, T., Kawamura, N., Ariga, T.*, et al.* (2006). Human tyrosine kinase 2 deficiency reveals its requisite roles in multiple cytokine signals involved in innate and acquired immunity. Immunity *25*, 745-755.

Minegishi, Y., Saito, M., Tsuchiya, S., Tsuge, I., Takada, H., Hara, T., Kawamura, N., Ariga, T., Pasic, S., Stojkovic, O.*, et al.* (2007). Dominant-negative mutations in the DNA-binding domain of STAT3 cause hyper-IgE syndrome. Nature *448*, 1058-1062.

Mio, T., Yamada-Okabe, T., Arisawa, M., and Yamada-Okabe, H. (2000). Functional cloning and mutational analysis of the human cDNA for phosphoacetylglucosamine mutase: identification of Munkley J., Vodak D., Livermore K.E., James K., Wilson B.T., Knight B, Mccullagh P., Mcgrath J, Crundwell M., Harries L.W., Leung H.Y, Robson C.N., Mills I.G., Rajan P., Elliott D.J. (2016). Glycosylation is a global target for androgen control in prostate cancer cells. EBioMedicine. 8: 103–116.

the amino acid residues essential for the catalysis. Biochim Biophys Acta *1492*, 369-376.

Nagel, A.K., and Ball, L.E. (2015). Intracellular protein O-GlcNAc modification integrates nutrient status with transcriptional and metabolic regulation. Adv Cancer Res *126*, 137-166.

Nathan, C., and Ding, A. (2010). SnapShot: Reactive Oxygen Intermediates (ROI). Cell *140*, 951-951.e952.

Ngoh, G.A., Hamid, T., Prabhu, S.D., and Jones, S.P. (2009). O-GlcNAc signaling attenuates ER stress-induced cardiomyocyte death. Am J Physiol Heart Circ Physiol *297*, H1711-1719.

Nishitani, Y., Maruyama, D., Nonaka, T., Kita, A., Fukami, T.A., Mio, T., Yamada-Okabe, H., Yamada-Okabe, T., and Miki, K. (2006). Crystal structures of N-acetylglucosamine-phosphate mutase, a member of the alpha-D-phosphohexomutase superfamily, and its substrate and product complexes. J Biol Chem *281*, 19740-19747.

Oka, N., Nakahara, S., Takenaka, Y., Fukumori, T., Hogan, V., Kanayama, H.O., Yanagawa, T., and Raz, A. (2005). Galectin-3 inhibits tumor necrosis factor-related apoptosis-inducing ligand-induced apoptosis by activating Akt in human bladder carcinoma cells. Cancer Res *65*, 7546-7553.

Olden, K., Breton, P., Grzegorzewski, K., Yasuda, Y., Gause, B.L., Oredipe, O.A., Newton, S.A., and White, S.L. (1991). The potential importance of swainsonine in therapy for cancers and immunology. Pharmacol Ther *50*, 285-290.

Olivari, S., Galli, C., Alanen, H., Ruddock, L., and Molinari, M. (2005). A novel stress-induced EDEM variant regulating endoplasmic reticulum-associated glycoprotein degradation. J Biol Chem *280*, 2424-2428.

Olivier-Van Stichelen, S., Guinez, C., Mir, A.M., Perez-Cervera, Y., Liu, C., Michalski, J.C., and Lefebvre, T. (2012). The hexosamine biosynthetic

pathway and O-GlcNAcylation drive the expression of β-catenin and cell proliferation. Am J Physiol Endocrinol Metab *302*, E417-424.

Oren, M., and Rotter, V. (2010). Mutant p53 gain-of-function in cancer. Cold Spring Harb Perspect Biol *2*, a001107.

Ozcan, S., Andrali, S.S., and Cantrell, J.E. (2010). Modulation of transcription factor function by O-GlcNAc modification. Biochim Biophys Acta *1799*, 353-364.

Palorini, R., Cammarata, F.P., Cammarata, F., Balestrieri, C., Monestiroli, A., Vasso, M., Gelfi, C., Alberghina, L., and Chiaradonna, F. (2013a). Glucose starvation induces cell death in K-ras-transformed cells by interfering with the hexosamine biosynthesis pathway and activating the unfolded protein response. Cell Death Dis *4*, e732.

Palorini, R., Simonetto, T., Cirulli, C., and Chiaradonna, F. (2013b). Mitochondrial complex I inhibitors and forced oxidative phosphorylation synergize in inducing cancer cell death. Int J Cell Biol *2013*, 243876.

Palorini, R., Votta, G., Pirola, Y., De Vitto, H., De Palma, S., Airoldi, C., Vasso, M., Ricciardiello, F., Lombardi, P.P., Cirulli, C*., et al.* (2016). Protein Kinase A Activation Promotes Cancer Cell Resistance to Glucose Starvation and Anoikis. PLoS Genet *12*, e1005931.

Pang, H., Koda, Y., Soejima, M., and Kimura, H. (2002). Identification of human phosphoglucomutase 3 (PGM3) as N-acetylglucosamine-phosphate mutase (AGM1). Ann Hum Genet *66*, 139-144.

Panieri, E., and Santoro, M.M. (2016). ROS homeostasis and metabolism: a dangerous liason in cancer cells. Cell Death Dis *7*, e2253.

Penque, B.A., Hoggatt, A.M., Herring, B.P., and Elmendorf, J.S. (2013). Hexosamine biosynthesis impairs insulin action via a cholesterolgenic response. Mol Endocrinol *27*, 536-547.

Perkins, N.D. (2012). The diverse and complex roles of NF-κB subunits in cancer. Nat Rev Cancer *12*, 121-132.

Rael, E.L., Marshall, R.T., and McClain, J.J. (2012). The Hyper-IgE Syndromes: Lessons in Nature, From Bench to Bedside. World Allergy Organ J *5*, 79-87.

Rajapakse, A.G., Ming, X.F., Carvas, J.M., and Yang, Z. (2009). The hexosamine biosynthesis inhibitor azaserine prevents endothelial inflammation and dysfunction under hyperglycemic condition through antioxidant effects. Am J Physiol Heart Circ Physiol *296*, H815-822.

Robey, R.B., and Hay, N. (2009). Is Akt the "Warburg kinase"?-Akt-energy metabolism interactions and oncogenesis. Semin Cancer Biol *19*, 25-31.

Rozanski, W., Krzeslak, A., Forma, E., Brys, M., Blewniewski, M., Wozniak, P., and Lipinski, M. (2012). Prediction of bladder cancer based on urinary content of MGEA5 and OGT mRNA level. Clin Lab *58*, 579-583.

Ryczko, M.C., Pawling, J., Chen, R., Abdel Rahman, A.M., Yau, K., Copeland, J.K., Zhang, C., Surendra, A., Guttman, D.S., Figeys, D*., et al.* (2016). Metabolic Reprogramming by Hexosamine Biosynthetic and Golgi N-Glycan Branching Pathways. Sci Rep *6*, 23043.

Salvatore, S., Heuschkel, R., Tomlin, S., Davies, S.E., Edwards, S., Walker-Smith, J.A., French, I., and Murch, S.H. (2000). A pilot study of N-acetyl glucosamine, a nutritional substrate for glycosaminoglycan synthesis, in paediatric chronic inflammatory bowel disease. Aliment Pharmacol Ther *14*, 1567-1579.

Sassi, A., Lazaroski, S., Wu, G., Haslam, S.M., Fliegauf, M., Mellouli, F., Patiroglu, T., Unal, E., Ozdemir, M.A., Jouhadi, Z*., et al.* (2014). Hypomorphic homozygous mutations in phosphoglucomutase 3 (PGM3)

impair immunity and increase serum IgE levels. J Allergy Clin Immunol *133*, 1410-1419, 1419.e1411-1413.

Saul, R., Chambers, J.P., Molyneux, R.J., and Elbein, A.D. (1983). Castanospermine, a tetrahydroxylated alkaloid that inhibits beta-glucosidase and beta-glucocerebrosidase. Arch Biochem Biophys *221*, 593-597.

Schulz, B.L., Stirnimann, C.U., Grimshaw, J.P., Brozzo, M.S., Fritsch, F., Mohorko, E., Capitani, G., Glockshuber, R., GrVºtter, M.G., and Aebi, M. (2009). Oxidoreductase activity of oligosaccharyltransferase subunits Ost3p and Ost6p defines site-specific glycosylation efficiency. Proc Natl Acad Sci U S A *106*, 11061-11066.

Schwarz, F., and Aebi, M. (2011). Mechanisms and principles of N-linked protein glycosylation. Curr Opin Struct Biol *21*, 576-582.

Sevier, C.S., and Kaiser, C.A. (2008). Ero1 and redox homeostasis in the endoplasmic reticulum. Biochim Biophys Acta *1783*, 549-556.

Slawson, C., and Hart, G.W. (2011). O-GlcNAc signalling: implications for cancer cell biology. Nat Rev Cancer *11*, 678-684.

Slawson, C., Lakshmanan, T., Knapp, S., and Hart, G.W. (2008). A mitotic GlcNAcylation/phosphorylation signaling complex alters the posttranslational state of the cytoskeletal protein vimentin. Mol Biol Cell *19*, 4130-4140.

Slawson, C., Zachara, N.E., Vosseller, K., Cheung, W.D., Lane, M.D., and Hart, G.W. (2005). Perturbations in O-linked beta-N-acetylglucosamine protein modification cause severe defects in mitotic progression and cytokinesis. J Biol Chem *280*, 32944-32956.

Son, J., Lyssiotis, C.A., Ying, H., Wang, X., Hua, S., Ligorio, M., Perera, R.M., Ferrone, C.R., Mullarky, E., Shyh-Chang, N*., et al.* (2013). Glutamine

supports pancreatic cancer growth through a KRAS-regulated metabolic pathway. Nature *496*, 101-105.

Spiro, R.G. (2002). Protein glycosylation: nature, distribution, enzymatic formation, and disease implications of glycopeptide bonds. Glycobiology *12*, 43R-56R.

Stanley, P. (2007). A method to the madness of N-glycan complexity? Cell *129*, 27-29.

Stray-Pedersen, A., Backe, P.H., Sorte, H.S., MƲƬrkrid, L., Chokshi, N.Y., Erichsen, H.C., Gambin, T., ElgstƲƬen, K.B., BjƲƬrƲ•s, M., Wlodarski, M.W*., et al.* (2014). PGM3 mutations cause a congenital disorder of glycosylation with severe immunodeficiency and skeletal dysplasia. Am J Hum Genet *95*, 96-107.

Szalai, G., Krishnamurthy, R., and Hajnóczky, G. (1999). Apoptosis driven by IP(3)-linked mitochondrial calcium signals. EMBO J *18*, 6349-6361.

Szegezdi, E., Logue, S.E., Gorman, A.M., and Samali, A. (2006). Mediators of endoplasmic reticulum stress-induced apoptosis. EMBO Rep *7*, 880-885.

Tadic, V., Prell, T., Lautenschlaeger, J., and Grosskreutz, J. (2014). The ER mitochondria calcium cycle and ER stress response as therapeutic targets in amyotrophic lateral sclerosis. Front Cell Neurosci *8*, 147.

Tan, E.P., Villar, M.T., E, L., Lu, J., Selfridge, J.E., Artigues, A., Swerdlow, R.H., and Slawson, C. (2014). Altering O-linked β-N-acetylglucosamine cycling disrupts mitochondrial function. J Biol Chem *289*, 14719-14730.

Thurston, T.L., Wandel, M.P., von Muhlinen, N., Foeglein, A., and Randow, F. (2012). Galectin 8 targets damaged vesicles for autophagy to defend cells against bacterial invasion. Nature *482*, 414-418.

Toleman, C., Paterson, A.J., Whisenhunt, T.R., and Kudlow, J.E. (2004). Characterization of the histone acetyltransferase (HAT) domain of a bifunctional protein with activable O-GlcNAcase and HAT activities. J Biol Chem *279*, 53665-53673.

Tong, X., Zhao, F., Mancuso, A., Gruber, J.J., and Thompson, C.B. (2009). The glucose-responsive transcription factor ChREBP contributes to glucose-dependent anabolic synthesis and cell proliferation. Proc Natl Acad Sci U S A *106*, 21660-21665.

Tu, B.P., and Weissman, J.S. (2002). The FAD- and O(2)-dependent reaction cycle of Ero1-mediated oxidative protein folding in the endoplasmic reticulum. Mol Cell *10*, 983-994.

Vasconcelos-Dos-Santos, A., Oliveira, I.A., Lucena, M.C., Mantuano, N.R., Whelan, S.A., Dias, W.B., and Todeschini, A.R. (2015). Biosynthetic Machinery Involved in Aberrant Glycosylation: Promising Targets for Developing of Drugs Against Cancer. Front Oncol *5*, 138.

Veerababu, G., Tang, J., Hoffman, R.T., Daniels, M.C., Hebert, L.F., Crook, E.D., Cooksey, R.C., and McClain, D.A. (2000). Overexpression of glutamine: fructose-6-phosphate amidotransferase in the liver of transgenic mice results in enhanced glycogen storage, hyperlipidemia, obesity, and impaired glucose tolerance. Diabetes *49*, 2070-2078.

Vibjerg Jensen, R., Johnsen, J., Buus Kristiansen, S., Zachara, N.E., and Bøtker, H.E. (2013). Ischemic preconditioning increases myocardial O-GlcNAc glycosylation. Scand Cardiovasc J *47*, 168-174.

Wang, Z.V., Deng, Y., Gao, N., Pedrozo, Z., Li, D.L., Morales, C.R., Criollo, A., Luo, X., Tan, W., Jiang, N.*, et al.* (2014). Spliced X-box binding protein 1 couples the unfolded protein response to hexosamine biosynthetic pathway. Cell *156*, 1179-1192.

WARBURG, O. (1956). On the origin of cancer cells. Science *123*, 309-314.

Wellen, K.E., Lu, C., Mancuso, A., Lemons, J.M., Ryczko, M., Dennis, J.W., Rabinowitz, J.D., Coller, H.A., and Thompson, C.B. (2010). The hexosamine biosynthetic pathway couples growth factor-induced glutamine uptake to glucose metabolism. Genes Dev *24*, 2784-2799.

Wells, L., Gao, Y., Mahoney, J.A., Vosseller, K., Chen, C., Rosen, A., and Hart, G.W. (2002). Dynamic O-glycosylation of nuclear and cytosolic proteins: further characterization of the nucleocytoplasmic beta-N-acetylglucosaminidase, O-GlcNAcase. J Biol Chem *277*, 1755-1761.

Wenling, C., Duohui, J., Jiamou, L., Yandao, G., Nanming, Z., and Xiufang, Z. (2005). Effects of the degree of deacetylation on the physicochemical properties and Schwann cell affinity of chitosan films. J Biomater Appl *20*, 157-177.

Whelan, S.A., Lane, M.D., and Hart, G.W. (2008). Regulation of the O-linked beta-N-acetylglucosamine transferase by insulin signaling. J Biol Chem *283*, 21411-21417.

Whisenhunt, T.R., Yang, X., Bowe, D.B., Paterson, A.J., Van Tine, B.A., and Kudlow, J.E. (2006). Disrupting the enzyme complex regulating O-GlcNAcylation blocks signaling and development. Glycobiology *16*, 551-563.

Wise, D.R., DeBerardinis, R.J., Mancuso, A., Sayed, N., Zhang, X.Y., Pfeiffer, H.K., Nissim, I., Daikhin, E., Yudkoff, M., McMahon, S.B.*, et al.* (2008). Myc regulates a transcriptional program that stimulates mitochondrial glutaminolysis and leads to glutamine addiction. Proc Natl Acad Sci U S A *105*, 18782-18787.

Wong, K.K., Engelman, J.A., and Cantley, L.C. (2010). Targeting the PI3K signaling pathway in cancer. Curr Opin Genet Dev *20*, 87-90.

Wu, G., Hitchen, P.G., Panico, M., North, S.J., Barbouche, M.R., Binet, D., Morris, H.R., Dell, A., and Haslam, S.M. (2016). Glycoproteomic studies of IgE from a novel hyper IgE syndrome linked to PGM3 mutation. Glycoconj J *33*, 447-456.

Yang, L., Fliegauf, M., and Grimbacher, B. (2014). Hyper-IgE syndromes: reviewing PGM3 deficiency. Curr Opin Pediatr *26*, 697-703.

Yang, X., Zhang, F., and Kudlow, J.E. (2002). Recruitment of O-GlcNAc transferase to promoters by corepressor mSin3A: coupling protein O-GlcNAcylation to transcriptional repression. Cell *110*, 69-80.

Yi, W., Clark, P.M., Mason, D.E., Keenan, M.C., Hill, C., Goddard, W.A., Peters, E.C., Driggers, E.M., and Hsieh-Wilson, L.C. (2012). Phosphofructokinase 1 glycosylation regulates cell growth and metabolism. Science *337*, 975-980.

Ying, H., Kimmelman, A.C., Lyssiotis, C.A., Hua, S., Chu, G.C., Fletcher-Sananikone, E., Locasale, J.W., Son, J., Zhang, H., Coloff, J.L*., et al.* (2012). Oncogenic Kras maintains pancreatic tumors through regulation of anabolic glucose metabolism. Cell *149*, 656-670.

Zhang, Q., Davis, J.C., Lamborn, I.T., Freeman, A.F., Jing, H., Favreau, A.J., Matthews, H.F., Davis, J., Turner, M.L., Uzel, G*., et al.* (2009). Combined immunodeficiency associated with DOCK8 mutations. N Engl J Med *361*, 2046-2055.

Zhang, Y., Yu, X., Ichikawa, M., Lyons, J.J., Datta, S., Lamborn, I.T., Jing, H., Kim, E.S., Biancalana, M., Wolfe, L.A*., et al.* (2014). Autosomal recessive phosphoglucomutase 3 (PGM3) mutations link glycosylation defects to atopy, immune deficiency, autoimmunity, and neurocognitive impairment. J Allergy Clin Immunol *133*, 1400-1409, 1409.e1401-1405.

Zheng, M., Fang, H., Hakomori, HS. (1994). Functional Role of N-Glycosylation in a5pl Integrin Receptor. J Biol Chem. 22;269(16):12325-31.

Zhou, F., Su, J., Fu, L., Yang, Y., Zhang, L., Wang, L., Zhao, H., Zhang, D., Li, Z., and Zha, X. (2008). Unglycosylation at Asn-633 made extracellular domain of E-cadherin folded incorrectly and arrested in endoplasmic reticulum, then sequentially degraded by ERAD. Glycoconj J *25*, 727-740.

Zhu, Q., Zhou, L., Yang, Z., Lai, M., Xie, H., Wu, L., Xing, C., Zhang, F., and Zheng, S. (2012). O-GlcNAcylation plays a role in tumor recurrence of hepatocellular carcinoma following liver transplantation. Med Oncol *29*, 985-993.

Zito, E. (2015). ERO1: A protein disulfide oxidase and H2O2 producer. Free Radic Biol Med *83*, 299-304.

List of pubblications

Transcriptional profiling of immortalized and K-ras-transformed mouse fibroblasts upon PKA stimulation by forskolin in low glucose availability.
Chiaradonna F, Pirola Y, Ricciardiello F, Palorini R.
Genom Data. 2016 Jul 7;9:100-4. doi: 10.1016/j.gdata.2016.07.004

Protein Kinase A Activation Promotes Cancer Cell Resistance to Glucose Starvation and Anoikis.
Palorini R, Votta G, Pirola Y, De Vitto H, De Palma S, Airoldi C, Vasso M, Ricciardiello F, Lombardi PP, Cirulli C, Rizzi R, Nicotra F,Hiller K, Gelfi C, Alberghina L, Chiaradonna F.
PLoS Genet. 2016 Mar 15;12(3):e1005931. doi: 10.1371/journal.pgen.1005931.

Ringraziamenti

A conclusione della mia tesi di dottorato desidero ringraziare il mio tutor, Ferdinando Chiaradonna, in primis per avermi accolta nel proprio laboratorio e soprattutto per l'aiuto (e anche la pazienza) e la competenza con cui mi ha indirizzata nelle occasioni di dubbio.

Ringrazio Roberta per i suoi insegnamenti e tutti coloro che lavorano e hanno lavorato nel laboratorio 5048 tra cui Claudia, Humberto e tutti i tesisti/stagisti: ognuno, anche se in maniera diversa, mi ha insegnato qualcosa aiutandomi nella mia crescita intellettuale e non solo.

Un doveroso ringraziamento va alla Prof.ssa La Ferla e a tutto il team dei chimici i quali mi hanno permesso di svolgere parte della tesi presso il loro laboratorio.

Ringrazio il laboratorio 5051, in special modo Federica e Matteo per le risate e il loro sostegno (anche a distanza), Laura e Valeria del lab Granucci, con le quali ho condiviso "gioie e dolori" dell'ultimo periodo. Ringrazio Michael, Aurora e Salvo per gli incoraggiamenti e per le chiacchierate fatte il sabato sera.

Ringrazio ancora i miei genitori, le mie nonne, Massimo, Giusi, Fabio, Antonio e i miei zii che mi hanno sostenuta e incoraggiata ogni giorno: dedico a loro il frutto di tre anni di lavoro.